

Investigations of Tribological Behaviour in Machining Operation for a Single Point Cutting Tool in Presence of Coolant

A Thesis submitted to the Delhi Technological University, Delhi in fulfilment of the requirements for the award of the degree of

DOCTOR OF PHILOSOPHY

in

Mechanical Engineering

by

ANURAG SHARMA

(2K16/PhD/ME/019)

Under the Supervision of

Dr. RAMESH CHNADERA SINGH

(Professor)

Dr. RANGANATH M.SINGARI

(Professor)



**DEPARTMENT OF MECHANICAL ENGINEERING
DELHI TECHNOLOGICAL UNIVERSITY**

Shahbad Daultpur Bawana Road

DELHI-110042, INDIA

OCTOBER, 2020

DECLARATION

I hereby declare that the thesis work entitled “**Investigations of Tribological Behaviour in Machining Operation for a Single Point Cutting Tool in Presence of Coolant**” is an original work carried out by me under the supervision of Dr. Ramesh Chandra. Singh, Professor, Department of Mechanical Engineering, Delhi Technological University, Delhi, and Dr. Ranganath M. Singari, Professor, Department of Mechanical Engineering, Delhi Technological University, Delhi. This thesis has been prepared in conformity with the rules and regulations of the Delhi Technological University, Delhi. The research work presented and reported in the thesis has not been submitted either in part or full to any other university or institute for the award of any other degree or diploma.

ANURAG SHARMA

(Regd. No: 2K16/PhD/ME/19)

Deptt. of Mechanical Engineering

Delhi Technological University,

Delhi

Date: 27.10.2020

Place: Delhi

CERTIFICATE

This is to certify that the thesis entitled “**Investigations of Tribological Behaviour in Machining Operation for a Single Point Cutting Tool in Presence of Coolant**” submitted by **Mr. Anurag Sharma** to the Delhi Technological University, Delhi for the award of the degree of **Doctor of Philosophy in Mechanical Engineering** is a bonafide record of original research work carried out by him under our supervision in accordance with the rules and regulations of the University. The results presented in this thesis have not been submitted, in part or full, to any University or Institute for the award of any degree or diploma.

Dr. Ramesh Chandra Singh

Professor,

Department of Mechanical Engineering

Delhi Technological University,

Delhi, India

Dr. Ranganath M. Singari

Professor,

Department of Mechanical Engineering

Delhi Technological University,

Delhi, India

ACKNOWLEDGMENTS

The completion of my research work and compilation into thesis work is a successful task which is a deep encouragement from very important and special persons who are of course my supervisors. I feel a great pleasure that I have reached at this stage of time when I would like to express my deep gratitude and special thankfulness foremost to supervisors Prof. Ramesh Chandra Singh and Prof. Ranganath M. Singari who have always been like a searchlight in the dark night for me. Their guidance and future perception always remain successful.

I would like to extend my deep sense of gratitude and thankfulness to Prof. S. Arvindan, Indian Institute of Technology, Delhi (IITD) who was kind enough to spare time from his busy schedule in clearing confusions and solving problems related to my research work.

I would like give my thanks and indebtedness to the respected distinguished Prof. R. S. Mishra Chairman, DRC, Prof. Vipin Head of the Department, Mechanical Engineering, and SRC members Prof. Sabah Khan (JMI), Prof. Surjit Angra (NIT Kurukshetra), Prof. Rajiv Chaudhary, Prof. D. S. Nagesh, Prof. Vikas Rastogi, Prof. Ramesh Srivastava for their valuable and important suggestions for improvement in bringing out a successful thesis in the presented format.

I am thankful to Prof. Jai Gopal Sharma Head of the Department Bio-Technology (DTU) for encouragement and motivation.

My sincere thanks are for my special friends Mr. Abhishek Singh, Mr. Deepak Kumar (Research Scholars, IIT Delhi), Pawan Kumar (Project Associate, IIT Delhi) and Sumit Chaudhary (PhD, D.T.U)

I convey my sincere thanks to Mr. Rajesh Bohra, Mr. Sunil Kumar, Mr. Chail Bihari, Mr. Manmohan, Ms. Niharika Gupta (Research Scholar, DTU), Ms. Shine Augustine (Research Scholar, DTU) and Ms. Shikha Gupta (Research Scholar) for their technical and experimental support. I am thankful for everyone who is directly or indirectly involved in my research work.

I also extend my thankfulness to my family members especially my wife Mrs. Mridula Sharma who helped me in every manner keeping me relaxed from children and other house hold activities which has increased my concentration power of brain.

I have found myself with no words in my vocabulary to mention the gratefulness for my parents though heavenly abode but always remain a source of inspiration and courage since childhood days. I find that their blessings are always with me.

I am always grateful and thankful to ALMIGHTY GOD in providing me with good health, energy and patience in every best and worst situation. An encouragement with a sense for being in stable behavior for every victory and failure is given by THY GRACE.

(Anurag Sharma)

Delhi

October 2020

List of contents

Description		Page No.
Declaration		i
Certificate		ii
Acknowledgements		iii
List of contents		v
List of Figures		ix
List of Tables		xii
List of Abbreviations		xiv
Abstract		xvi
CHAPTER 1	INTRODUCTION	1-10
1.1	Historical Background	1
1.2	Terminology of Single Point Cutting Tool	2
1.3	Major Angles of Single Cutting Tool	3
1.4	Tool Angles Specifications System	5
1.5	Dry machining	7
1.6	Conventional cutting fluid	7
1.7	Minimum Quantity Lubrication (MQL)	8
1.8	Nano-cutting fluids	8
1.9	Cryogenic Cooling	9
1.10	Classification of cutting Fluids	9
CHAPTER 2	LITERAURE REVIEW	11-67
2.1	Tribology at interface of cutting tool and workpiece	11
2.2	Friction at interface of cutting tool and workpiece	14
2.3	Wear at interface of cutting tool and workpiece	18
2.4	Lubrication at interface of cutting tool and workpiece	25
2.5	Metal Cutting of workpiece by cutting tool	28

2.6	Thermal Effects on cutting tool and workpiece	41
2.7	Cutting Fluids/High Pressure Fluids for metal cutting	45
2.8	Effects of Nano particles in cutting fluids	49
2.9	Nano Particles in lubricants	54
2.10	Cryogenic Cooling	59
2.11	Research gaps	66
2.12	Objectives	67
CHAPTER 3	EXPERIMENTATION	68-78
3.1	Pin-on-disc tribometer	68
3.2	Specially made delivery system	69
3.3	Pin and Disc	70
3.4	IR Thermal imaging non contact type camera	71
3.5	Digital microbalance	72
3.6	Single point cutting insert and tool holder	73
3.7	Lathe machine	74
3.8	Piezo electric lathe tool dynamometer	75
3.9	Surface roughness tester	76
3.10	CNC Vision Inspection Machine	76
CHAPTER 4	NANO-CUTTING FLUIDS AND CHARACTERIZATION	79-88
4.1	Characterization of Nanoparticles	79
4.2	Preparation of nano-cutting fluids	81
4.2.1	Nano-cutting fluid with TiO ₂ nanoparticles	81
4.2.2	Nano-cutting fluid with Al ₂ O ₃ nanoparticles	83
4.3	Characterization of prepared nano-cutting fluids by TEM images	84
4.4	Characterization of prepared nano-cutting fluids by Raman Shift	85
4.5	Rheological Properties of nano-cutting fluids	87
CHAPTER 5	EXPERIMENTATION PROCESS	89-93

5.1	Experiments performed on pin-on-disc tribometer (dry and cryogenic)	89
5.2	Experiments performed on pin-on-disc tribometer (wet and nano-cutting fluids)	91
5.3	Experiments performed on lathe machine (dry and cryogenic)	91
5.4	Experiments on Lathe machine (Wet and Nano-cutting fluids)	93
CHAPTER 6	RESULTS AND DISCUSSION	94-129
6.1	Experiments on pin-disc tribometer (dry and cryogenic)	94
6.1.1	Wear volume loss	96
6.1.2	Optimization on the basis of Taguchi (S/N ratio)	97
6.1.3	Confirmation Tests	100
6.1.4	Wear of pin	100
6.1.5	Wear of disc	101
6.2	Experiments on Pin-on- Disc tribometer (Wet and Nano-cutting fluids)	102
6.3	Experiments on lathe machine (dry and cryogenic)	105
6.4	Taguchi Based Optimization (Signal to Noise ratio)	108
6.3.1	Surface roughness	112
6.3.2	Cutting force	114
6.3.3	Tool wear (Flank wear length)	116
6.3.4	Temperature	118
6.3.5	Confirmation Experiments	120
6.3.6	Surface morphology	122
6.4	Experiments on lathe machine with wet and nano-cutting fluids	123
6.4.1	Surface roughness	123

6.4.2	Tool Wear (Flank Wear length)	124
6.4.3	Cutting Force	125
6.4.4	Temperature	126
6.4.5	Machining time	127
6.4.6	Chip compression ratio	128
Chapter 7	CONCLUSIONS AND FUTURE SCOPE	131-154
Conclusions		131
Future scope		133
References		135-153
Patent		153
Research Papers Published/Accepted in Journals		153
Research Papers Published/ Accepted in International / National Conference Proceedings		154
Research Papers presented in International/National Conferences		154

List of Figures

Figure No.	Description	Page No.
Figure 1.1	Single Point Cutting Tool (SPCT)	3
Figure 1.2	Layout of Single Point Cutting Tool	4
Figure 3.1	Schematic sketch of (a) Dry sliding (b) Cryogenic sliding with Liquid N ₂	69
Figure 3.2	Specially made delivery system of nano-cutting fluid in Pin-on-disc tribometer	70
Figure 3.3	(a) TiN coated carbide pin and (b) AISID3disc	71
Figure 3.4	IR Thermal imaging non-contact type camera	72
Figure 3.5	Digital microbalance	73
Figure 3.6	Single point cutting insert and tool holder	73
Figure 3.7	Lathe machine with self-made supply of controlled drop wise supply of nano-cutting fluid	74
Figure 3.8	(a) piezo electric dynamometer (b) digital display of lathe tool dynamometer	75
Figure 3.9	Surface roughness tester	76
Figure 3.10	CNC Vision Inspection Machine	77
Figure 4.1	(a) SEM image and (b) EDS of nanoparticles Al ₂ O ₃	80
Figure 4.2	(a) SEM image and (b) EDS of nanoparticles TiO ₂	80
Figure 4.3	4.3 Magnetic stirrer for nano-cutting fluid with nanoparticles TiO ₂	82
Figure 4.4	Water bath ultrasonicator	83
Figure 4.5	TEM image at a magnification of 40000X and (b) 60000X of prepared Al ₂ O ₃ nano-cutting fluid	84
Figure 4.6	(a) TEM image at a magnification of 40000X and (b) 60000X	85

	of prepared TiO ₂ nano-cutting fluid	
Figure 4.7	Raman shift pattern for Al ₂ O ₃ in prepared nano-cutting fluid	86
Figure 4.8	Raman shift pattern for TiO ₂ in prepared nano-cutting fluid	86
Figure 4.9	Viscosity of nano-cutting fluids with time at room temperature 25°C	87
Figure 6.1	Probability plot for Wear volume	94
Figure 6.2	Wear volume obtained during experimental run L ₁₈ DoE	96
Figure 6.3	Diversification of (a) mean S/N ratio wear volume (b) means of mean wear volume with various factor levels	98
Figure.6.4	(a) Field scanning electron microscope (FSEM) image of used pin during dry sliding at sliding speed = 90m/min, sliding load = 75N, sliding distance = 1200m (b) with LN ₂ sliding	101
Figure 6.5	(a) Field scanning electron microscope (FSEM) image of wear tracks on disc formed during dry sliding at sliding distance = 90m/min, sliding load = 75N, sliding distance = 600m (b) with LN ₂ sliding distance = 1200m	102
Figure.6.6	Coefficient of friction during different sliding conditions	103
Figure.6.7	Specific wear rate during different sliding conditions	104
Figure 6.8	Probability plots for (p) surface roughness, (q) cutting force, (r) flank wear length and (s) temperature	105
Figure 6.9	Experimental Ra' in accordance with DoE	112
Figure 6.10	(a) Modification of mean S/N ratio Ra' (b) Modification of mean Ra' with various factor levels	113
Figure 6.11	Experimental Fc' in accordance with DoE	114
Figure 6.12	(a) Modification of S/N Fc' (b) Modification of means Fc' with various factor levels	115

Figure 6.13	Experimental V_b' in accordance with DoE	116
Figure 6.14	(a) Modification of S/N of V_b' (b) Modification of mean V_b' at various factor levels	117
Figure 6.15	Experimental T' in accordance with DoE	118
Figure 6.16	(a) Modification of mean S/N of T' (b) Modification of mean temperature T' at various factors	119
Figure 6.17	(a) SEM image of the used cutting insert during dry turning at V_c' 60m/min., F_o' 0.14mm/rev. & D_c' 0.35mm (b) cryogenic turning with LN_2	121
Figure 6.18	(a) SEM image (b) EDS of the machined surface during dry turning at V_c' 60m/min., F_o' 0.14mm/rev. and D_c' 0.35mm	122
Figure 6.19	(a) SEM image (b) EDS of the machined surface during cryogenic turning with LN_2 at V_c' 60m/min., F_o' 0.14mm/rev. and dc' 0.35 mm	123
Figure 6.20	Surface roughness (μm) during different machining conditions	124
Figure 6.21	Flank wear length (μm) during different machining condition	125
Figure 6.22	Cutting force (N) during different machining condition	126
Figure 6.23	Temperature ($^{\circ}C$) during different machining condition	127
Figure 6.24	Machining time (seconds) during different machining conditions	128
Figure 6.25	Chip compression ratio (ψ) during different machining condition	129

List of Tables

Table no.	Description	Page no.
Table 2.1	Review regarding tribology at the interface of cutting tool and workpiece	11
Table 2.2	Review regarding friction at the interface of cutting tool and workpiece	14
Table 2.3	Review regarding wear at the interface of cutting tool and workpiece	18
Table 2.4	Review regarding lubrication at the interface of cutting tool and workpiece	26
Table 2.5	Review regarding metal cutting by of workpiece by cutting tool	28
Table 2.6	Review regarding thermal effects at interface of cutting tool and workpiece	41
Table 2.7	Review regarding cutting/high-pressure fluids at interface of cutting tool and workpiece	45
Table 2.8	Review regarding nanoparticles in cutting fluids at the interface of cutting tool and workpiece	50
Table 2.9	Review regarding nanoparticles in lubricants	54
Table 2.10	Review regarding cryogenic cooling	59
Table 3.1	Chemical analysis of carbide pin	70
Table 3.2	Elements found through chemical analysis	71
Table 4.1	Properties of nanoparticles	79
Table 5.1	Control factors with different level values Sliding Parameter	89
Table 5.2	L ₁₈ Taguchi orthogonal array for experiments performed pin-on-disc tribometer	90
Table 5.3	Control factors with different level values Machining Parameter	91
Table 5.4	L ₁₈ Taguchi orthogonal array experiments performed on lathe machine	92
Table 6.1	L ₁₈ Taguchi orthogonal array [OA]	95

Table 6.2	Response table for S/N ratio Wear volume (mm ³)	97
Table 6.3	Response table for means Wear volume (mm ³)	97
Table 6.4	Analysis of variance for means of Wear volume (mm ³)	99
Table 6.5	L ₁₈ Taguchi orthogonal array basis of performance of experiments	106
Table 6.6	Experimental results of responses with respective S/N value as per Taguchi L ₁₈ orthogonal array	107
Table 6.7	Response table for S/N ratio of surface roughness (Ra'), cutting force (Fc'), flank wear length (Vb') and temperature (T')	108
Table 6.8	Response table for means of surface roughness (Ra'), cutting force (Fc'), flank wear length (Vb') and temperature (T')	109
Table 6.9	Analysis of variance for means of surface roughness (Ra'), cutting force (Fc'), flank wear length (Vb') and temperature (T')	110
Table 6.10	Regression models	120

List of abbreviations

Symbols	Description
[OA]	Orthogonal array
Dc'	Depth of cut (mm)
DoE	Design of Experiment
E'	Sliding Environment
Ets	Elements
Fc'	Cutting force (N)
Fo'	Feed (mm/rev.)
LN ₂	Liquid nitrogen
M'	Machining condition
Nano A	Nano-cutting fluid with nanoparticle TiO ₂
Nano B	Nano-cutting fluid with nanoparticle Al ₂ O ₃
Ra'	Surface roughness (μm)
SPCT	Single point cutting tool
SD'	Sliding distance (m)
SL'	Sliding load (N)
SS'	Sliding speed (m/min.)
T'	Temperature (°C)

V_b'	Flank wear length (μm)
V_c'	Speed (m/min.)
$W_g\%$	Weight percentage
W_v'	Wear volume (mm^3)
λ'	Inclination angle
α'	Orthogonal rake angle
β'	Orthogonal clearance angle of principal flank
γ'	Auxiliary orthogonal clearance angle
ϕ'	Auxiliary cutting edge angle
θ'	Principal cutting edge angle
r'	Nose radius(mm)

ABSTRACT

Dry turning is considered environmentally safe but the manufacturing rate may be slow due to the effect of combined machinability parameters (i) speed, (ii) feed and (iii) depth of cut. The cutting tool has relative velocity insitu contact with the workpiece. The possibility of sticking material and plastic deformation of the cutting tool may be increased. The surface morphology may get affected due to adhesive particles and other cutting parameters and finally dimensional accuracy of workpiece depends on the same. Conventional cutting fluids may be used to smoothen the process but do not show more remarkable improvement due to recent development of new hard engineering materials and strict high standards of manufacturing. Straight oils and mineral oils were used by researchers at the interface of cutting tool and workpiece but lubrication was found more effective than cooling. Servocut cutting oils with water emulsions were used but the majority of conventional cutting fluids provided marginal improvement in machinability characteristics like surface roughness, tool wear, surface morphology etc. The need was found for the preparation of novel cutting fluid and supplied in the control way to the cutting tool surface to prevent wastage. Therefore, cutting fluids with nanoparticles were developed of Al_2O_3 and TiO_2 separately in distilled water of 1.0% W/W separately. Biocompatible (Tween 20) surfactant was used for preventing agglomeration of particles. Nano-cutting fluids were used on pin-on-disc tribometer for determining tribological properties during sliding and on lathe machine for observing machinability characteristics. Cryogenic cooling was done with a direct supply of LN_2 at the interface of pin-on-disc of tribometer and the rake surface of single point cutting tool on lathe machine. Tribological properties and machinability characteristics of prepared nano-cutting fluids were compared with dry, wet, and cryogenic cooling condition.

It has been found that the lowest value coefficient of friction and specific wear rate was found at direct supply LN_2 and increasing order with nano-cutting fluid with nanoparticles TiO_2 tribometer. The coefficient of friction was 0.93 and specific wear rate was $4.365 \times 10^{-5} \text{ mm}^3/\text{Nm}$ during the dry sliding condition. On comparing with the dry condition, coefficient friction was lowered by 4.3%, 12.9%, 15% and 17.2% for wet with conventional cutting fluid, nano-cutting fluid TiO_2 , nano-cutting fluid Al_2O_3 and cryogenic cooling with LN_2 respectively. On comparing with a dry condition, specific wear rate was lowered by 22.5%, 29.5%, 37.92% and 98.5% for wet with conventional cutting fluid, nano-cutting fluid TiO_2 , nano-cutting fluid Al_2O_3 and cryogenic cooling with LN_2 respectively.

Surface roughness, flank wear length, cutting force, temperature, machining time and chip compression ratio were found at 1.85 μm , 245 μm , 110N, 127 $^{\circ}\text{C}$, 49.31seconds and 2.3 respectively during dry turning and declined by 30.27%, 54.28%, 49.09%, 53.54%, 30.26% and 54.35% during cryogenic cooling on comparing with respective values during dry machining condition. It was found that values of machining properties were higher during dry machining condition and followed by decreasing pattern as (i) dry, (ii) wet, nano-cutting fluid with TiO_2 , nano-cutting fluid with Al_2O_3 and cryogenic cooling with LN_2 . It has been found that wastage is associated with liquid nitrogen due to its property and boiling point temperature of -196 $^{\circ}\text{C}$. During experimentation, the contact of liquid nitrogen with the atmosphere at room temperature created white fumes. This gave a need for the development of an alternative cooling process. A controlled and localized process was developed for supplying the conventional cutting fluid and nano-cutting fluids drop by drop at the interface of pin-on-disc tribometer and cutting insert-workpiece on lathe machine. The results of rigorous experiments showed that nano-cutting fluid with Al_2O_3 was better than dry, wet, nano-cutting fluid with TiO_2 and cryogenic LN_2 . The wastage of nano-cutting fluid has been found very low or negligible as compared with cryogenic cooling with LN_2 .

INTRODUCTION

This chapter has the content about the beginning of some important aspects of tribology from historical background and its influence on mankind to present-day modern machining techniques. The brief introduction of the terminology of single point cutting tool, principal angles, tool angle specification system, a different type of machining conditions like dry, conventional cutting fluid, minimum quantity lubrication (MQL), nano-cutting fluids, cryogenic cooling and classification of cutting fluids.

1.1 Historical Background.

Influence of tribology can be seen from the pre-historic time of the Paleolithic period. The early man at that time used this knowledge in the sharpening of tools over other stones. Those sharpened tools were used for hunting of animals for food and clothes.

The friction generated by two stones over each other produced sparks and later discovered fire. The sharpened edges of stones were used to drill holes.

Discovery of wheel reduced the sliding friction and was converted into rolling friction. This made easy in moving heavy items from one place to another. Carts were discovered which later pulled by horses, bulls, camels, etc. Potter's wheel influenced the fabrication of utensils, pots etc. prepared by clay.

Modern day's applications and impact of tribology can be remarked from Leonardo da Vinci performed a series of experiments regarding friction between contacting objects in 1400s and invented the sketches for the discovery of laws of friction

The law of governing motion regarding the rectangular block bearing over a flat surface was discovered. An introduction was made for the relationship of coefficient of friction to normal load.

In the 1960s, many engineers from iron and steel plants in one conference of UK Cardiff expressed the failures of machines due to seizure. This reported the heavy losses of time and economy.

Later on, Dr. H. Peter Jost made acceptance in the study and discovered the word Tribology which means friction, wear and lubrication.

The combination of Greek work “Tribos” means rubbing and “logy” means study results in the Tribology. Good tribological knowledge results in negligible wastage of energy and time. In machining, we find a situation that with every movement of the tool on metal workpiece we get fresh exposed new metal surface and preventing that surface from the atmosphere is a challenging task [1, 2].

Good tribological knowledge results for less wastage of energy, time and long life of the cutting tool. Tribological study provides a better finished product during machining. The new metal surface must be protected from atmospheric reactive conditions exposed during machining with the cutting tool on workpiece.

The relative motion of chip and cutting tool surfaces in the presence of lubricants plays a significance role to produce surface finish, requirement of energy and tool life.

1.2 Terminology of Single Point Cutting Tool

The parts of (SPCT) used for metal cutting are fabricated by proper grinding of cutting tool square bar as shown in Figure 1.1. The shank is firmly held in a tool holder or tool post and prevented from vibrations and high shear stress.

The top surface of the tool between shank and the point of tool is called rake face. In cutting action the chips flow along this surface.

The lowest portion of the side cutting edges is a heel and the portion of cutting tool which faces the workpiece is called flank face.

The nose radius which is formed at the sharp point of cutting tool, it provides more strength to the tip, long tool life with a superior surface finish

Its value varies from 0.4mm to 1.6 mm depending on other factors like depth of cut, type of cut, etc. [3].

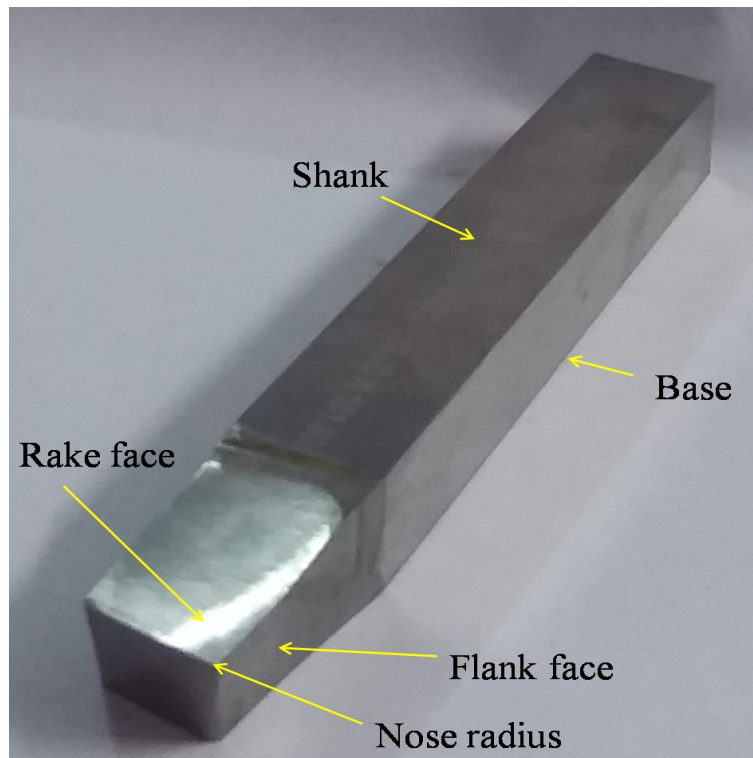


Figure 1.1 Parts of Single point cutting tool (SPCT)

1.3 Major Angles of Single Cutting Tool

Rake Angle: The angle formed between the face of the tool and a plane parallel to its base. If the inclination is towards the shank, it is called back rake angle or top rake angle or positive rake angle and it varies from 10° to 12° , when it is measured towards the side of the tool, it is called side rake angle and varies from 10° to 12° for high speed steel tool for machining mild steel workpiece, when the face of is made in such a way that, it slopes upwards from the point is called negative rake angle, when no rake is provided then on the tool, then it is called zero rake angle.

The increase in rake angle results in easy chip flow, reduction of cutting force & power consumption and improved surface finish

Higher rake angles show thinner chips and low dynamic shear strain. Therefore, cutting tools with higher rake angles are used for machining soft or ductile materials for easy chip flow and cutting tool with a small rake angle are used for machining hard material or brittle materials.

The angle between the face and the flank of the tool is called lip angle. The angle which is formed by the front or side surfaces of the tool which are adjacent and below the cutting

edge, when the tool is held in a horizontal position are called clearance angles. They decrease friction between flank surface and workpiece.

The selection of clearance angles depends on the type of material and cutting conditions.

A large clearance angle is used in machining soft or ductile materials and small clearance is required for machining hard materials or brittle materials

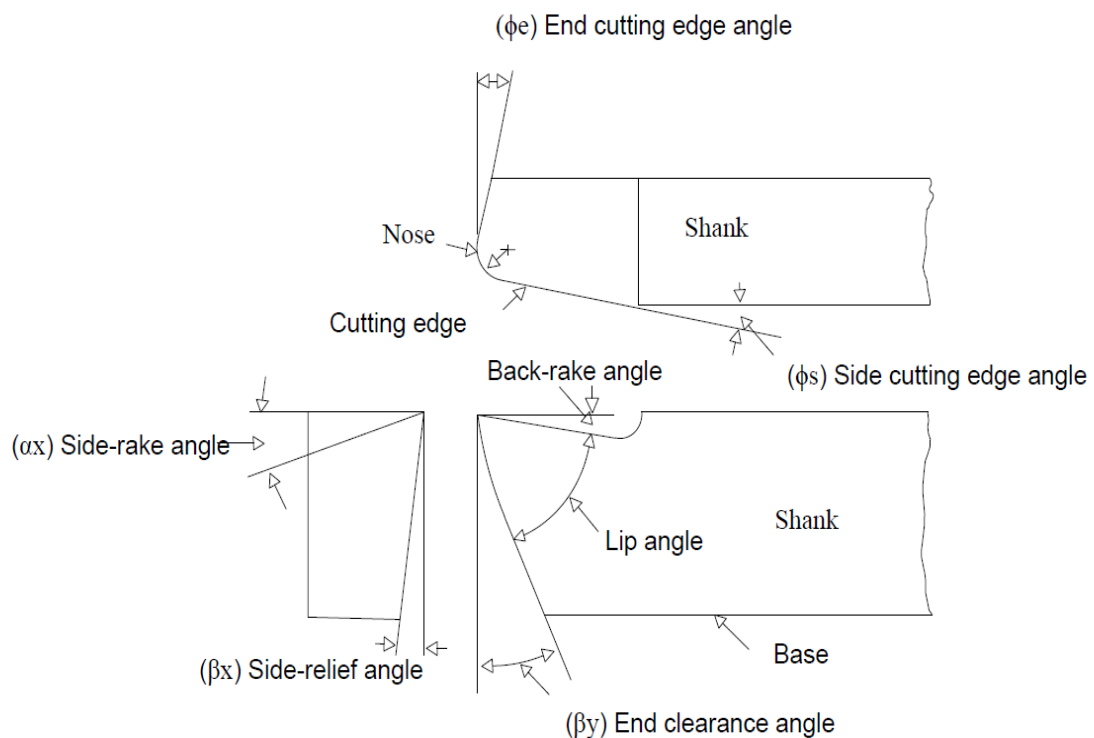


Figure 1.2 Layout of Single Point Cutting Tool

Clearance angles play an important role in improving tool life by reducing friction. The clearance angles are classified as below:

When the surface is considered is in front of the tool is called front clearance angle and varies from 6° to 8° . When the surface below the side cutting edge is considered the angle formed is called side clearance angle and varies from 6° to 8° .

The angle formed between the flank of the tool and a perpendicular line drawn from the cutting point to the base of the tool is called relief angle. The angle formed between the tool face and

a line through the point, which is a tangent to the machined surface of the work at that point is called cutting edge angle.

The side cutting edge angle is provided to side of turning tool and varies from 0° to 90° .

A knife edge turning tool has a side cutting edge angle of 0° and cutting edge is perpendicular to the work surface. It is used in a slender type of work.

A square nose tool has a side cutting edge angle equal to 90° and cutting edge is parallel to the work surface. It is used in finish turning with a very fine depth of cut and coarse feed.

The end cutting edge angle is provided to the front of turning tool and prevents the front cutting edge from rubbing against the workpiece. It varies from 8° to 15° .

Nose radius: The pointed edge of side cutting edge angle and end cutting edge angle is slightly made round is called nose radius. It reduces the stress concentration of the sharp edge of turning tool and improves the surface finish of the workpiece and it varies from 0.8 mm to 1.6mm. A large nose radius is recommended for brittle materials with discontinuous chips [4].

1.4 Tool Angles Specifications System

ASA System: It stands for American Standards Association System is called a transverse plane. The horizontal plane which contains tool shank is known as a base plane.

The second reference plane is the longitudinal plane which is perpendicular to the base plane but parallel to the longitudinal feed direction.

The third reference plane is perpendicular to both the planes

The sequence of angles adopted in ASA system is as follows: The horizontal plane which contains tool shank is known as base plane.

The second reference plane is the longitudinal plane which is perpendicular to the base plane but parallel to the longitudinal feed direction. The third reference plane is perpendicular to both the planes

$\alpha_y, \alpha_x, \beta_y, \beta_x, \phi_e, \phi_s, r$ are the designations for various angles.

ORS system: It stands for orthogonal rake system. The horizontal plane which contains tool shank is known as base plane.

The second reference plane is called cutting plane which is perpendicular to the base plane but parallel to the side cutting edge/principal cutting edge.

The third reference plane is called orthogonal plane which is perpendicular to both the planes.

The sequence of angles adopted in ORS system is as follows:

$\alpha_o, \delta_p, \delta_a, \gamma_a, \gamma_p, r$ are the pattern of different angles.

ISO means International Standards Organization which also called NRS system: It stands for normal rake system.

The horizontal plane which contains tool shank is known as base plane. The second reference plane is called cutting plane which is perpendicular to the base plane but parallel to the side cutting edge/principal cutting angle.

The third reference plane is called a normal plane which is perpendicular to the side cutting angle/ principal cutting edge angle. In this system, the axes are chosen in such a way that every angle is a true angle. Tool grinding becomes easy since no angle corrections are required during grinding.

The sequence of angles adopted in NRS system is as follows:

$\alpha_n, \delta_{pn}, \delta_{an}, \tau_a, \tau_p, r$ are the various types of angles.

During machining the tool wear takes place. The rake and flank surface of turning tool get deteriorated. The wear is of two types as crater wear and flank wear.

Crater Wear: The wear in which tool – chips interface form a depression on the tool face is called crater wear. This is due to the pressure of the hot chips sliding the face of the tool.

Flank Wear: The wear in which a flank portion is worn out behind the cutting edge is called flank wear.

The tool and workpiece become hot due to rise in temperature while machining which is one of the undesirable effects. The temperature distribution is not uniform.

It is highest at the tool-workpiece interface means highest at tool point and immediate contact chip, so, distribution of temperature in the form of the zone is as follows:

Shear Zone: The highest amount of heat is generated which makes the material deform plastically. The chips carry away the heat during movement.

Chip- tool interface zone: The deformation takes place due to hot chips and cutting insert/tool. The temperature rise is due to higher cutting speed. The hardness of workpiece material increases the friction with same machining parameters.

Work – tool interface zone: The temperature rise takes place due to workpiece and that portion of tool which is in immediate contact. The rubbing action of cutting insert has significant effect. [5, 6].

1.5 Dry machining:

In this machining condition, cutting tool and the workpiece may work in dry condition like without the use of any coolant or lubrication. This may increase the temperature at the interface of cutting tool and workpiece and deteriorated tool and surface of the workpiece.

In the case of steel as workpiece, the chips were long, staggered at both sides with material outflow to both of the sides.

The process may be considered as eco-friendly and economical but the manufacturing rate was slow due to machining at low machinability parameters for the optimum tool wear and surface roughness. Researchers have proposed some harder tool material with a coating of TiN, diamond powder etc. [7].

1.6 Conventional cutting fluid:

In this machining condition, a conventional cutting fluid used at the interface of tool and workpiece. This may include natural oils, straight oils, vegetable oil and emulsions may vary with oil (1-20%) approximately in the remaining water.

The supply rate could be from 500-20,000 ml per hour. Researchers have found that tool wear and surface roughness were (20-31%) lower as compared with dry machining.

The amount of cutting fluid may vary further depending upon the type of workpiece material. But, environmental and health issues like skin infections, itching, nausea etc. may emerge during the handling and recycling of debris and chips.

The chips contaminated with the ingredients of cutting fluid may be difficult in separating and economically cost elevating. The fumes generated with conventional cutting fluids and contact with hands may increase skin infections, itching in eyes, sometimes nausea etc. [8].

1.7 Minimum Quantity Lubrication (MQL):

The oil in small quantity generally 100-500ml/hour used during machining at the interface of cutting tool and workpiece. One method was continuous drop wise flow and another method was mixing oil and compressed air in equal proportionate.

The mist generated was supplied at the interface of the cutting tool and workpiece. This method may be environmentally friendly depending upon the type of oil.

Vegetable and biocompatible oils can make this method which has negligible effect on environment and health issues of human beings. The chips or debris created may be found clean and free from impurities and further recycled with almost negligible cost [9].

1.8 Nano-cutting fluids:

Nanoparticles are in the range of 1 to 100 nm. Researchers have tried to mix nanoparticles in oils for lubrication and cooling purpose.

The selection of nanoparticles was based on the type of base fluid like some nanoparticles were found easily mixing with oil but the same may not be mixing with water.

Nanoparticles increase the thermal conductivity of the base fluid and lower the tool wear and surface roughness of workpiece during machining.

Eco-friendly nano-cutting fluids can be made by selecting biodegradable oil and nanoparticles like nanoparticle of MoS₂ in sunflower or olive oil.

The surfactant if used should be biocompatible. Water-based nano-cutting fluid can be economical due to easily availability of water and further conversion into distilled water.

The heat transfer coefficient of water was found to be more than oil. This may improve the heat carrying capacity and a further improvement in machinability properties. Besides, increasing cooling capacity of base fluids lubrication property may be imparted.

The fluid may provide a cooling and lubricating effect. Nanoparticles in water based fluid with oil (1-10%) may be known as water emulsion.

The percentage of oil may vary with the type of oil and the amount of lubrication needed [157-160].

1.9 Cryogenic cooling:

Liquid nitrogen (LN₂) is odourless, non-toxic and having a boiling point of -196°C. The process may not produce any harmful ingredients that may be harmful to human health.

The direct supply of liquid nitrogen at the interface of cutting tool and workpiece may lower down the tool wear and surface roughness. The working environment during machining remained neat and clean without any splashing.

Researchers have used a hybrid combination of cryogenic cooling (direct supply of LN₂) and lubrication (MQL) and found that marginal difference of tool wear and surface roughness [185-187].

1.10 Classification of cutting fluids:

Those fluids which absorb the heat, generate cooling and provide lubrication during machining operations are called cutting fluids. They reduce the coefficient of friction between tool and workpiece. The cutting fluids are classified as follows:

Water based fluid: Water is the base fluid and small amount of other ingredients which increase the cooling and lubrication capacity are mixed in fixed proportionate.

Oil based fluids: Oil act as base fluid and small amount of ingredients are added which increase the lubrication and may also provide cooling effect during machining.

Straight oils: The straight oils are mineral oil like petroleum oils for example, kerosene oil and fatty oils containing animal, vegetable oil. They are good coolant and lubricant

Mixed oils: The mixture of straight oil and fatty oil make good cutting oil which is used during machining operations with low machining paraters.

Chemical additive oil: Sulphur as additive is used in machining tough, stringy, low carbon steels. Chlorine as additive is used promoting anti weld properties.

Chemical compounds: Rust inhibitor are used with high percentage of water in making cutting fluid and micro biocides are added to prevent any organic growth

The cutting fluid acts as a barrier between fresh machined surface and atmosphere and prevent corrosion of material. The cutting forces and energy consumption become less. [3, 4]

Summary

- The main salient features from Pre historic, Paleolithic period have been discussed.
- Facts regarding the discovery of word tribology and modern days application to machining have been discussed.
- Main parts, angles and importance to machining are shown.
- Importance of cutting fluids are studied.

LITERATURE REVIEW

Literature review of presented research work is categorised into eleven categories. The number of research paper for each category as, Introduction-9, Tribology at the interface of cutting tool and workpiece-10, Friction at the interface of cutting tool and workpiece-15, Wear at the interface of cutting tool and workpiece-8, Metal cutting from workpiece by cutting tool-48, Thermal effects on cutting tool and workpiece-14, Effects of nanoparticles in cutting fluids-12, Effects of nanoparticles in lubricants-19, Cutting fluids/High pressure fluids for metal cutting -16, Cryogenic cooling-27

2.1 Tribology at the interface of cutting tool and workpiece

Steel in various forms has used in engineering applications. In machining, the basic concept is used that workpiece like soft material and the cutting tool is made up of hard material. In making tools harder depends upon material selection and further enhanced by hard coating materials. Table 2.1 gives some details of research work related to reduce tribological properties which can be used in machining.

Table 2.1 Review regarding tribology at the interface of cutting tool and workpiece

Sno.	Author, year, reference no.,	Work done	Results/findings
1	Rech 2006 [10]:	The experiments were performed for the investigation of change in friction with the use of coatings like TiN, TiAlN and TiAlN + MoS ₂ deposited on a WC-Co carbide	It was found that TiN and (Ti, Al) + MoS ₂ coatings depicted better behavior in tribological property as compared to uncoated tools and reduced tool-chip contact length.
2	Samad et al. 2010 [11]:	The wear tests performed for finding out the influence of the polymer coating on tool steel with a	It has been found that tribological characteristics were improved with the effect of polymer coating.

		diameter 4mm silicon nitride ball on disc tribometer.	
3	Jin et al. 2014 [12]	N + Zr ions were implanted to bearing material surface like of Cr4Mo4Ni4V steel	It has been found that hardness in the implantation depth was improved significantly. Five times improvement was made in fatigue life.
4	Barnes et al. 2004 [13]	Surface roughness (Ra) approximately 1-10 μ m were generated on the glass surfaces.	Positive feelings were generated during rubbing finger over a smooth surface like glass and negative feelings were generated during rubbing a finger over a rough surface.
5	Tichy et al. 2000 [14]:	This review paper is concerned about the role of solid mechanics in the field of tribology.	The solid mechanics improved and made advancement in tribology field which further created an improvement in the field engineering and science and technology.
6	Olah et al. 2016 [15]:	TiC/amorphous carbon (TiC/a:C) nanocomposites thin film was investigated for determining the relationship between structure, elemental composition mechanical	It has been found that the samples of coating have influenced the tribological properties.

		and tribological properties.	
7	Kovalchenko et al. 2014 [16]	Ductile mode of removal of silicon provided greater depth of cut, avoiding cracks, reduce silicon brittleness due to thermal softening	A diamond tool was used for material removal. The surface of silicon was smooth and defects were absent on the surface of material.
8	Kopac et al. 2001 [17]	The carbide end mill tools were coated with TiAlN (1-3 μ m), other with 3 μ m coating of TiAlN and another with multiple coating of TiAlN/TiN and were used on CNC milling machine on workpiece of alloy steel X38CrMoV5.1	It has been found that coatings prevented the surface of end mill tool by protecting from outside environment.
9	Errico, et al. 1997 [18]	The cutting tool was coated by PVD techniques TiN and TiN + TiC _N coating deposited each by a cathodic arc and an iron-plating technique on a commercial insert.	The microhardness and thickness influenced anti-erosion resistance. It was found that no direct relation between anti-wear behaviour of milling with anti-erosion resistance and coating adhesion.
10	Recherger et al. 2013 [19]	The cutting tool shape was inspired by biting teeth geometry. This work gave an overview of biological principles and described a biomimetic approach for designing a cutting tool.	The tool showed outstanding mechanical properties and provided evidence that self-sharpening effects and high abrasive resistance.

2.2 Friction at the interface of cutting tool and workpiece

Composite materials are becoming more popular and solutions to various engineering applications are investigated about the friction properties between composite and cutting tool. This section gives details of research work done in reducing friction between tool and workpiece. The different types of friction models have been proposed and validated. The predicted values and values arrived during the performance of experiments are very close to each other. Table 2.2 gives some details about the reduction of friction performed by researchers.

Table 2.2 Review regarding friction at the interface of cutting tool and workpiece

Sno.	Author, year, reference no.,	Work done	Results/findings
1	Chardon et al. 2015 [20]	The experiments were performed for investigating the effect of friction during machining between composite and cutting materials. The simulations were done to examine the machining the composite by an original tribometer.	It has been found that the sliding velocity had a lower influence on coefficient of friction at high velocities
2	Bonnet et al. 2008 [21]	A friction model was made for describing the coefficient of friction at the interface during dry machining of an AISI 316 L steel with titanium nitride coated carbide tool.	It was found that coefficient of heat portion towards tool-chip was depended on the sliding velocity.
3	Grzesik 2000 [22]	Experimentally investigated about temperature, contact loads and friction during tool-	The multilayer coatings improved the wear rate. The coefficient of friction was varied between 0.4-

		work interface during orthogonal machining process at the chatter-free end turning.	0.8 which was similar to ceramic-ceramic contact.
4	Grzesik 1999 [23]	The experiments were performed for investigating the effect of adhesion in determining the friction at the tool-chip interface.	It was found that during orthogonal machining steels and uncoated carbides had high adhesion at the tool-chip interface. The maximum value of the interfacial coefficient of friction was 0.7 and 0.4 for carbon steel and stainless steel respectively.
5	Pottirayil 2010 [24]	The friction was measured during an experimental setup during cutting made by a tool and a spherical pin measured the friction of the nascent fresh cut under complete assembly dipped in lubrication.	It has been found that friction was 20-30% higher for un-cleaned surface
6	Saoubi et al. 2015 [25]	Presented an overview of progress made the efficient type of aviation use alloys and other composites. The detailed applications of technology used in the fabrication of high-quality aviation components have been discussed.	Result showed that machine tools were key factors in advanced material machining.
7	Chamani et al. 2016 [26]	An analytical model was generated for the	The results found during finite element simulation

		ploughing and adhesive friction co-efficient of metals during the scratch test with Berkovich indenters at various tip orientations.	and experimentation were in close agreement to each other.
8	Grzesik et al. 2014[27]	The experiments were performed with ceramic tools with large negative rake angle for oblique machining.	It has been found that during higher loads and velocity coefficient of friction was declined to 0.3. The tool wear evolution influenced the difference between coefficient of friction during orthogonal and oblique cutting.
9	Grzesik et al. 2013 [28]	The experiments were made for the investigations of the effect of inclination angle in Merchants model and new friction model was developed.	The tool inclination angle was significant for determining friction which was more for negative angles.
10	Schuh et al. 2016 [29]	Asymmetric depth profile was generated on 6 mm thick plate of Rheometer. The experiments were performed under full film lubrication for textured symmetric and asymmetric textures.	The result showed that symmetric texture produced normal forces below experimental limits, but asymmetric textures produced normal forces of higher than the experimental limit.
11	Abdelali et al. 2012 [30]	A new tribometer was developed. The workpiece was holding in CNC	It has been found that with the increase in sliding velocity the apparent

		machine and a carbide pin with a spherical head was used with hydraulic control creating the similar conditions of cutting	coefficient of friction declined.
12	Brinksmeier et al. 2015 [31]	The historical background of metalworking fluids with mechanisms has been discussed.	It was found that tribological tests showed that with the application metalworking fluids coefficient of friction was decreased due to making boundary layer film as compared to dry conditions.
13	Kawasegi et al. 2009 [32]	Femtosecond laser technology was used for texturing the cutting insert for different dimensions of depth and directions.	It was found that friction, cutting force were declined in nanotextured as compared to microtextured.
14	Smolenicki et al. 2014 [33]	To measure actual cutting process conditions, certain changes were made in tribometer. So, that every rotation gave freshly generated workpiece surface	It has been found that friction coefficient decreased with increasing speed.
15	Rech et al. 2009 [34]	The development of new tribometer was almost very close in simulating the movement of cutting insert on workpiece during turning. A modified pin on ring system was validated.	The coefficient of friction was dependent on sliding velocity. A normal force of 1000N was applied onto the pin of diameter 9mm which resulted in the pressure range of 1-2 GPa.

2.3 Wear at the interface of cutting tool and workpiece

The wear of cutting tool is influenced by the machining conditions, machining parameters and environmental conditions. In dry machining at high machining parameters and elevated environment conditions, the tool wear and surface roughness of machined workpiece are higher. The application of hard coatings on cutting tools has incremented the hardenability, helpful in retaining the shape and cutting ability.

Table 2.3 Review regarding wear at interface of cutting tool and workpiece

Sno.	Author, year, reference no.,	Work done	Results/findings
1	Tlili et al. 2016 [35]	The stresses emerged during heat treatment of coatings were reduced by adding ceramic powder with sol-gel.	It has been found that deposited alumina coating showed δ - Al ₂ O ₃ through sol-gel technique. The uncoated and nitrided steel wear more as compared to coated by newly developed technique.
2	Wang et al. 2016 [36]	The experiments were performed in analyzing the behaviour of epoxy-based composites in orthogonal machining with the influence of two different filler materials.	It has been found that cutting force for epoxy materials declined with incremented tool rake angle. The lower depth of cut improved the quality of cut surface due to the transition from the brittle to ductile.
3	Yahiaoui et al. 2016 [37]	The excavation forces emerged during cutting action with a contact of cutter/rock were analyzed while performing	It has been found that impact friction force was dependent on impact angle and velocity of rock particles on the front face

		experiments on vertical lathe machine	of the cutter.
4	Kurniawar et al. 2016 [38]	The elliptical vibrating tool was used for texturing at the distance of 5 μ m above the workpiece of Al-6061.	It was found that mathematical and experiment results were very close to each other. Surface roughness was related to the roughness of the tool nose radius.
5	Granados et al. 2016 [39]	The cutting mechanism at micro/nanoscale with the application of non-rigid tool holder was developed.	It was found that cutting mechanism worked successfully on different topography of surfaces like plane, inclined and curved surface with constant cutting depth.
6	Sugihara et al. 2012 [40]	The cutting tool was modified by developing micro texturing. The experiments were performed to investigate the efficiency of the tool.	It has been found that modified design of cutting tool improved the anti-adhesive properties.
7	Ahmed et al. 2009 [41]	Composites of AlMg B ₁₄ with 0, 30 and 70 wt% of TiB ₂ were prepared by mechanical alloying and hot pressing.	On incrementing, load wear rate was increased for all compositions of materials. AlMg B ₁₄ - 70 wt% TiB ₂ showed lower crater and tool flank wear.
8	Shalaby et al. 2014 [42]	Turning tools of different coating materials were selected like PCBN (Polycrystalline Cubic Boron Nitride), TiN, and	It was found that mixed alumina ceramic coating tool had a longer life and lower cutting components than coating tools.

		mixed alumina (Al ₂ O ₃ +TiC) coatings were used for performing turning experiments.	
9	Pilkington et al. 2013 [43]	AlCrO _x N _{1-x} coatings were arc deposited over HSS drills and WC- Co end mills at N ₂ /O ₂ ration of 0.9 - 0.75 using DC or 10 Khz pulse bias and experiments were performed.	AlCrO _x N _{1-x} coating deposited with N ₂ /O ₂ ration of 0.9/0.1 had hardness values of 32 GPa and were harder than coatings made with N ₂ /O ₂ ratio of 0.75/0.25 which had hardness values of 24 GPa.
10	Ramaujachar et al. 1996 [44]	Tool crater wear was investigated during for free cutting steels with and without lead addition i.e. AISI 12L14 and AISI 1215 respectively at moderately high cutting speed 140-200m/minute using cemented carbide cutting tools.	Dissolution wear was the dominant mechanism of crater were in both lead added AISI 12L14 and non lead AISI 1215 steel during machining at high speed. Coating of HFN on tool acted as an effective diffusion barrier.
11	Komanduri et al. 2000 [45]:	Molecular dynamics (MD) simulation of nanometric cutting was conducted on single crystal aluminum in specific combinations of crystal orientation (111), (110) (001) and cutting directions [110], [211] and positive [100]and with tool positive rake angles 0°,10°	Aluminum crystal was orientated in [111] plane and cut in [-110] direction, plastic deformation ahead of the tool was found to be predominately compression along with shear in cutting direction.

		and 40° to investigate nature of deformation.	
12	Nouri et al. 2007 [46]	A planer machine was used for orthogonal cutting. The image of the tool-chip interface was captured by high-resolution camera. The series of images were used for understanding the wear mechanism.	The wear behaviour of uncoated tool during dry machining was well illustrated and understood.
13	Zhu et al. 2015 [47]	The microscopic model of ploughing was developed. A robotic arm was used for measuring force component of abrasive belt.	The cutting force, specific energy and energy efficiency were found to be independent of the ideal depth of cut of robot-assisted grinding but dependent on the depth of grain penetration.
14	Bhat et al. 1995 [48]	The analysis was done in understanding the effect of polishing on diamond coated tools and influence on material machining.	It has been found that diamond had a significant improvement in the surface finish and a reduction of forces.
15	Komanduri et al. 1998 [49].	Molecular Dynamic (MD) simulations of nanometric cutting on a single crystal aluminum were used to investigate the nature of the chip formation process with crystal orientations.	It was found that three modes of deformation were observed in the shear zone. The material deformed parallel to the cutting direction and shear angle below 45° such variation in the

			mode of deformation were not discussed earlier.
16	Komanduri et al. 1998 [50]	Investigated effect of tool geometry in nanometric cutting, molecular dynamics (MD) simulations of nanometric cutting were carried out with tools of different edge radii relative to the depth of cut, tool edge radius r (3.62 - 21.72mm) and depth d (0.362 - 2.172mm) $d/r=0.1,0.2$ and 0.3 .	In conventional cutting, the edge radius was small and negligible but in nanometric cutting edge radius was 20-70nm. To study the effect of depth of cut tools of different edge radii, it was necessary to maintain d/r to be constant.
17	Kosaraju et al. 2015 [51]	The optimization was based on Taguchi in selecting out effective machining parameters for machining characteristics.	Confirmation tests showed that predicted and experimental values were very close to each other.
18	Yuefeng et al. 2010 [52]	The wear information of 873 samples of tools was collected and the more suitable tool was selected regarding wear rate.	Tool life was influenced by WRUMP (wear rate in uniform wear period).
19	Bahi et al. 2015 [53]	A hybrid model was developed having combined analytical and numerical approach to solve non-linear thermomechanical problem on chip and predicted the nature of friction	It was found that due to combined effect of high normal load, high temperature and shear flow stress a plastic deformation zone took place along tool chip interface.

20	Caliskan et al. 2015 [54]	The effect of carbon nitride/ titanium aluminium nitride coating during machining of titanium alloy Ti6Al4V was investigated.	It was found that coating had influenced machining characteristics
21	Buse et al. 2016 [55]	A new tribological simulation model was developed a modified pin-on-disc system was used for cutting CFRP and other hard composite materials.	The wear mechanisms of hard materials tools when cutting or making contact with CFRP was mainly characterized by cobalt phase removal
22	Sugihara et al. 2013[56]	The cutting tools were modified with micro stripe textured surface on rake and flank faces.	It has been found that texturing on flank face gave better resistance to wear.
23	Thakur et al. 2016 [57]	The research work related to nickel based alloy regarding applications, characteristics, machining processes and cooling strategies involved have been discussed.	It has been found that work hardening should be related to residual stresses at higher machining parameters.
24	Hakim et al. 2011[58]	An assessment of the performance of four cutting tool during machining medium hardened HSS polycrystalline c-BN (cBN +TiN), TiN coated polycrystalline CBN (c-BN+ TiN) ceramic mixed alumina (Al ₂ O ₃ +Tic) and	Mixed alumina and ceramic and coated carbide had longer tool life as compared with c-BN tools. The high chemical and thermal stability of Al ₂ O ₃ tribo film protected the tool substrate as it prevented heat generated at tool chip

		coated tungsten carbide.	from entering the tool core.
25	Monaghan et al. 1999 [59]	Finite Element methods were used to determine the influence of various coated and uncoated tungsten carbide tools on the machining of nickel based super alloy Inconel 718	The results of finite element models correlated closely with those of experimental cutting tests
26	Zhou et al. 2006 [60]	The experiments were performed by using conventional turning and with assisted ultrasonic vibration	It was found that assisted ultrasonic vibration turning performed better in relation to machining characteristics.
27	Ozbek et al. 2016 [61]	The uncoated carbide cutting inserts were cryogenically treated and used for turning of AISI 316 alloy.	It has been found that grain size elongated of cutting insert. The treated cutting inserts showed improvement in wear.
28	Remadna et al. 2006 [62]	The experiments were performed on tempered steel with CBN tool with constant speed. In another method, speed was continuously varied.	It was found that surface roughness was $0.64\mu\text{m}$ which was considered as good.
29	Kumar et al. 2006 [63]	The machining tests were conducted using SiC whisker reinforced alumina ceramic cutting tool and Ti [C, N] mixed alumina ceramic cutting tool on martensitic	Flank wear and crater wear in Ti [C, N] mixed alumina ceramic cutting tool was lower than SiC whisker reinforced

		stainless steel grade 410 and EN 24 steel work pieces.	
30	Woydt et al. 2015 [64]	The sliding tests were performed with alumina as pin and binder niobium carbide (NiC) and cobalt – bonded NbC at sliding speed 0.1-8.m/s at 22°C and 400°C	The wear rates at 400°C of HP-Nbc and NbC 8Co remained generally below 10-6mm ³ /Nm regardless of applied sliding speed
31	Settineri et al. 2006 [65]	Nanocomposite coatings were tested on ball erosions tests, Rockwell indentation, scratch test, ball on disc test at room temperature and a high temperature as well as nanoindentation and roughness measurements.	It was found that results obtained from laboratory tests and cutting tests were in very close values to each other.

2.4 Lubrication at the interface of cutting tool and workpiece

Lubrication reduces the coefficient of friction between two contacting bodies/ surfaces and prevents deterioration.

The lubricants keep the surface cool by absorbing heat and releasing to the atmosphere.

The debris generated is absorbed by the oil and keep the contacting surfaces clean.

Table 2.4 shows the details of lubricants used by researchers during machining

Table 2.4 Review regarding lubrication at the interface of cutting tool and workpiece

Sno.	Author, year, reference no.,	Work done	Results/findings
1	Talib et al. 2016 [66]	The composition of jatropha oil was modified and tested for viscosity index, coefficient of friction. The modified oil was used on NC lathe machine for AISI 1045 steel as workpiece and uncoated carbide cutting insert. The newly developed oil was supplied at the interface of workpiece and cutting insert.	The results showed that cutting force and cutting temperature, was reduced to 5-12%.and 6-11% as compared to synthetic ether.
2	Simonovic et al. 2016 [67]	An empirical model was made by using sequences of statistical methods for steel-steel and steel-DLC contacts with oil.	It has been found that developed models were strictly valid within the parameter range.
3	Sugihara et al. 2009 [68]	Nano/microtextures were made on the cutting tool by using femtosecond laser technology.	The results showed that cutting fluid retention on cutting surface was improved which increased anti-adhesion effect.
4	Claudin et al. 2010[69]	The coefficient of friction was measured during dry sliding and with the application of lubricating oil.	It has been found that straight oil was efficient in penetrating the pin-workpiece material interface even at very high pressure..

5	Pottirayil et al. 2011 [70].	The experiments were formed on steel disc by using a cut by single point cutting tool followed by a spherical pin for measuring coefficient of friction of the freshly cut surface. The whole assembly was immersed in a bath of water emulsion in the oil.	The coefficient of friction to lypophilic emulsifier was lower than that to a more hydrophilic surfactant.
6	Zhao et al. 2014[71]	Investigated the effect of surface modification of Zinc borate ultrafine powder [ZBUFPs] on their tribological; properties as lubricative additives in liquid paraffin (LP). ZBUFPs were successfully modified by hexadecyltrimethoxy silane (HD TMOS) and Oleic acid (OA).	ZBUFP as a lubricant additive in LP played an important role in the outstanding anti wear property.
7	Enomoto et al. 2011 [72]	The surface engineering approach was used to solve cutting of aluminum alloy due to the chips adhesion to cutting tool surface by texturing with nano/micro technic.	It was found that adhesion between chip and tool was declined by nano/micro texturing.
8	Batterz et al. 2016 [73]	The experiments were performed on ball-on-disc reciprocating tribometer	It was found that at 20Hz tests wear volume was lower due to thicker

		during constant frequency of 15Hz with variable load (4-120N) for testing tribological behaviour of methyltrioctylammonium bis (trifluoromethylsulfonyl) imideionic liquid as neat lubricant	tribofilm formation
--	--	--	---------------------

2.5 Metal cutting of workpiece by cutting tool

The process involves various types of conventional and modified cutting tools, inserts during the metal cutting process by machining.

The surface of tool is developed by texturing for reducing friction and cutting forces. The applications of cutting fluid with textured tool increase the cutting ability of tool. The temperature is declined as compared with dry machining.

Table 2.5 depicts the work done by researchers in the field of metal cutting. The different types of machining processes with cutting tools have been discussed.

Table 2.5 Review regarding metal cutting by of workpiece by cutting tool

Sno.	Author, year, reference no., title of research paper	Work done	Results/findings
1	Sheya et al. 2015 [74]	The experiments were performed on lathe machine titanium alloy Ti6Al4V as workpiece and carbide cutting insert in the presence of vegetable based cutting fluids. The surface roughness and flank wear length were	Ra was ranged from 0.56 to 1.81 μ m. Flank wear length incremented according to high cutting parameters.

		observed	
2	Deshayes 2007 [75]	Original approach based on the experimental estimation of friction coefficient and enabled to simplify complex groove geometry in a flat rake was presented	The cutting speed range used in turning for machining a steel alloy with the industrial grooved cutting face was assessed by combining experimental result and finite element simulations.
3	Zhu et al. 2010 [76]	The nanometric cutting process of copper by diamond cutting tool was in accordance with atomic force model which was further analyzed by three dimensional molecular dynamics.	The coefficient of friction (cutting resistance) on nanoscale decreased with increased tool angle as predicted by macroscale theory. Higher cutting velocity resulted in larger chip volume in front of tool
4	Klocke et al. 1999 [77]:	The method to test, evaluate and influence the properties of tool coatings were presented	CVD diamond coatings were very successful in machining non ferrous materials.
5	Romero et al. 2014 [78]	Studied the dynamics interaction among the tool, the experimental setup and sheet blank during the forming process. It is the use of single point forming manufacturing process.	The manufacturing machine parameters used to process metallic sheet blanks resonance forming tool behaviour did not appear.
6	Mansori et al. 2007 [79]	Examined the application of external electromotive	With magnetic field the final shape of chip was

		force sources (EMF) e.g. magnetic field as an integral part of nearing no wear conditions when cutting dry.	characterized as steady state type (continuous chips) and remained constant irrespective of cutting speed.
7	Gao et al. 2015 [80]	Dedicated to draw the stability lobe diagram for vibration assisted machining (VAM) and compared it to conventional machining (CM) finally cutting experiments about surface roughness was carried out to verify theoretical conclusion.	The roughness figure for CM was 1.79 μm while VAM is only 0.3 μm VAM increased cutting stability.
8	Coscon et al. 2015 [81]	The orthogonal turning forces in three directions like x, and z, torque and power consumption through machining path of non-axisymmetric parts were predicted by a newly developed mechanistic model	Results from simulation were valid with a real machining tests with a good agreement
9	Sagapuram et al. 2015 [82]	The experiments were performed for plain –strain cutting on linear planning, low speed HSS tool and rotary strain on high speed radial plunge turning with carbide tool.	The flow was unsteady and at variance with usual models of cutting. The work surface was related with starting the instabilities.
10	Wang et al. 2007 [83]	The collection of research	It was found that new

		work regarding the better performance of machining and selection of optimum methodology.	method was proposed for the selection of tool.
11	Rao et al. 2014 [84]	Tool life, power, cutting force surface roughness and material removal rate were analyzed by varying one factor and keeping other two constants. The machining parameters were rotated on by one for turning aluminium as workpiece and tungsten carbide as cutting tool.	It has been found that tool life was declining as cutting force, material removable and cutting speed were incrementing, optimum process parameters.
12	Agapiou et al. 2000 [85]	The tools were analyzed in terms of (i) significance of machining parameters on tool life. (ii) tool stiffness and damping, tool holder interface	Productivity and quality of machining operations enhanced.
13	Elamadagli et al. 2003 [86]	Metallographic sections were taken from commercially pure copper samples and were examined to determine the displacement gradients and local gradients in the material a head of cutting tool tip.	The microstructure corresponded to a Dynamic equilibrium state in which stress, strain, temperature and profiles remained constant in time.
14	Beauchamp et al. 1996 [87]	The experiments were performed on lathe machine for investigating	It was found that small tool length gave lower surface roughness as compared to

		the effects of cutting parameters on the surface roughness during boring operation.	long tool length.
15	Venuvinod et al. 1995 [88]	Focused on stress distribution for single edge oblique cutting. It was assumed that progressive deformation of work material into chip material occurred within the effective plane.	The new model demonstrated a rigorous and direct approach to the modelling of stress distributions on the lower boundary of shear zone in oblique cutting.
16	Grzesik et al. 2009 [89]	The experiments were performed on lathe machine with pearlitic ferritic nodular iron as workpiece. The three different types of cutting tools were used. Thermal imaging camera was fixed at a constant distance near the cutting tool.	It was found that higher temperature generated at the interface of tool and workpiece was tolerable by silicon nitride with negligible damage as compared to uncoated cutting insert.
17	Shoba et al. 2015 [90]	The experiments were performed on a lathe machine with aluminium as matrix material and silicon carbide with rice husk as reinforcing materials with different compositions.	It has been found that cutting force was higher for an unreinforced alloy.
18	Kilic et al. 2016 [91]	Presented unified modelling for mechanics and dynamics of metal	The dynamic model predicted the vibrations, surface location errors

		cutting processes. The distribution of chip thickness, along cutting edges of tools were evaluated using generalized geometric and kinematic model of operations.	and chatter stability for any operation with arbitrary operations
19	Wegener et al. 2016[92]	Explained the changing trends of cutting processes of Materials according to the properties of materials	Research results and recent development in machine tools showed how to combine the requirement from ecology, economy and quality. Machine tool, tool and process were the building blocks of success in cutting
20	Tanaka et al. 2016 [93]	Turning and orthogonal cutting experiments on Inconel 718 were conducted to evaluate tool life and identify wear mechanisms at a wide range of cutting speed PCBN (Polycrystalline cubic boron nitride) with high CBN (Cubic Baron Nitride) and with low CBN content below 60%.	PCBN tool with a high CBN content (PCBN-A) showed the same tendency as observed in conventional studies. (PCBN-B) low context of CBN showed better wear resistance at cutting speed over 300m/min
21	Sparham et al. 2016 [94]	The cutting process in CNC lathe machine generated cutting force,	It has been found that linear guideways experienced lower friction

		longitudinal force and radial force. The effect of different forces was transferred towards guideways which were analyzed.	force as compared to Z-direction.
22	Alagan et al. 2016 [95]	The experiments were performed on CNC lathe machine with cast alloy 718 and textured cutting insert with one nozzle spray at rake face and other on flank face.	It has been found that flank wear for Nusselt channel insert was lower as compared with Nusselt insert.
23	Huang et al. 2016 [96]	Residual stress on the surface layer of workpiece has significant effects on service life of parts, including fatigue strength and corrosion resistance, stress of a point during cutting was time dependent. Proposed a criterion to determine initial stress state in stress relaxation process.	The computed result showed that residual stress component in cutting speed direction was higher than that in axial direction.
24	Su et al. 2016 [97]	The experiments were performed on lathe machine with compacted graphite iron and TiCN – Al ₂ O ₃ coated carbide cutting insert. The high pressure jet was supplied at rake and flank face	It was found that during dry turning chipping and adhesive wear on the faces of cutting insert. Abrasion was on the face of cutting tool during high pressure cutting fluid.

		individually.	
25	Katuku et al. 2012 [98]	(cBN-TiC) sintered cubic boron nitride was placed in between autempered ductile iron (ADI) on both the sides like ADI-(cBN-TiC)-ADI and in other sample cBN-Tic- was placed between Si silicon wafers like Si-(cBN-TiC) - Si static interaction experiments were run in the temperature range 1000-1100°C under argon for a holding time of 60 minutes and a pressure of 200MPa.	The result showed that interaction of cBN grains with ADI was relatively slight. cBN-Tic cutting tools and their reprecipitation in as fe and Sic1- X resulted in reduced wear resistance of cBN cutting tools.
26	Goel et al. 2016 [99]	Molecular dynamics was used to study the mechanisms of plasticity during cutting of mono-crystalline and poly crystalline silicon. (i) cutting a single crystal silicon work piece with a single crystal diamond tool (ii) cutting a polysilicon workpiece with a single crystal diamond tool(iii) cutting a single crystal silicon workpiece with a polycrystalline diamond tool	MD simulation results should that a unique phenomenon of brittle cracking typically inclined angle of 45°-55° to the cut surface

27	Schneider et al. 2016 [100]	The formation of chips during micro-machining of cp-titanium with ultrafine cemented carbide cutting tool was analyzed.	It was found that rake angle influenced the chips and surface roughness. On incrementing rake angle plastic deformation and surface roughness declined respectively.
28	Mauclair 2015[101]	Investigated the effect of intensity gradient on the spots line for micro-cutting on stainless steel.	Successfully applied an efficient technique to increase the cutting speed and energy efficiency of ultrafast laser micro-cutting by generating a line of N laser spots in the focal plane of lens.
29	Sonam et al. 2014 [102]	The influence of electricity of direct control mode was investigated for tool wear and surface roughness of workpiece during dry and wet with cutting fluid were analyzed.	It was found that flank wear was lower during positive polarity as compared to negative polarity.
30	Abouridouance et al. 2015 [103]	The friction mechanism was investigated by developing a new model. Infra red thermal camera and a high speed image camera.	The newly developed model was validated by finite element simulation.
31	Piska et al. 2015 [104]	The coefficient of friction, and cutting performance of PVD coated HSS taps were analyzed during machining of carbon steel	It was found that surface roughness was below $1.6\mu\text{m}$ and 1000 threads was tool life for forming tool.

		C45 and forming of 42CrMo4V.	
32	Chengzhang et al. 2015 [105]	The two types of Johnson-Cook Model during turning of titanium alloy were developed for chip study, plastic deformation, forces and temperature.	It was found that for lower hardening parameters the values of chip thickness was in acceptable limit fo ALE and CEL.
33	Baksa et al. 2014[106]	The experiments were performed by using four different types of end mills of similar diameter but different edge radius .	It has been found that elaton too with edge radius of 3-5µm performed better as compared with other tools.
34	Pilkington et al. 2013 [107]	HSS Drills and WC-Co end mills were coated by AlCrN and AlCr _x N _{1-x} with arc and gas respectively.	It was found that hardness of coating prevented the wear of end mills and drilled a large number of blind holes.
35	Venkateson et al. 2014 [108]	The experiments were performed on lathe machine with different power of laser beam focused at 60° angle from workpiece.	It was found that for laser power of 1250w cutting force was declined by 60%as compared with conventional turning.
36	Shihab et al. 2014 [109]	The experiments were performed with multilayered cutting insert with three levels of variation in machining parameters	It has been found that predicted values were close to experimental values
37	Kannan et al. 2006 [110]	Presented an analytical tool flank wear rate model	The developed model was validated with the

		for orthogonal cutting process. In this approach wear volume loss was formulated based on the process parameters and reinforcement properties	orthogonal cutting tests conducted on 6061 aluminium MMC (Metal Matrix Composites) reinforced with Al ₂ O ₃ (alumina) particulates.
38	Dhananchezian et al. 2011 [111]	The experiments were performed on lathe machine in wet condition and with some modifications in tool holder for the close supply of LN ₂ .	It has been found that tool wear and surface roughness wear was lower in LN ₂ supply as compared with wet condition.
39	Jiang 2014 [112]	Presented the analysis of 3 dimensional nano structured coating on serrations created on carbide cutting insert during turning of 4340 hardened steel. The coating design inspired by sea urchin and shark teeth architecture delivered serrated cutting edges and self-sharpening. The coating design inspired by sea urchin and shark teeth architecture delivered serrated cutting edges and self-sharpening.	3-D coating coated inserts demonstrated a superior tool life and delivered much smoother workpiece surface finish than all other conventional cutting tools.
40	Soussia et al. 2013 [113]	Investigations were performed the effect of coating type on the	CVD MNL[Monolayer diamond coated] cutting tool had best resistance to

		properties of both fiber and matrix phases when cutting glass/epoxy composites. Cutting experiments were performed on three different specimens with glass fibers oriented at 0°,45° and 90° in accordance with respect to cutting direction	wear in cutting glass/epoxy with 0° fiber orientations but it almost failed in 45° and 90° orientations CVD MTL (CVD multilayers titanium carbonitride / ceramic / titanium nitride coated) tool gave better performance.
41	Lakic et al. 2013 [114]	The experiments were performed on lathe machine using conventional flooding and controlled supply of vegetable oil.	It was revealed that MQL was better than conventional lubrication
42	Kramer 1993 [115]	The various types of tool wear mechanisms were discussed with mathematical and experimental models	Experimental models and mathematical models developed had almost near values to each other.
43	Gupta et al. 2016 [116]:	The experiments were performed in dry, wet and cryogenic condition with direct supply of LN ₂ at the interface of tool and workpiece.	It was found that during cryogenic cooling with LN ₂ specific cutting force and surface roughness were lower than wet and dry conditions.
44	Mandal et al. 2016 [117]:	A newly developed zirconia toughened cutting inserts were used on performing experiments on lathe machine for	It was found that predictive values were very close to experimental values.

		analyzing surface roughness.	
45	Nagpal et al. 2016 [118]	The complete model was analyzed using finite element method based software ANSYS Different materials of workpiece were analyzed to the sensitivity of stress concentration factor	Composite material workpiece were found to have high strength to weight ratios, high strength, high stiffness, low density and long fatigue life.
46	Sundeepan et al. 2016 [119]	Mechanical and tribological characteristics of acrylonitrile- butadiene styrene matrix / titanium dioxide (TiO ₂) composites were investigated Tensile modulus, tensile strength, flexural modulus and hardness were evaluated	Tensile and flexural modulus increased with an increase in filler content while tensile and flexural strength increased upto 10% weight filler content. Normal load had the highest influence on friction and wear rate followed by filler content and sliding speed.
47	Bleicher et al. 2016 [120]	Cooling strategies (external, internal) and cutting fluid quality showed significant influence. An internal cooling of cutting insert allowed a reduction of built up edge by reducing temperature at rake face.	A combined internal and external cutting fluid supply of a tool insert with an internal flow channel significantly reduced the built up edge formation on rake face of cutting tool
48	Shokoohi et al. 2016 [121]	Presented the role of machining in manufacturing and the	Results showed that suitable nanofluids, optimum utilizing for

		importance of lubrication fluids during metal cutting. Nanofluids were utilized in machining operations.	cooling and lubrication purposes were beneficial in different machining operations.
--	--	--	---

2.6 Thermal effects on cutting tool and workpiece

Temperature rise is associated with heating effects. High temperature means high heating effects.

The excess heat generated in machining operation result in poor surface finish and sometimes changes in metallurgical properties so, temperature control is necessary.

Table 2.6 shows the work done by researchers in controlling and lowering down the high temperature generated between cutting tool and workpiece.

Table 2.6 Review regarding thermal effects at interface of cutting tool and workpiece.

Sno.	Author, year, reference no.,	Work done	Results/findings
1	Rech et al. 2004 [122]	Experimentally associated an inverse heat conduction method signified the beneficial effects of coatings upon the interactions in the tool - chip interface	TiN and (Ti, Al) + MoS ₂ coatings gave better tribological properties as compared to (Ti, Al) N. These coatings allowed an important decreased in the heat flux transmitted in to the tool even if decreased in feed force was minimal.
2	Komanduri et al. 2001 [123]	An analytical model was formed for understanding the heat distribution and elevating temperature in moving and stationary tool	It was found that model developed remained faster, easier and more accurate than other models previously used.

		by considering friction heat source at chip-tool interface stationary tool	
3	Moufki et al. 2004 [124]	An analytical approach was used to model oblique cutting process. The chip formation was supposed to occur mainly by shear within a thin primary zone	The flow within the band was supposed to be adiabatic and strain sensitivity was weak
4	Rajifar 2015 [125].	Advanced coolants such as nanofluids as PCM slurries (Phase change materials) are realized and reported as effective substitutions for conventional coolants	Results showed that using the proposed configuration, the cooling performance of the system was enhanced.
5	Cotterell et al. 2013 [126]	Models were developed for the measurement of strain and temperature by using Ernst-Merchant theory and 2 D steady state heat conduction problems.	It was found that the values of temperature measured through infra red radiation thermometer and predicted by the model were in very close to each other.
6	Chiffre et al. 2000 [127]	The performance of cutting fluids were investigated in different types of metal cutting process considering availability, economical, handling work done by previous researchers,	It was found that tool life tests were with limited repeatability ($\sigma = 50\%$) and resolution (σ/ρ) ranging from ($\sigma/\rho = 0.25-0.75$) with costs ranging 1000 to 2000 pounds.
7	Gosai et al. 2016 [128]	The temperature of cutting tool was investigated by a thermocouple during	It has been found that mathematical model was found to be valid by

		turning of EN 36 workpiece by a coated carbide cutting insert. carbide	experimental tests with error in temperature less than 10%. optimized values of cutting parameters were 98.9% which was highly acceptable.
8	Savan et al. 2005 [129]	The thin films of MoS ₂ and Ti were deposited by using radio frequency magnetron co-sputtering and further tested for tribological property on pin –on-disc tribometer.	MOSX-Ti composite showed good lubrication properties up to 350°C and not to deteriorate with storage over 12 months period.
9	Augspurger et al. 2016 [130]	Experimentally investigated the thermal boundary conditions at characteristic regions of metal cutting i.e. shear zone, contact zone of chip and tool, the clearance face workpiece surface by infrared thermal images.	Temperature measurements at considered areas yielded significant errors due to constraints imposed by experimental set up a comprehensive analysis of the boundary conditions was conducted by means of numeric calculations
10	Courbon et al. 2013 [131]	The experiments were performed for orthogonal cutting of steel during dry machining condition with TiN coated carbide cutting insert. The interaction between tool and chip was analysed by SEM-EDS	Results from simulations were compared to experimental data in terms of average machining force, heat flux, cutting velocity and tool chip contact length. It was numerically shown

			that TCR (Thermal contact Resistance) was not significantly affecting macroscopic outputs when using ALE (Arbitrary Lagrangian Eulerian) numerical simulations but directly governing heat transfers.
11	Makaddem et al. 2016 [132]	Related the tribological reality of TiAlN-based PVD coatings face to TiN based CVD, coating in cutting FRP(Fiber Reinforced polymers).	Abrasion dominated wear upon CVD coating regardless the types of fiber. The location of TiAlN within PVD coating was of great role in controlling wear.
12	Nanty et al. 2009 [133]	The high pressure cooling jets were directed into tool chip interface to sufficiently penetrate and change thermal, frictional and mechanical conditions in cutting zone.	The results showed significant improvement in tool life. It was about 250% over conventional wet environment.
13	Jawhir et al. 2016 [134]	The applications of cryogenic supply are related to manufacturing processes. An assessment is done of the collected research work in cryogenic field to other available processes.	It has been found that role of cryogenic is emerging at faster rate. The improvement in tribological, machining, manufacturing, thermal properties have been reported by different researchers which is essential for complete

			sustainable process.
14	Madanchi et al. 2015 [135].	Machining processes use different cutting fluid strategies flood, dry and minimum quantity lubrication (MQL).	The application(1) without any fluid i.e. dry machining used high electricity power in running as compared to others.

2.7 Cutting Fluids/High Pressure Fluids for metal cutting

Cutting fluids are used in machining processes for providing coolant and lubrication. Generally, cutting fluids are supplied by the in housed pump fitted in machine

The speed of supply of cutting supply is almost fixed. The cutting fluid moves in a closed cycle and comes back to the pump after filtration.

Table 2.7 depicts the workdone by researchers during use of cutting fluids and high pressure fluids

Table 2.7 Review regarding cutting/high pressure fluids at interface of cutting tool and workpiece

Sno.	Author, year, reference no.,	Work done	Results/findings
1	Naves et al. 2013 [136]	The experiments were performed on lathe machine using AISI 316 as workpiece and coated carbide cutting insert with supply of high pressure cutting fluid at different levels of concentration and pressure.	It was found that tool wear and tool chip length were declined on comparing with other concentration of cutting fluid. The amount of wear was lowest at higher concentration of cutting fluid and pressure.
2	Mosleh et al. 2017 [137]	The experiments were performed on four-ball tester for checking and	It has been found that wear scar length was shorter in prepared fluid

		analyzing the wear properties of balls under prepared fluid with MoS ₂ at different concentrations varied from 2-4% and .5-1% for diamond.	of MoS ₂ for all concentration as compared with diamond particles.
3	Paul et al. 2016 [138]	The experiments were performed in different machining conditions like dry, wet with conventional cutting fluid and minimum quantity lubrication.	It was found the tool wear and surface roughness was lower in minimum quantity lubrication as compared with dry and wet with conventional with cutting fluid.
4	Shokrani et al. 2012 [139]	The processes involved in machining of hard materials with different types of cooling techniques used by researchers have been discussed.	It was found that cooling technique was dependent on type of quality of machining, machining parameters and ease in availability.
5	Jayal et al. 2009 [140]	The experiments were performed in different machining conditions. The nozzle was kept at overhead position of cutting chip during machining.	It was found that tool life was lower in dry condition as compared with other machining conditions
6	Verochaka et al. 2014 [141]	Investigated the effect of Filtered cathodic vacuum arc deposition (FCV AD) coatings on carbide inserts. Cutting parameters were selected in accordance to	The results showed the cutting tool life of inserts in more than two times as compared to conventional coated carbide inserts.

		industrial applications.	
7	Bork et al. 2014 [142]	The experiments were performed by using new product jatropha vegetable base soluble cutting oil in relation to the canola oil (vegetable), synthetic (jatropha ester) and semi-synthetic (mineral) traditionally used in machining aluminium alloy.	Jatropha cutting oil presented best result in relation to lubrication mean roughness index, life span of cutting tool increased by 30% as comparative to other oils.
8	Sokovic et al. 2001[143]	The properties of available cutting fluid were discussed and a newly cutting fluid was developed.	It has been found that newly developed cutting fluid gave better results of machining than available cutting fluids. Dry cutting and MQL could be encouraged for ecological balance.
9	Hermoso et al. 2014 [144]	The influence of additives on viscosity and different concentrations were analyzed for change in rheological properties at for oil base drilling fluids.	It was found that organoclay and concentration highly effect the viscous flow of oil..
10	Khan et al. 2009 [145]	The experiments were performed on lathe machine under dry, wet and minimum quantity lubrication for AISI 9310 as steel workpiece.	It has been found that minimum quantity lubrication gave lower machining properties like tool wear, surface roughness, cutting temperature as compared

			to other machining conditions with ecofriendly behavior.
11	Lv et al. 2016[146]	The influence of oil mixed with LN ₂ in a mixing chamber and directly supplied at the interface of cutting tool and workpiece was compared with traditional cutting fluid for milling operation.	It has been found that cooling strategy with LN ₂ gave lower tool wear and surface roughness.
12	Baradie 1995 [147]	Studied the issues of clean machining technology concerned with recycling and disposal of cutting fluids.	Many pollution problems have been found to be solved on treating of cutting fluids with solvents that my reduced the toxic and other unwanted chemical effects as negligible .Then disposal problem was not an issue and became pollution free.
13	Lotierzo et al. 2016 [148]	Investigated the physical properties, wetting, lubricating and corrosion behavior, of primary / tertiary amines in oil-in-water emulsions (as metal working fluids towards brass) MWFs.	Experimental result showed that number of carbon atoms in amines played a pivotal role in reducing brass corrosion
14	Rabic et al. 2002 [149]	The process of selection metal working fluids on the basis tribological	ISO-L-MAG (Synthetic concentrate) gave longer life as compared to ISO-

		property for milling machines were investigated	L-MAE (Micro emulsion)
15	Courbon et al. 2011 [150]	The influence of high pressure jet assisted cooling during turning operation was investigated with numerical model considering mechanical load and thermal effects.	The numerical model was validated by FEM simulation using ALE approach.
16	Xavior et al. 2009 [151]	The effects of different cooling methods were analyzed. The cooling was done individually by coconut oil, soluble oil and straight cutting oil with carbide tool.	It has been found that tool wear and surface roughness were lower with coconut oil as compared with other cooling methods.

2.8 Effects of Nano particles in cutting fluids

Nanoparticles are very fine particles of magnitude of 10^{-9} m. These particles change various parameters during machining applications.

In accordance with the type of nanoparticles can give lubrication effect, cooling effects and abrasive effects.

Nanoparticles are water soluble and oil soluble. Generally, oil soluble nanoparticles cannot become soluble in water or vice versa. The nano-cutting fluids are supplied in very controlled way at the surface of tool.

Table 2.8 shows the research work done by using nanoparticles in cutting fluids.

Table 2.8 Review regarding nanoparticles in cutting fluids at the interface of cutting tool and workpiece

Sno.	Author, year, reference no.,	Work done	Results/findings
1	Chan et al. 2013 [152]	The conventional cutting fluid was used for preparing for four samples of coolants. One sample was made with 5% cutting oil and 95% water (w/w), sample two was made with 2.5% cutting oil and 97.5 water (w/w). Sample three was made by treating composition by nanodropltes of 5% cutting oil, sample four was made by treating 2.5% nanodroplets and sample five was pure water. Each sample was characterized by contact angle and experiment was performed on lathe machine.	In cutting experiments NDCF had high contact angles and gave better lubrication effect. The surface roughness was lower for sample of cutting fluid with 5%cutting oil remaining water with nanodroplets.
2	Zong et al. 2008[153]:	An ultraprecision lathe machine was made with running accuracy of 550nm and the range of moving guide way was 100nm for grooving of mooncrystalline silicon (111) as workpiece.	It has been found that the machined silicon surface depicted silicon carbide and diamond like carbon structure.
3	Yin et al. 2003 [154]	The concentration of	It was found that elastic

		cobalt was varied from 0, 3%,5% and 8% for preparing a composite with alumina varied 59%, 56%, 54% and 51%.TiC remained constant on the basis of particle size. The samples were tested for mechanical properties..	modulus was declined with increase in temperature.
4	Kumar et al. 2016 [155]	A nano fluid was developed by using multiwalled nanocarbon tubes in sunflower oil as base fluid by 1% (w/w). The experiments were performed by using synthetic oil, sunflower oil and developed nanofluid on tribometer and grinding.	Tribological properties got improved Wear rate of wheel was significantly minimized. The surface finish of workpiece was improved by using nanofluid as compared of soluble oil cutting fluid.
5	Zhang et al. 2015 [156]	First nano-scale surface textured tools were then deposited with Ti55 Al45N hard coating, the second one Ti55Al45N hard coatings were deposited on carbide tools, nano-scale surface texturing was then produced on coated tool surface.	The firstly coated and then nano-scale textured tools (CNT) were more effective in reducing cutting forces, cutting temperature co-efficient of friction and tool wear compared with firstly nano-scale textured and then coated tools (NCT).
6	Amrita et al. 2014 [132]	Four samples of	Functionalised nano

		nanofluids were prepared with nano graphite, functionalized nano graphite, nano boric acid and nano molybdenum sulphide with emulsion 0.3%(w/w). Emulsion was made from 20 parts of water and 1 part of conventional cutting oil. The experiments were performed on lathe machine by using different types of nanofluids at constant machining parameters.	graphide (FNG) showed good stability in emulsifier oil based cutting fluids than nano graphide (NG). With respect to surface roughness, nano MOS ₂ (Nano molybdenum disulphide). Tool wear, surface roughness and cutting forces were lower during turning with nano MoS ₂ as compared with other nanofluids
7	Sharma et al. 2016 [158]	The samples of nano fluids were prepared by using Al ₂ O ₃ (0%, 0.25%, 0.5% 1.0%, 1.5%, 2% and 3%) by volume with oil-water emulsion. The experiments were performed on lathe machine at constant machining parameters during dry, wet and minimum quantity lubrication	It has been found that Al ₂ O ₃ with 1% concentration had better thermal conductivity and viscosity (considering pressure drop relation with viscosity). The Surface roughness, tool wear were cutting force declined as compared with other machining conditions.
8	Sharma et al. 2016 [159]	A nano fluid was developed by mixing TiO ₂ nanoparticle conventional cutting oil with water emulsion in different	It has been found that performance of TiO ₂ nanofluid in terms of surface roughness, tool wear, cutting force was

		concentrations. 1% by volume of TiO ₂ was selected Its machining performance was examined in turning workpiece of AISI 1405 steel using MQL	found better compared to dry machining wet/MQL machining with conventional cutting fluid.
9	Padmini et al. 2016 [160]	The experiments were performed on lathe machine with dry, and samples of nano fluids prepared by blending nano MoS ₂ with (0%, 0.25%, 0.5%, 0.75% and 1%) in conventional coconut oil, sesame oil and canola oil at constant machining parameters.	It was found that composition with coconut oil with 0.5% nano MoS ₂ particles gave better results as compared other compositions for machining characteristics
10	Uysal et al. 2015 [161]	The experiments were performed on milling machine in dry, conventional cutting oil and nano fluid developed by using 1% MoS ₂ (w/w) with vegetable oil emulsion with water.	It has been found that experimental result values showed that nano fluid decreased the tool wear and surface roughness. As compared to other machining c
11	Wu et al. 2015 [162]	AlCrN (aluminum chromium nitride) coating & AlCrSiN Multilayer and nano composite coatings were designed and deposited on the surface of	The service life of AlCrSiN nano composite coating tool was increased 40% longer than AlCrN coated tool.

		HSS cutters.	
12	Dobrzanski et al. 2005 [163]	The harden ability of cutting tool was increased by depositing many layers of nano composites on high speed steel cutting tool.	It has been found that silicon imparted higher hardness and more grain refinement in the coating. This incremented the cutting ability .

2.9 Nano Particles in lubricants

Nanoparticles mixed with lubricants then lubricity of lubricants get increase many times. The hybrid use of more than one nanoparticles have increased the viscosity and film thickness.

The higher temperature has negligible effect on viscosity of nanolubricant as compared to base fluid (without nanoparticles).

Table 2.9 shows the research work done by developing nanolubricants.

Table 2.9 Review regarding nanoparticles in lubricants

Sno.	Author, year, reference no.	Work done	Results/findings
1	Esfe et al. 2017 [164]	The viscosity was investigated of nano lubricants prepared by mixing multi walled carbon tubes (90%) and zinc oxide (10%) by volume in engine oil of grade SAE 40 in different concentrations from (0-1%).	It has been found that nano lubricants followed Newtons law of viscosity. The maximum ride in viscosity of nanolubricant was 33%.
2	Ali et al. 2016 [165]	The experiments were performed on prepared nano lubricants by mixing	It has been found that 0.25% concentration gave better results. Coefficient

		nano alumina and titanium in different compositions for analyzing the tribological properties.	of friction and wear rate were declined
3	Asadi et al. 2016 [166]:	The samples were prepared with nano magnesium oxide and multi walled carbon nano tube in different compositions with lubricating oil SAE 50 and analysed for change in viscosity at a particular range of temperature.	It has been found that dynamic viscosity declined with increment in temperature. At room temperature the dynamic viscosity was lowest for all samples of nanolubricants.
4	Ali et al. 2016 [167]	Investigated nano-additive for reducing frictional power automotive engine parts and gave a cleaner environment.	It has been found that of composition of 0.05wt% of nano alumina and titanium oxide gave better results in terms of frictional losses and wear rate as compared to other compositions of lubricants.
5	Esfe et al. 2017 [168]	The samples of nanolubricants were prepared with different composition of Nanoparticles SiO_2 in lubricating oil SAE 40 and investigated for change in rheological properties.	It was found that all samples of nanolubricants followed Newtons law of viscosity.
6	Maheswaran et al. 2016 [169]	Presented the study of the effect of dispersion of	The result showed that prepared nano fluids were

		0.25, 0.50 and 0.75 wt% of nano garnet particles in commercially available SN500 lubricant oil in its viscous behaviour.	highly stable upto 500°C and viscous behavior was found to enhance according to the nano particles concentrations.
7	Callisti et al. 2014 [170]	A self lubricant W-S-C coating with different Ni-Ti-(CU) interlayers was fabricated by magnetron sputtering.	The resistance to adhesion damage W-S-C coating was improved by using Ni-Ti (CU) interlayers.
8	Afrand et al. 2016 [171]	A new correlation was proposed to predict the relative viscosity of MWCNTs SiO ₂ / AE40 Nano-lubricant using experimental data. Forty-eight experimental data were used to feed the model.	The correlation outputs showed that there was a deviation margin of 4% The result obtained from optimal artificial neural network presented a deviation margin of 1.5%
9	Kumar et al. 2015 [172]	During machining Al ₂ O ₃ nano particles were sprayed over it. A thin layer over the surface was formed that changed the properties like surface roughness and hardness. The workpiece was of mild steel.	Nano particles Al ₂ O ₃ on mild steel changed surface roughness at constant speed of 500rpm.
10	Cho et al. 2013[173]	Investigated the possible lubricating effects of aqueous dispersions of hexagonal boron nitride (h-BN) nano sheets.	Results indicated that even small amounts of h-BN nano-sheets enhanced wear resistance and reduced friction co

			efficient. After 30 days of synthesis, the tribological properties of dispersions were not degraded with time.
11	Shahnazar et al. 2016 [174]	Nanotechnology offered the opportunity to improve the performance of lubricant oil via the utilization of nano additives.	Nano particles delivered excellent lubrication properties.
12	Hu et al. 2015.[175]	The samples were prepared by using nanoparticle of copper in the base fluid of normal octane. Molecular dynamic and simulations models were formed for understanding mechanisms.	It was found that nanolubricant could bear higher load without film breakage which was supported by both the models.
13	Liv et al. 2017 [176]	Novel double hollow-sphere MoS ₂ (DHSM) nanoparticles with an average diameter of 90nm were synthesized on sericite mic (SM)	The DHSM/SM composited was used an additive in polyalphaolefin oil friction and wear were decreased by 22.4% and 63.5% respectively.
14	Tao et al. 2014 [177]	The samples with different composition of treated and untreated nanoparticles AlN were mixed with lubricating oil and characterisation was	It was found that nano particles improved the modified effect and enhanced dispersion stability in base oil. The composition of 0.3%

		performed.	concentration of nanoparticles performed better as compared to remaining samples.
15	Zheng et al. 2017 [178]	Carbon nanohoops firstly fabricated by CH ₄ plasma treatment served as toughening and lubricant agents in TiN (Titanium nitride) porous films.	TiN porous films with carbon nanohoops successfully possess flexible, hard, lubricant and antiwear effects.
16	Yang et al. 2016 [179]	Oleic acid surface - modified Lanthanum trifluoride graphene oxide (OA-LaF ₃ -GO) nanohybrids were successfully prepared by surface modification technology.	Tribological results showed that OA-LaF ₃ GO nanohybrids had excellent friction reduction and anti wear ability at the loading of 0.5wt/ of OA-LaF ₃ - GO nano hybrids compared to liquid paraffin alone.
17	Xiang et al. 2014 [180]	The samples were prepared with magnetic nano flakes with different composition with base lubricating oil and tested on four ball tester for tribological properties.	It was found that the composition of 1.5% magnetic ferric oxide performed better in delivery of results. The coefficient of friction and wear scar diameter were declined by 18.06% and 11.20% respectively.
18	Zovari et al. 2014 [181]	Investigated the friction and wear behavior of electrostatically sprayed polyester powder coatings on an aluminium substrate	The additions of graphite or hBN were effective in enhancing the wear life of polyester powder coatings.

		and focused the response of thermosetting coatings to micromechanical deformation under scratch test loading.	
19	Tang et al. 2014 [182]	The properties of lubricants were improved by adding some additives which reduced friction of lubricants and wear rate of contacting surfaces. The modifications made by researchers have been discussed.	It has been found that organomolybdenum compounds reduced friction and wear rate to higher extent as compared to other available compounds.

2.10 Cryogenic Cooling

Cryogenic cooling means cooling the surface below 0°C to - 196°C. At lower temperature the metallurgical properties of materials get changed e.g. porous materials become hard.

The cooling process is done by liquid nitrogen, solid carbondioxide or other refrigerated non toxic gas and chilled air.

On cryogenically treating the cutting inserts in cryoprocessor and reheating to room temperature bring change in hardenability which reduces the wear rate.

The direct supply of LN₂ is used at the interface of workpiece and cutting insert reduces the temperature many times. The coefficient of friction, cutting forces, and tool wear declined.

Table 2.10 depicts the work done by using cryogenic cooling by LN₂, solid CO₂, chilled air etc. during machining

Table 2.10 Review regarding cryogenic cooling

Sno.	Author, year, reference no.,	Work done	Results/findings
1	Mputz et al. 2016 [183]	Investigated approach to	Liquid Nitrogen used to

		enhance machinability with cryogenic cooling during cutting elastomer components.	cool down elastomers before machining. The surface quality was improved.
2	Birmingham et al. 2011 [184]	Investigated the effectiveness of cryogenic coolant during turning of Ti-6Al-4V at constant speed and material removal rate (125m/min, 48.5cm ³ /min) with different combinations of feed rate and depth of cut.	Cryogenic coolant was effective in extending tool life compared to dry cutting for all machining parameters.
3	Huang et al. 2014 [185]	Experimental studied the effect of cryogenic cooling on milling stability using a dedicated cryogenic cooling system for applying liquid nitrogen (LN ₂) jet to cutting zone.	Cryogenic cooling was enhanced the stability limits in end milling by 50-100%
4	Yuvaraj et al. 2016 [186]	Cutting aluminium alloy with abrasive water jet and cryogenic assisted abrasive water jet: A comparative study of the surface integrity approach.	CAAW Cutting process enhanced the functional performance of cut surface and uniform surface roughness pattern.
5	Schoop et al. 2013[187]	Investigate the influence of cryogenic pre-cooling time and depth of cut on the attainable surface morphology of porous tungsten.	Result showed that increased pre-cooling significantly altered the deformation mechanism during machining.
6	Aggarwal et al. 2008 [188]	Optimized multiple	Models developed were

		characteristics (tool life, cutting force, surface roughness and power consumption) in CNC turning of AISI-20 tool steel using nitrogen as coolant.	adequate in explaining the effect of independent parameters on responses.
7	Hong et al. 2001[189]	Introduced an innovative and economical dispensing method that directed LN ₂ through microjets to the flank, rake or both near the cutting edge in the turning of Ti6Al-4V alloy.	It was found that application of LN ₂ was better in lowering down cutting temperature as compared to other emulsion type coolants.
8	Aslantas et al. 2016 [190]	Presented a hybrid system for cooling and lubrication in micro-milling of Ti6Al4V alloy. Hybrid system was based on mixing oil with chilled air.	Result showed that hybrid system gave minimum tool wear and burr size.
9	Fredj et al. 2006 [191]	Presented evaluation of ground surface quality improvements of the austenitic stainless steel AISI 304 resulting from the application of cryogenic cooling.	Due to cryogenic cooling surface roughness reduced by 40%.
10	Chiffre et al. 2007 [192]	Investigated efficiency of cryogenic CO ₂ and compared a commercial water based cutting fluid in terms of tool life, surface finish, chips	Results showed that cryogenic CO ₂ was an alternative as compared to water based cutting fluid.

		disposal etc.	
11	Wu et al. 2017 [193]	Presented the GNP _s /Al ₂ O ₃ (Graphene nano platelets reinforced alumina) fabricated by colloidal process. The optimum content of GNP _s in GNP _s /Al ₂ O ₃ composite was 1.0 vol%.	Presented the GNP _s /Al ₂ O ₃ (Graphene nano platelets reinforced alumina) fabricated by colloidal process. The optimum content of GNP _s in GNP _s /Al ₂ O ₃ composite was 1.0 vol%.
12	Kayank et al. 2013 [194]:	Examined the effects of cryogenic cooling on tool-wear rate and progressive tool-wear by comparing new findings from cryogenic machining with MQL and dry machining.	Cryogenic cooling was effective on reducing tool-wear rate at high cutting speeds and reducing flank wear and notch wear.
13	Chinchanikar et al. 2015 [195]	Presented a comprehensive literature review on machining of hardened steels using coated tools, studies related to hard turning, different cooling method and attempt so far to machining performance	It was found that optimum condition was lower feed and lower depth of cut with higher cutting speed for reducing machining force and surface roughness.
14	Rubio et al. 2015 [196]	Collected the review and analysed the cooling systems based on cold compressed air.	Results showed that cold compressed air is a real environmental friendly alternative to other conventional lubrication / cooling systems.
15	Sharma et al. 2009 [197]:	Presented an overview of major advances in techniques as minimum	Result showed that coconut oil as coolant was encouraging at lower

		quantity lubrication (MQL) / near dry machining (NDM), high pressure coolant (HPC) cryogenic cooling, compressed air cooling and used of solid lubricants coolants.	speeds. All types of cooling techniques gave good response with almost all tool material, particular with carbide (coated/uncoated) and PCBN.
16	Courbon et al. 2013 [198]	The experiments were performed with titanium alloy and inconel in dry and cryogenic conditions over fabricated tribometer having round pin sliding over the rotating workpiece (like Lathe machine)	Neither liquid nor gas nitrogen was able to decrease the co-efficient of friction and material transfer when Ti6Al4V and uncoated carbide pins were used, but a significant improvement was noted for Inconel 718 and TiN coated pins
17	Gao et al. 2016 [199]	Investigated the effects of deep cryogenic treatment on microstructure and properties of WC-Fe-Ni cemented carbides. The specimens were treated about -196° C for 2,1 2 and 24 hours.	The martensite transformation temperature for WC-Fe-Ni cemented carbide was approximately - 23.28°C. The hardness and TRS of WC-FE-Ni cemented carbides after deep cryogenic treatment was higher than untreated ones.
18	Tyshchenko et al. 2010 [200]	The tool steel X220 CrV Mo 13-14 (DIN 1.2380) containing (mass%) 2.2C, 13 Cr, 4V,1Mo and the	The results showed that, there was an increase in the density of dislocations, captured of

		binary alloy Fe ₂ O ₃ mass% C were studied using transmission electron microscopy. It was cryogenically cooled to - 50°C.	immobile carbon atoms by moving dislocations and strain induced partial dissolution of carbide phase.
19	Shokrani et al. 2016 [201]	Presented first comprehensive investigation on the effects of cryogenic cooling using liquid nitrogen on surface integrity of Ti-6Al-4V titanium alloy workpiece in milling operations	Results showed that 39% and 31% lower surface roughness when compared to dry and flood cooling methods respectively.
20	Schoop et al. 2016 [202]	Investigated cryogenic machining of porous tungsten was developed as alternative sustainable process to current industry practice of machining plastic infiltrated workpieces.	Results showed that by using modified polycrystalline diamond cutting tool, high speed cryogenic machining of porous tungsten by ductile shear was achieved. Cutting speed of 400m/min and low surface roughness Ra ~ 0.4 µm.
21	Podgornik et al. 2012 [203]:	Investigated the effect of deep cryogenic treatment parameters (time and temperature) in combination with plasma nitriding on the tribological performance of powder -metallurgy	Results showed that deep cryogenic treatment contributed to improved abrasive wear resistance plasma nitriding improved tribological properties of P/M high speed steel and reduced

		(P/M) high speed steel.	the effect of austenizing temperature
22	Li et al. 2013 [204]	Presented an internal frictional behaviour of cold work tool steel subjected to different heat treatment schedules to get insight to segregation of carbon and refinement of carbide particles due to deep cryogenic treatment.	Results showed that interstitial carbon atoms migrated and segregated near by dislocations of shrinking strain energy during deep cryogenic treatment.
23	Hong et al. 2001 [205]	Presented an environmentally safe approach of micro manipulation of cutting temperature in machining AISI /SAE 1008 low carbon steel.	Results showed that chip breaking was improved by cryogenic cooling the chip to below the embrittlement temperature -55°C the tool wear decreased and increased tool life..
24	Pusavec 2012 [206]	Experimentally studied on high performance machining of porous tungsten under cryogenic conditions	Cryogenic method was compared with traditional carbide tools PCD, CBN, ceramic etc. Results showed cryogenic was capable of producing unseamed surfaces. The surface finish was improved.
25	Leshovsek et al. 2012 [207]	Presented vacuum heat treatment deep cryogenic treatment and pulse plasma nitriding were efficient techniques to	Results showed that deep cryogenic treatment improved the micro structure of investigated P/M high speed steel.

		improve properties of tool and high speed steels.	
26	Dhokia et al. 2011 [208]	Presented the novel concept of cryogenic CNC machining of elastomers and development of a process control system for cryogenic CNC machining.	Results showed that the surface finish was very good as compared to other conventional methods.
27	Li et al. 2010 [209]	Studied deep cryogenic treatment (DCT) on microstructure of tool steel.	Results showed that retained austenite was present in a thin film between laths of martensite and stably existed even during prolonged soaking time in liquid nitrogen. Hardness and wear resistance on tool steel increased.

2.11 Research gaps

- The tribological properties of nano-cutting fluids have not been studied in details.
- The rheological properties of nano-cutting fluids have not been examined.
- The comparison of coefficient of friction and specific wear between different sliding conditions like dry, wet, nano-cutting fluids and cryogenic cooling with LN₂ have not been performed.
- The novel delivery system of cutting fluids and nano-cutting fluids have not been developed.
- The comparisons of machining characteristics in different machining conditions have not been done.

- The attention of most of the researchers are towards aerospace alloys, navigational alloys, composite alloys, etc. but very less interest is given to cold work steel which is commonly used in micro scale, small scale or medium scale industries in INDIA.
- .The simultaneous running of nano-cutting fluid with cryogenic LN₂ is not analyzed.
- The pre-mixing of nano-cutting fluids with cryogenic LN₂ is not performed and analyzed.

2.12 Objectives

1. To study the cutting parameters and analyze the tribological properties as well as surface roughness of materials of the workpiece / single point cutting tool (SPCT) in dry condition
2. To prepare a cutting fluid and to determine its rheological and tribological properties.
3. To investigate the tribological properties at the interface of the materials of workpiece and SPCT under cryogenic cooling and compare same with prepared cutting fluid.
4. To optimize cutting parameters of machining with single point cutting tool in turning process based on the investigations

Summary

- The research work done by previous researchers has been categorised.
- Every category has been discussed with research work.
- Research gaps have emerged from the literature review
- There is a need to discover nano-cutting fluid and delivery system which can supply in a controlled way

EXPERIMENTATION

This chapter consists of the description of tools and type of equipment used during the performance of experiments. The important specifications of instruments have been discussed like pin-on-disc tribometer, specially made delivery system, IR thermal imaging non-contact type camera, digital microbalance, single point cutting insert and tool holder, lathe machine, piezo electric lathe tool dynamometer, surface roughness tester and CNC vision inspection machine

3.1 Pin-on-disc tribometer

The pin-on-disc tribometer had stationary pin on rotating disc. The load was applied through weights placed on hanger connected to pin through a lever. The wear between pin and disc was measured by LVDT (Linear variable differential transducer).

The friction force was measured by sensors and depicted on the computer monitor. Enclosed chamber protected the materials (pin and disc) from atmospheric exposure and splashing of cutting fluids and gases which could spoil the surroundings. The disc could rotate from 200-2000 rpm.

The maximum range of frictional force measured was 200N with an accuracy of $0.1N \pm 2\%$ of the measured value in N.

Figure 3.1 (a) shows a schematic sketch of pin-on-disc during dry sliding condition. Hanger was used for carrying the desired weight. Load cell connected with a lever to pin for measuring the frictional force between pin and disc.

Figure 3.1 (b) shows a dewar container TA55 which was similar to well-insulated mirror polished thermoflask. The storage capacity was 51.5 litre of LN_2 . The height and outer diameter was 710mm and 460mm respectively.

The empty weight of the container was 15kg while filled with liquid nitrogen was 56.6 kg. An air compressor with a regulator was used to supply a controlled amount of air to dewar container. The compressor was single stage reciprocating air-cooled operated by single phase 220-230V half horse power electric motor. A safety relay valve was used to release extra air

pressure to atmosphere. The motor was fitted with auto shut-cut-off valve for closure of electric supply while exceeding the limit of air pressure inside the cylinder of air compressor.

The pressurised air with LN₂ was supplied at the interface of pin and disc in the closed chamber through well insulated pipe. The interaction between LN₂ and atmosphere became negligible. The cooling capacity of LN₂ might remain almost unchanged while moving from container to the designated position.

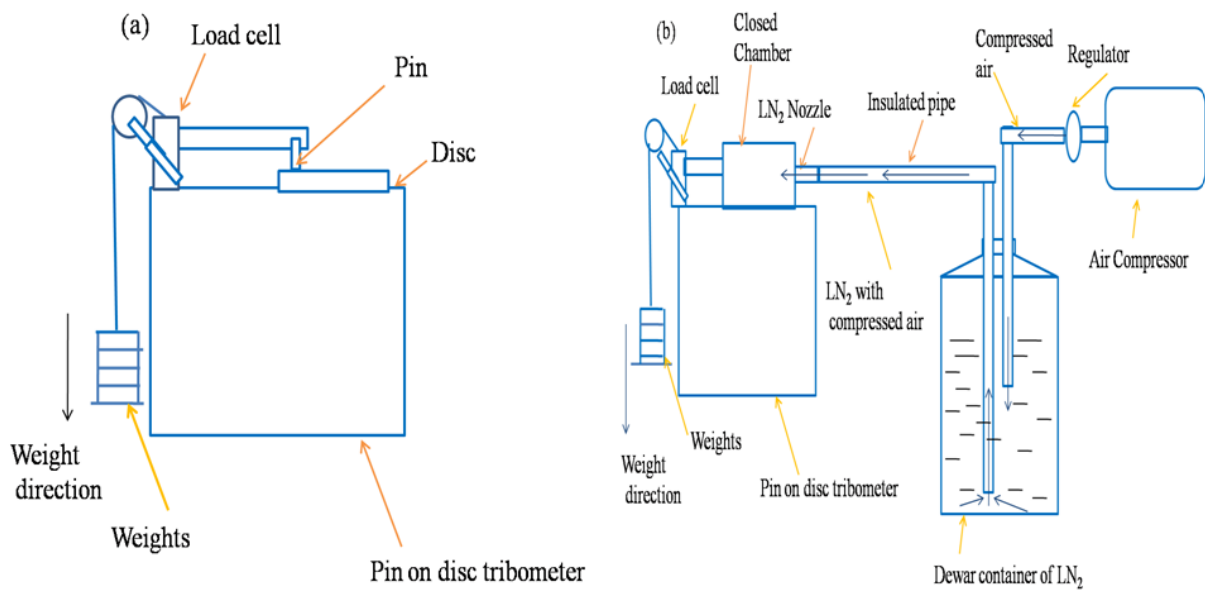


Figure 3.1 Schematic sketch of (a) Dry sliding (b) Cryogenic sliding with Liquid N₂

3.2 Specially made delivery system

Figure 3.2 shows a specially made delivery system was made to supply drop wise conventional cutting fluid and nano-cutting fluid at the interface of pin and disc. One litre container with a close lid fitted with 12V servo synchronous (direct current) motor with fluid pump.

The outlet diameter of transparent pipe was 5mm which was connected with nozzle. The delivery system could supply the fluid on the basis of viscosity at the rate of 100-500ml per hour.

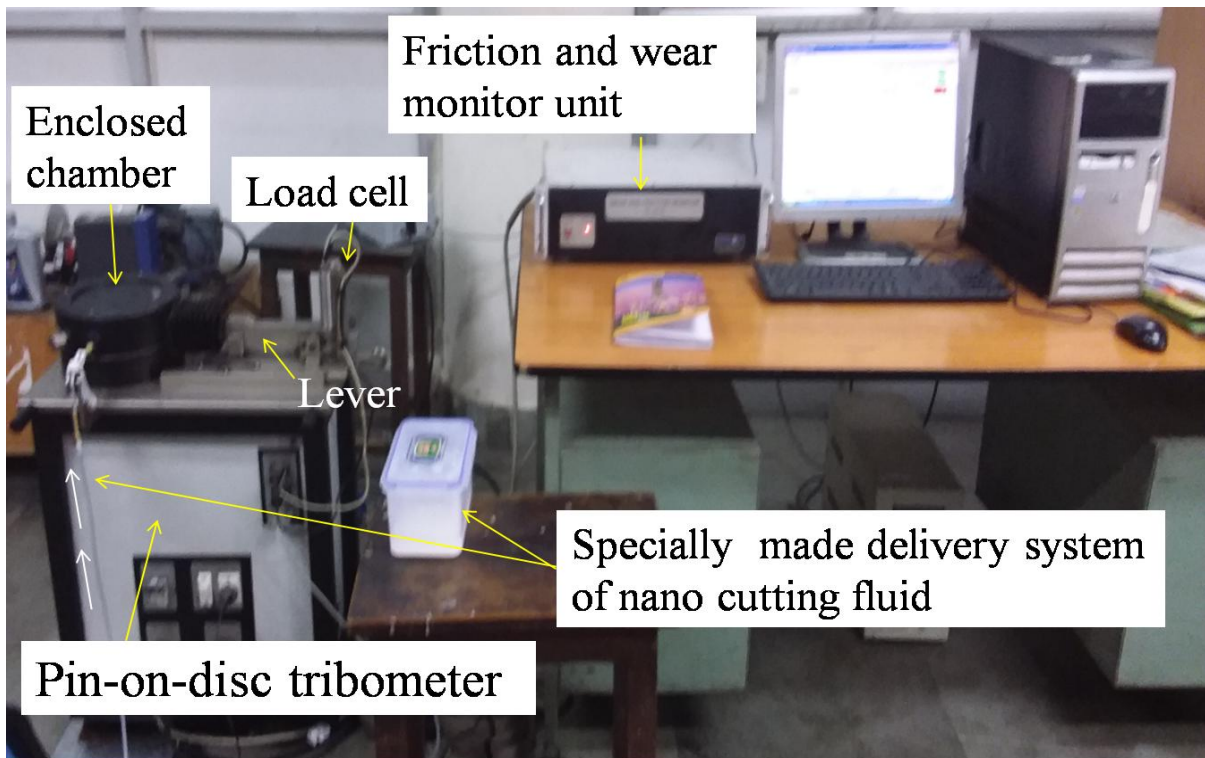


Figure 3.2 Specially made delivery system of nano-cutting fluid in Pin-on-disc tribometer.

3.3 Pin and Disc

Pin and disc were made according to ASTM G 99. Pin was made from carbide material in the shape of cylinder as shown in Figure 3.3 (a).

The height and diameter was 32mm and 10mm respectively. Coating of TiN of one micrometer thickness approximately was applied. The elements found during chemical analysis are depicted in Table 3.1.

Table 3.1 Chemical analysis of carbide pin

Elets	C	Co	Cr	Fe	W	Ti
Wt%	7.12	12.98	0.045	0.035	30.22	49.6

The disc was fabricated from AISI D3 steel in the diameter and thickness of 165mm and 8mm respectively as shown in Figure 3.3 (b).

Four holes of diameter 5mm were made on disc at the diameter of 150mm. The surface of the disc was grinded. Surface roughness was measured between 0.12 - 0.25 μ m.

The elements found during chemical analysis are depicted in Table 3.2.

Table 3.2 Elements found through chemical analysis

Ets	C	Si	Mn	S	P	Cr	Ni	Mo	Co	Nb	V	W	Fe
Wg%	2.03	0.255	0.432	0.026	0.019	11.05	0.073	0.07	0.013	0.021	0.040	0.086	85.525

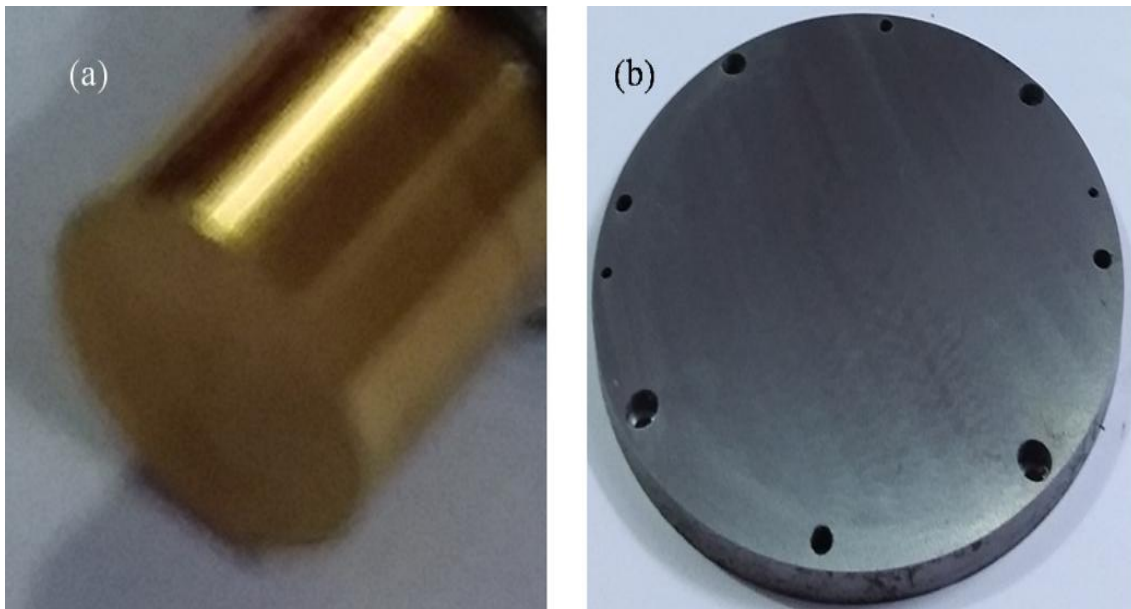


Figure 3.3(a) TiN coated carbide pin and (b) AISI D3 disc

3.4 IR Thermal imaging non contact type camera

Infra red thermal imaging non-contact type camera is shown in Figure 3.4. This can measure the temperature from -20 to 1200°C. Detector type of 320 X 240 pixels. Thermal sensitivity is less than 0.05°C at 30°C.

The laser beam was focused for measuring the temperature at the interface of pin and disc when experiments performed on tribometer and at rake face of cutting insert and workpiece during turning at a fixture of constant distance and angle of inclination.



Figure 3.4 IR Thermal imaging non-contact type camera

3.5 Digitalmicrobalance

Digitalmicrobalance was used for measuring the weight of pins before and after the performance of experiments. Every reading was repeated ten times and the average was calculated for a final value.

Every time of measurement zero reading was ensured by pressing Tare and wait for few seconds till zero appeared on the digital screen

The glass lid was closed every time of keeping the sample in the pan. Figure 3.5 depicts digital microbalance.

The glass enclosures prevent the disturbance from surroundings. The maximum measuring capacity is 200 grams.

The pan is used for placing the sample is of diameter 90mm. Response time for showing measurement is 2.5seconds.



Figure 3.5 Digitalmicro balance

3.6 Single point cutting insert and tool holder

Cutting inserts used during turning were in the shape of a diamond. The material was tungsten carbide with a coating of titanium nitride. ISO specification of cutting insert is DCMT 11T 3087 HQ with a grade of PV20 and tool holder is SDJCR 1212F 11. Tool geometry as per orthogonal rake system is $0^\circ, 0^\circ, 7^\circ, 7^\circ, 60^\circ, 93^\circ$ and 0.8mm ($\lambda', \alpha', \beta', \gamma', \phi', \theta'$ and r') respectively. Figure 3.6 depicts a tightened cutting insert in the holder



Figure 3.6 Single point cutting insert and tool holder

3.7 Lathe machine

The lathe machine used for the performance of turning experiments was three jaws conventional machine.

Figure 3.7 shows revolving centre for supporting the long workpiece in holding and rotating. Self made controlled drop wise supply of nano-cutting fluid at the rake face of cutting insert.

The maximum swing over bed is 400mm. Spindle size of diameter is 30mm. Square shaped tool holder of 12.5mm. The number of spindle speed is 6. Feed is of 4-60 thread per inch (tpi). An electric motor is fitted to supply power to head stock through an assembly of V – Belts. The rating of electric motor is 3 Phase with 440 volts with 2 horse power (H.P.)

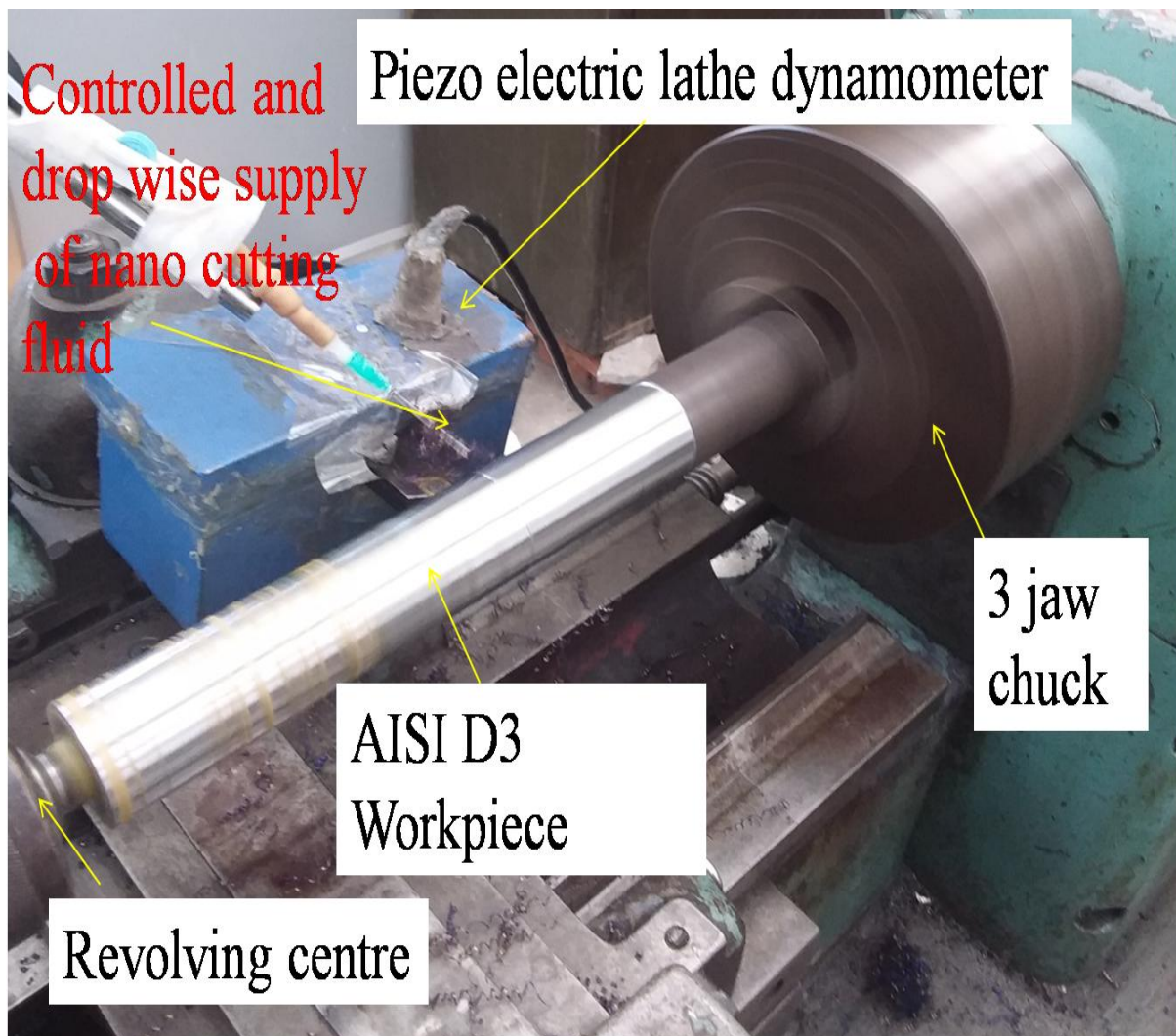


Figure 3.7 Lathe machine with self made supply of controlled drop wise supply of nano-cutting fluid

3.8 Piezo electric lathe tool dynamometer

Piezo electric lathe tool dynamometer was used for measuring cutting force during performing experiments on lathe machine.

Figure 3.8 (a) depicts an arrangement of tightened tool holder with cutting single point cutting insert in the slot of piezo electric lathe tool dynamometer. When cutting tool touches the workpiece the transmitted force gets converted into corresponding electrical signals. Further, into numerical values into digital display.

It was made assured that at the start of experiment the digital display showed zero readings as shown in Figure 3.8 (b). Each display is of 3.5 inches in length and 1 inch in breadth with light emitting diodes. The measuring capacity of cutting force, feed and axial thrust is 500kg each. The slot size for holding tool holder is square of 20mm side. Zero balancing is provided for each force in front panel with fine potentiometer.



Figure 3.8 (a) piezo electric dynamometer (b) digital display of lathe tool dynamometer

3.9 Surface roughness tester

Surface roughness was measured by Subtronic 3+ Taylor/ Habson surface roughness tester with a resolution of $0.01\mu\text{m}$. Ten readings were taken in six different axial positions. An average was calculated for the final value. Figure 3.9 depicts that workpiece is placed on V-blocks over levelled surface plate.

The probe of surface roughness tester is placed on the machined surface. When switch button is pressed the probe moves forward and backward. Probe consists of fine needle which remains always in contact with surface.

The movement passes through valleys and peaks of surface. The measured surface roughness is shown on the digital display of surface roughness tester

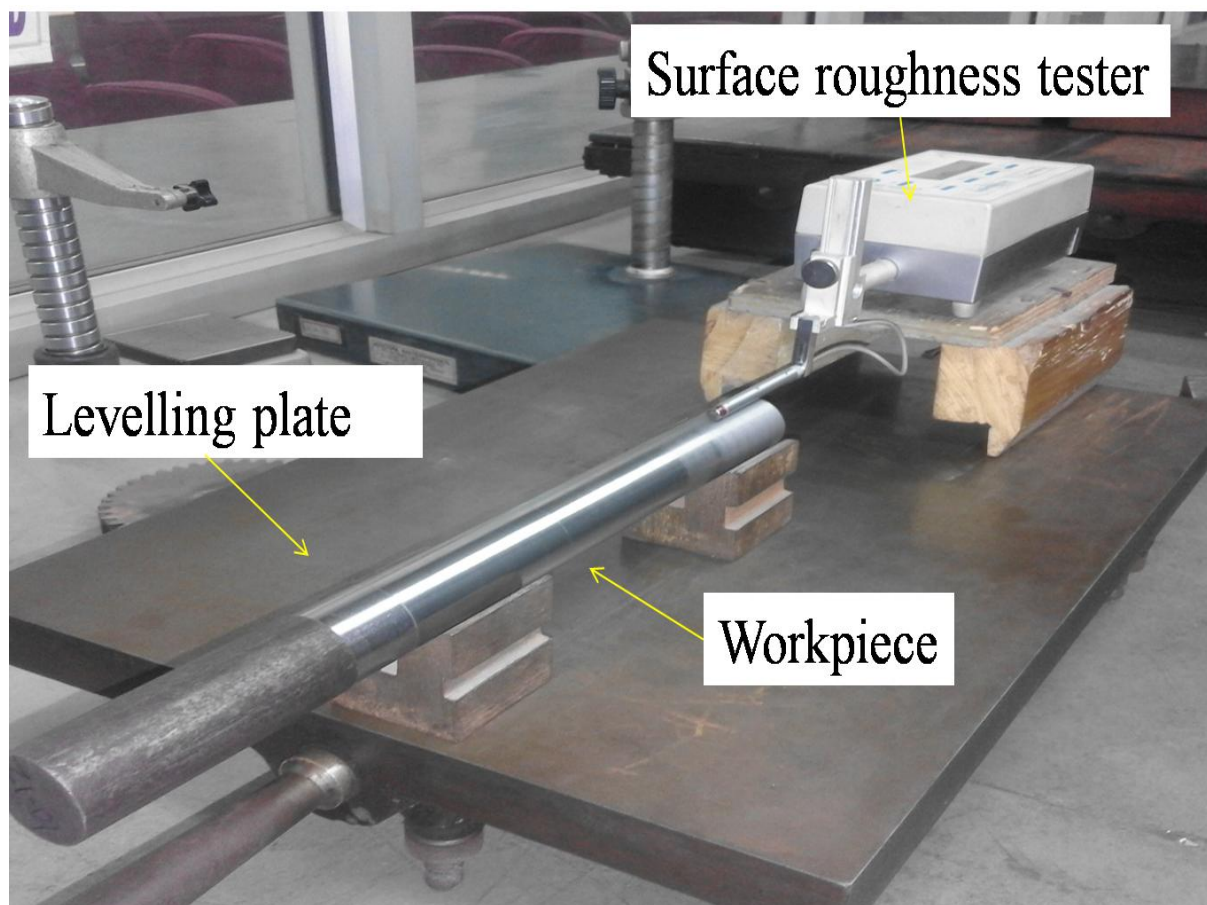


Figure 3.9 Surface roughness tester

3.10 CNC Vision Inspection Machine

CNC stands for computer numeric control. This machine can be used with designed coordinate system by computer or manually by quick release joy stick.

Figure 3.10 depicts a computer connected with vision inspection machine. The sample is placed on fixed glass surface of moving table. This can move in X and Y direction.

Vision has 1/3" High Resolution CCD camera which is fitted with sensor can move vertically in $\pm Z$ direction. The position of camera is controlled by joy stick. Every image is shown on computer screen.

After fixing the camera to the suitable position the magnification can be increased. Optical magnification is 0.7-4.5 times and magnification on computer screen is 35-225times.

The software used is IK 5000 / MSU3DPRO/M3. The measuring range is X-axis 500mm, Y-axis 400mm, Z-axis 300mm. The linear accuracy is $(3+L/200)$ micron. Repeatability is ± 0.002 mm. The measured dimensions with images are saved in computer software. This can be retrieved into image form which is readable in other commonly used softwares.



Figure 3.10 CNC Vision Inspection Machine

Summary

- Instruments used during experimentation in different sliding conditions for pin-on-disc tribometer have been discussed
- Instruments used during experimentation in different machining conditions for lathe machine have been discussed
- Major specifications of instruments are shown
- Emphasis is given for safety precautions like an assurance of zero reading before measuring weight and cutting force during turning operations etc.

NANO-CUTTING FLUIDS AND CHARACTERIZATION

This chapter consists of the steps involved in the characterization of nanoparticles through SEM, and preparation of nano-cutting fluids, TEM and Raman Analysis. Specifications of instruments used in the preparation like magnetic stirrer and ultrasonicator are discussed. Zeta potential tests have been performed for checking the stability. Rheological property like viscosity has been analyzed.

4.1 Characterization of nanoparticles

The comprehensive literature review has resulted in the selection of water based nanoparticles as Al₂O₃ and TiO₂.

It has been found that average grain size and range of particle size of nanoparticles of Al₂O₃ are greater than the grain size and range of particle size of nanoparticles TiO₂

The purity index of nanoparticles is very high in terms of percentage for both the selected nanoparticles.

The properties of nanoparticles are given in Table 4.1

Table 4.1 Properties of nanoparticles

SNo.	Properties	Nano-Al ₂ O ₃	Nano-TiO ₂
1	Average grain size	40nm	8nm
2	Particle size full range	5-100nm	8-25nm
3	Purity	99.99%	99.98%
4	Specific surface	> 10 m ² /g	50±10 m ² /g

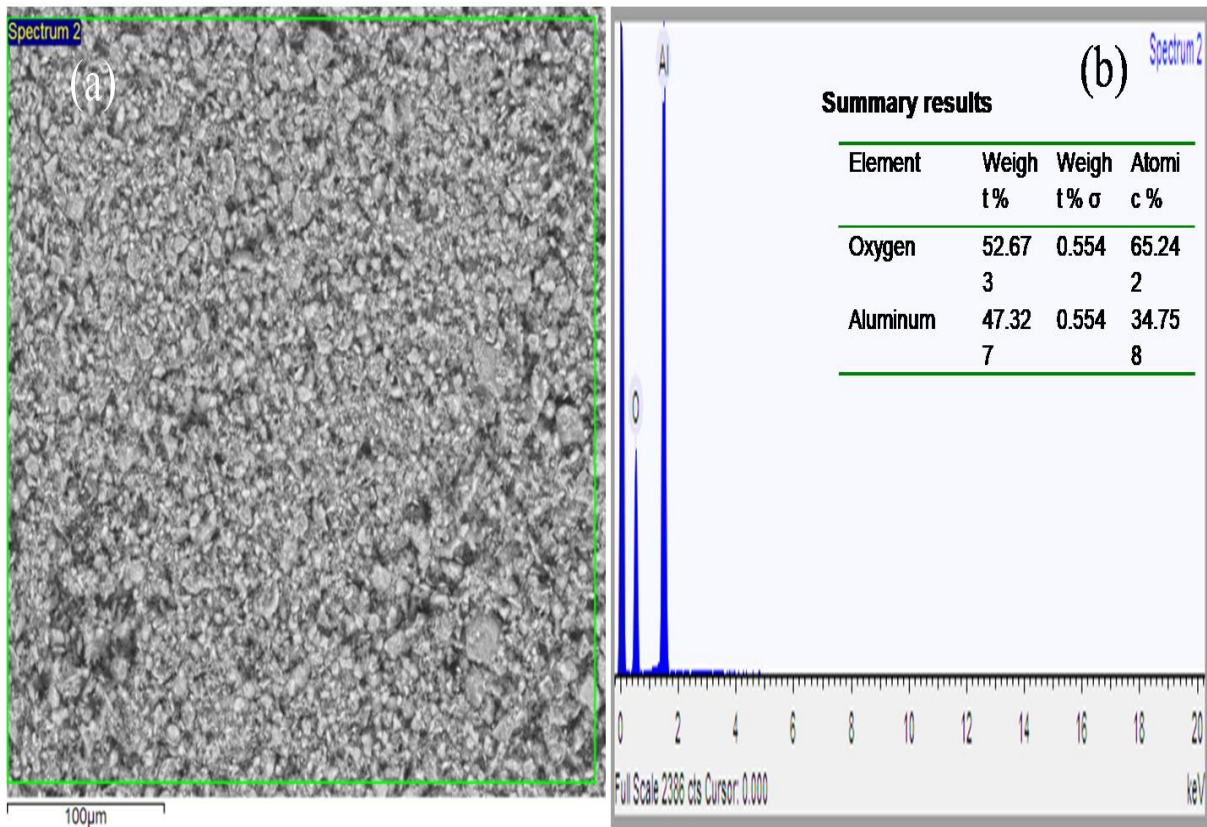


Figure 4.1 (a) SEM image and (b) EDS of nanoparticles Al_2O_3

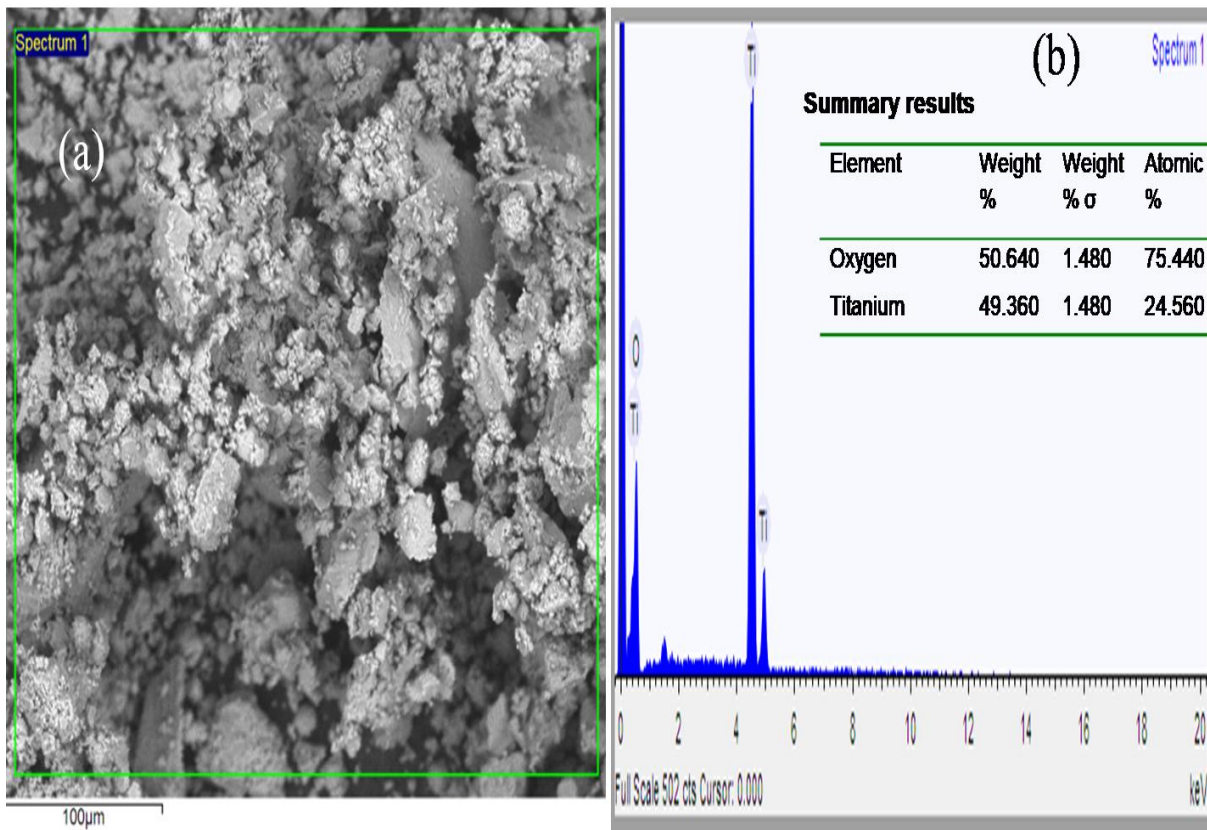


Figure 4.2 (a) SEM image and (b) EDS of nanoparticles TiO_2

Nanoparticles Al_2O_3 were characterized by SEM image and EDS. Figure 4.1 (a) depicts appearance of nanoparticles at $100\mu\text{m}$.

Figure 4.1 (b) shows high peaks of aluminium and oxygen. It has been found that percentage oxygen is more. The percentage of oxygen and aluminium in weight is depicted as 52.673% and 47.327% respectively.

Nanoparticles TiO_2 were characterized by SEM and EDS. Figure 4.2(a) depicts the appearance of TiO_2 at $100\mu\text{m}$.

Figure 4.2 (b) shows high peaks of titanium and oxygen. It has been shown that percentage of titanium is more. Comparatively oxygen is progressively lower. The percentage of titanium and oxygen in weight as 49.360% and 50.640%

4.2 Preparation of nano-cutting fluids

Two samples of nano-cutting fluids were prepared from two different nanoparticles. The composition was formed by considering weight by weight ratio with base fluid. In present research work base fluid is distil water.

The empty beaker was weighted on weighing scale. Then scale reading was made zero. The beaker was filled with distil water and weighed on scale.

Now, naonoparticles was weighed on micro scale in proportionate to 1% weight of water and mix in beaker.

4.2.1 Nano-cutting fluid with TiO_2 nanoparticles

Nanoparticles of TiO_2 were weighed on micro digital balance with an accuracy of ± 0.0001 grams. Sample of Nano cutting fluid was made with distill water in the proportion weight of 1% (weight by weight) of distilled water and abbreviated as Nano A

Figure 4.3 shows magnetic stirrer for blending of nanocutting fluid for 60 minutes at 520rpm at 21°C and rest was given for half an hour. Rest was given for half an hour for checking the sedimentation. The process of magnetic stirring was repeated for 60 minutes. This process was repeated 4-5 times

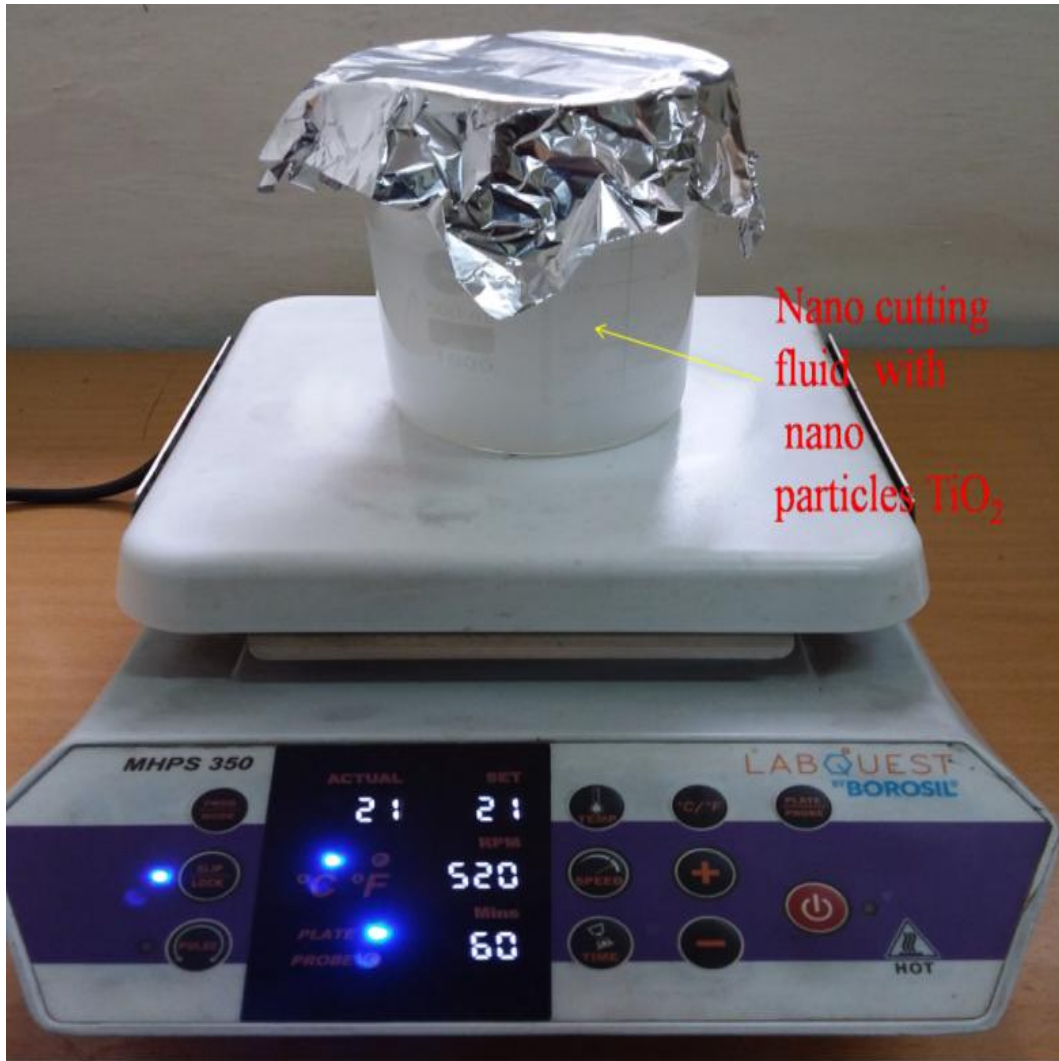


Figure 4.3 Magnetic stirrer for nano-cutting fluid with nanoparticles TiO_2

Ultrasonification was performed by water bath ultrasonicator. It was operated with single phase electric supply at 200-230Voltsat 50Hz.

One litre distil water was used for filing the water bath container. 30k Hz ultrasonification waves were generated. Initially, ultrasonification was performed for 30minutes.

Rest of five minutes was given. Then it was repeated for five times. Visual inspection did not show any sedimentation. Zeta potential test was conducted. The value was 32 which was in stable range.



Figure 4.4 Water bath ultrasonicator

4.2.2 Nano-cutting fluid with Al_2O_3 nanoparticles

Nanoparticles of Al_2O_3 were weighed on micro digital balance with an accuracy of ± 0.0001 grams. Sample of Nano cutting fluid was made with distilled water in the proportion weight of 1% (weight by weight) of distilled water and abbreviated as Nano B.

Magnetic stirring was done for blending of nanocutting fluid for 60 minutes at 520rpm at 21°C and rest was given for half an hour. This was repeated for 4-5 times and rest was given overnight for checking any sedimentation.

Most of the surfactant used by previous researchers are sodium based. Tween -20 Biocompatible surfactant has been found, which is non-toxic in nature. Initially, 0.25% was mixed with nano-cutting fluid.

Further, it was increased to 1% (weight by weight) of prepared nano-cutting fluid. Magnetic stirring was done at 520rpm at 21°C for 60 minutes.

Then ultrasonication was done for 30 minutes and repeated for 4-5 times. Zeta potential test was done and value was 21 which was in stability range.

4.3 Characterization of prepared nano-cutting fluids by TEM images

Characterization of prepared nano-cutting fluids by performing TEM image of samples. Figure 4.5 (a) shows TEM image at magnification of 40000 times and (b) shows TEM image at magnification of 60000times.of the prepared sample of nano-cutting fluid with nanoparticles of Al_2O_3 . Some agglomeration of particles are seen

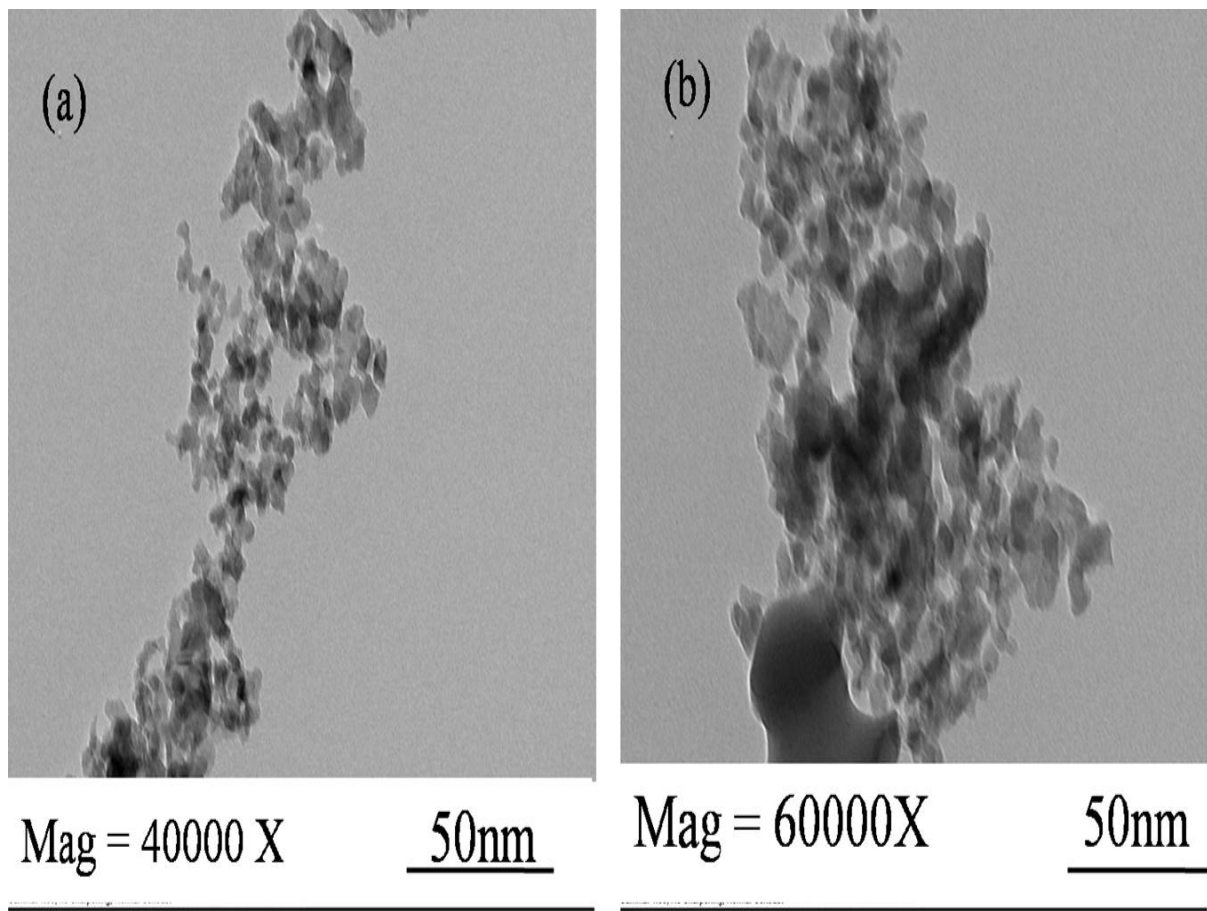


Figure 4.5 (a) TEM image at magnification of 40000X and (b) 60000X of prepared Al_2O_3 nano-cutting fluid

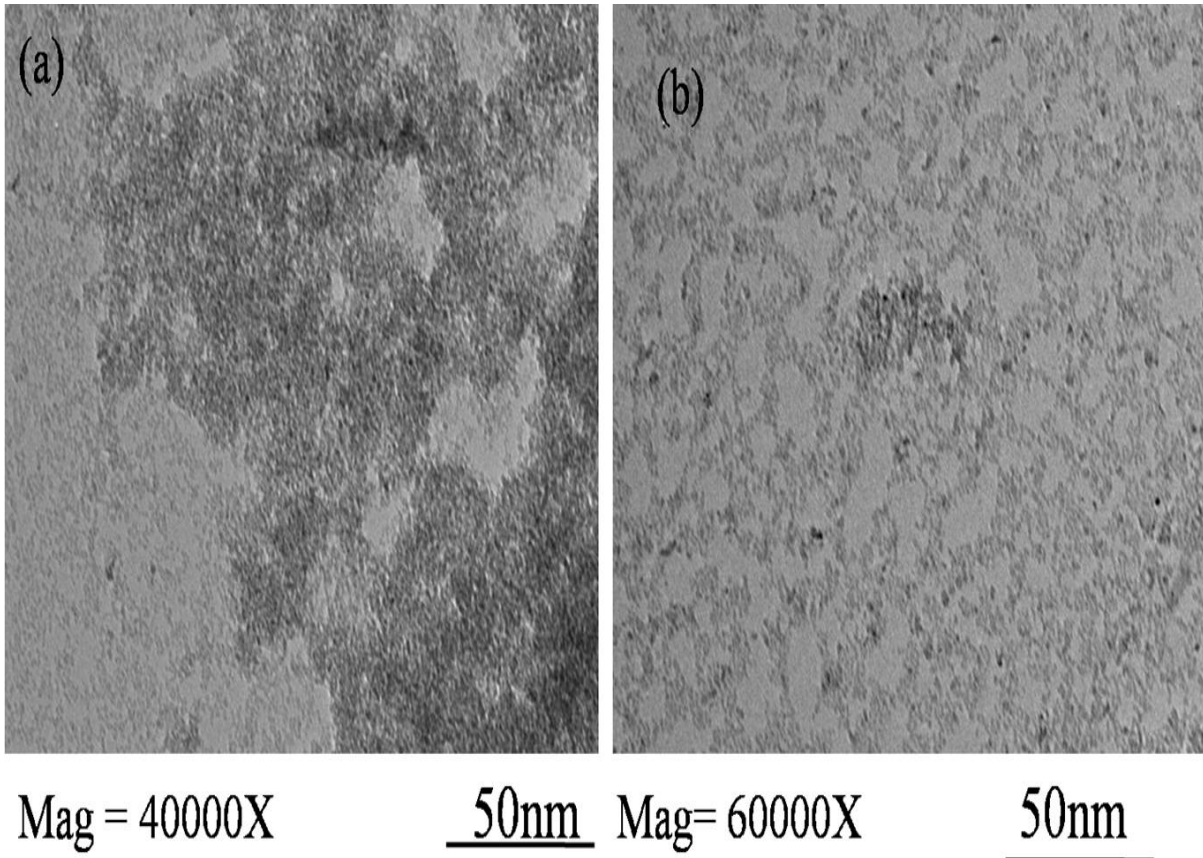


Figure 4.6 (a) TEM image at magnification of 40000X and (b) 60000X of prepared TiO₂ nano-cutting fluid

Figure 4.6 (a) shows TEM image at magnification of 40000 times and (b) shows TEM image at magnification of 60000times.of the prepared sample of nano-cutting fluid with nanoparticles of TiO₂. It has been seen that particle size is very fine and no agglomeration of particles are seen.

4.4 Characterization of prepared nano-cutting fluids by Raman Shift

It has been shown in Figure 4.7 that highest peak of Al₂O₃ is observed at 1100-1200 raman shift /cm⁻¹ for 380counts. This confirmed the presence of Al₂O₃. Other peak is observed at 2200-2300 raman shift /cm⁻¹ for 100counts.

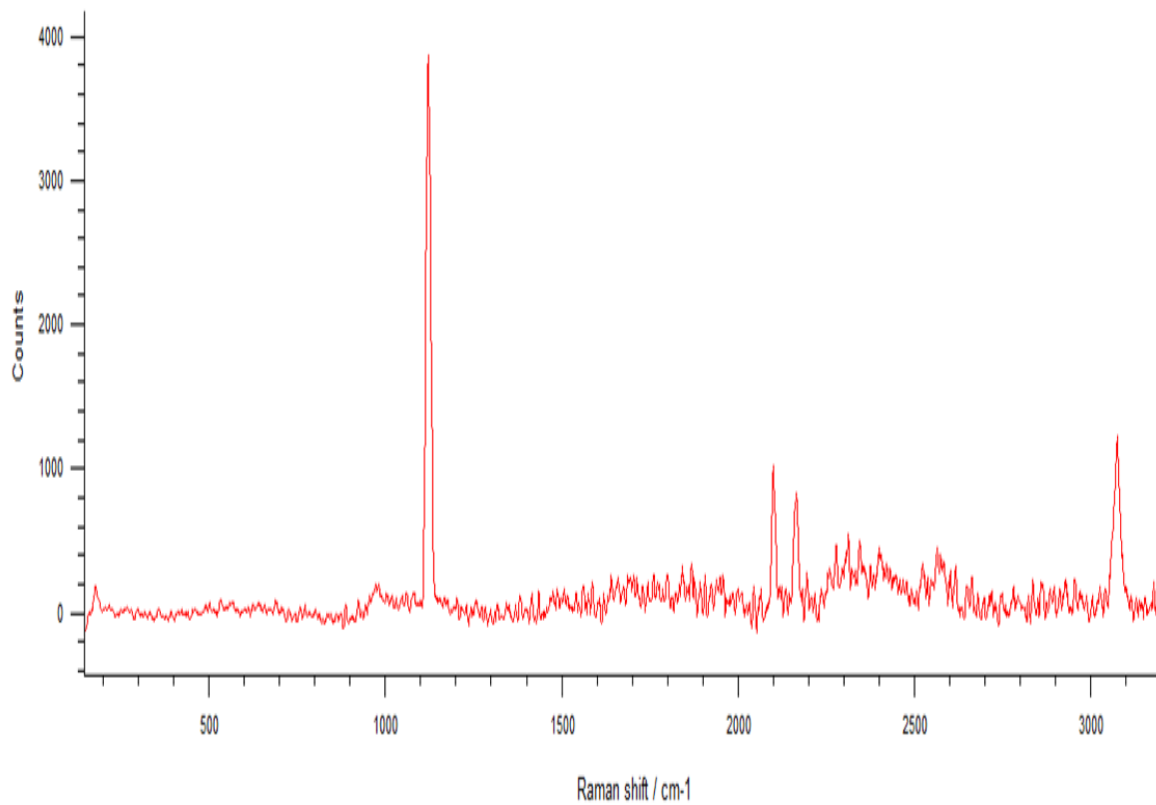


Figure 4.7 Raman shift pattern for Al₂O₃ in prepared nano-cutting fluid

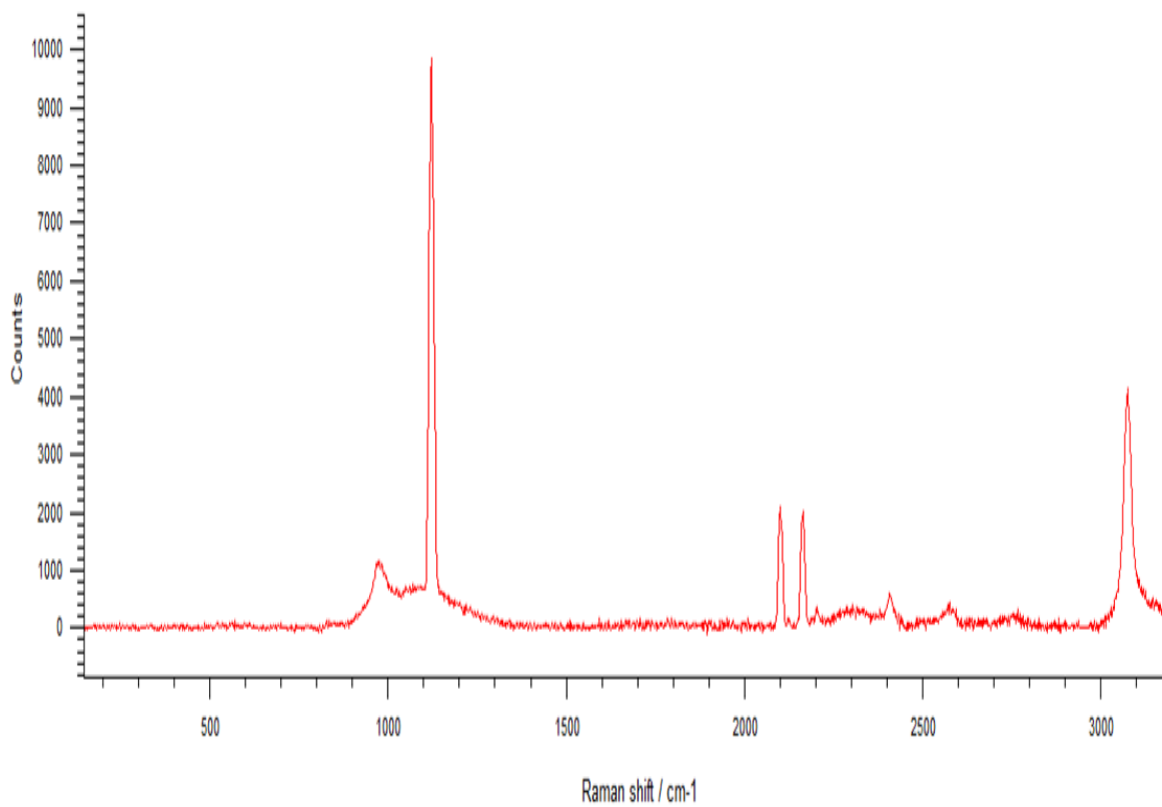


Figure 4.8 Raman shift pattern for TiO₂ in prepared nano-cutting fluid

Figure 4.8 depicts that highest peak is observed at 1200-1300 raman shift $/\text{cm}^{-1}$ for 980counts. This confirms the presence of TiO_2 in prepared nano-cutting fluid. Other high peak is observed at 3200-3300 raman shift $/\text{cm}^{-1}$ for 450counts.

4.5 Rheological Properties of nano-cutting fluids

Each sample was kept by a dropper at the cup and hob of Rheometer in the enclosed chamber. The temperature was adjusted at room temperature at 25°C .

The viscosity of Al_2O_3 and TiO_2 samples were 0.0930 and 0.0895 at the shear rate of 100/second. Figure 4.9 shows the change in viscosity for nano-cutting fluid with Al_2O_3 and TiO_2 .

It has been shown that viscosity is higher at the start of experiment and goes on decreasing with passing of time in seconds.

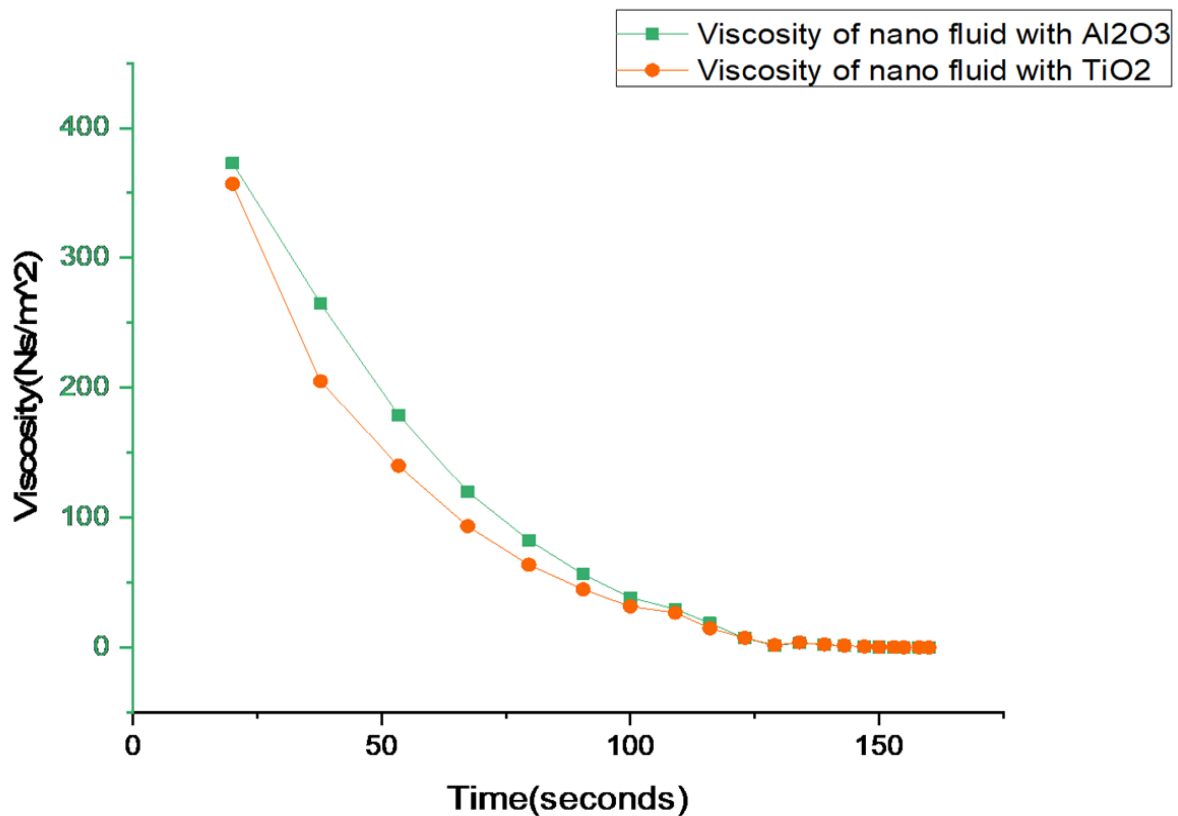


Figure 4.9 Viscosity of nano-cutting fluids with time at room temperature 25°C

Summary

- Nanoparticles are characterized then used for the preparation of nano-cutting fluids.
- Steps performed for preparing nano-cutting fluid have been discussed.
- Prepared nano-cutting fluid are characterized and checked for stability
- Change in viscosity is studied under rheological properties

EXPERIMENTAL PROCESS

This chapter consists of the description for selected sliding parameters during the performance of experiments on pin-on-disc tribometer and machining parameters during different created localized environmental condition at the vicinity of pin - disc and single point cutting tool-workpiece like dry, wet, nano A, nano B and direct supply of LN₂ respectively.

5.1 Experiments performed on pin-on-disc tribometer (dry and cryogenic)

The experiments were performed by using Taguchi [OA], mixed 2-3 level with L₁₈ DoE. The total input control variables were four like sliding speed (30, 60 and 90m/min.), load (35, 55 and 75N) and distance (600, 1200 and 1800m) varied to three levels (1, 2 and 3) respectively. One control factor was varied to two levels (1= Dry and 2= Cryogenic with LN₂). Table 5.1 shows the details of the control factors.

Table 5.1 Control factors with different level values Sliding Parameter

Levels	Sliding Condition	Sliding parameters		
		SS' (m/min.)	SL'(N)	SD'(m)
Level 1	Dry	30	35	600
Level 2	LN ₂	60	55	1200
Level 3	-	90	75	1800

The experiments were performed on pin-on-disc tribometer in two sliding conditions like dry and cryogenic with direct supply of LN₂ at the interface of pin and disc.

Table 5.2 shows the distribution pattern of coded and uncoded values of factors. Every numeral value has its unique representation which is clearly depicted.

Table 5.2 L₁₈ Taguchi orthogonal array for experiments performed pin-on-disc tribometer

Run	Coded Values of factors				Uncoded values of factors			
	E'	SS'	SL'	SD'	E'	SS' (m/min.)	SL'(N)	SD'(m)
1	1	1	1	1	Dry	30	35	600
2	1	1	2	2	Dry	30	55	1200
3	1	1	3	3	Dry	30	75	1800
4	1	2	1	1	Dry	60	35	600
5	1	2	2	2	Dry	60	55	1200
6	1	2	3	3	Dry	60	75	1800
7	1	3	1	2	Dry	90	35	1200
8	1	3	2	3	Dry	90	55	1800
9	1	3	3	1	Dry	90	75	600
10	2	1	1	3	Cr LN ₂	30	35	1800
11	2	1	2	1	Cr LN ₂	30	55	600
12	2	1	3	2	Cr LN ₂	30	75	1200
13	2	2	1	2	Cr LN ₂	60	35	1200
14	2	2	2	3	Cr LN ₂	60	55	1800
15	2	2	3	1	Cr LN ₂	60	75	600
16	2	3	1	3	Cr LN ₂	90	35	1800
17	2	3	2	1	Cr LN ₂	90	55	600
18	2	3	3	2	Cr LN ₂	90	75	1200

5.2 Experiments performed on pin-on-disc tribometer (wet and nano-cutting fluids)

Experiments were performed on pin-on-disc under wet and nano-cutting fluids at sliding speed =90m/min., sliding distance=1800m and load = 75N. Wet condition was created by using servo cut oil in the ratio of 1:20 and nano-cutting fluids A and B separately.

5.3 Experiments performed on lathe machine (dry and cryogenic)

Machining experiments were performed with four control factors. One factor machining condition was varied at two levels and three factors were varied at three levels. Former factor machining condition was varied to two levels (level 1 = Dry) and (level 2 = LN₂). Cutting parameters three levels of speed (30, 45 and 60 m/min.), feed (0.05, 0.08 and 0.14mm/rev.) and depth of cut (0.25, 0.35 and 0.45mm). Table 5.3 shows control factors with different level values. L₁₈ orthogonal array [OA]

Table 5.3 Control factors with different level values Machining Parameter

Levels	Machining Condition	Cutting parameters		
		Vc' (m/min.)	Fo' (mm/rev.)	Dc' (mm)
Level 1	Dry	30	0.05	0.25
Level 2	LN ₂	45	0.08	0.35
Level 3	-	60	0.14	0.45

The experiments were performed on lathe machine in two machining conditions like dry and cryogenic with direct supply of LN₂ at the interface of single point cutting insert and workpiece.

Table 5.4 shows the distribution pattern of coded and uncoded values of factors. Every numeral value has its unique representation which is clearly depicted.

Table 5.4 L₁₈ Taguchi orthogonal array experiments performed on lathe machine

Run	Coded Values of factors				Uncoded values of factors			
	M'	Vc'	Fo'	Dc'	M'	Vc' (m/min.)	Fo' (mm/rev.)	Dc' (mm)
1	1	1	1	1	Dry	30	0.05	0.25
2	1	1	2	2	Dry	30	0.08	0.35
3	1	1	3	3	Dry	30	0.14	0.45
4	1	2	1	1	Dry	45	0.05	0.25
5	1	2	2	2	Dry	45	0.08	0.35
6	1	2	3	3	Dry	45	0.14	0.45
7	1	3	1	2	Dry	60	0.05	0.35
8	1	3	2	3	Dry	60	0.08	0.45
9	1	3	3	1	Dry	60	0.14	0.25
10	2	1	1	3	LN ₂	30	0.05	0.45
11	2	1	2	1	LN ₂	30	0.08	0.25
12	2	1	3	2	LN ₂	30	0.14	0.35
13	2	2	1	2	LN ₂	45	0.05	0.35
14	2	2	2	3	LN ₂	45	0.08	0.45
15	2	2	3	1	LN ₂	45	0.14	0.25
16	2	3	1	3	LN ₂	60	0.05	0.45
17	2	3	2	1	LN ₂	60	0.08	0.25
18	2	3	3	2	LN ₂	60	0.14	0.35

5.4 Experiments on Lathe machine (Wet and Nano-cutting fluids)

Experiments were performed on lathe machine under wet and nano-cutting fluids at cutting parameters of speed =60m/min., feed 0.14(mm/rev.) and depth of cut 0.45mm. Wet condition was created by using servo cut oil in the ratio of 1:20 and nano-cutting fluids A and B separately.

Summary

- Design of experiments was according to Taguchi L₁₈ [OA] between dry and cryogenic sliding condition for pin -on-disc tribometer
- Design of experiments was in accordance to Taguchi ₁₈ [OA] between dry and cryogenic machining for lathe machine
- Taguchi based experiments saved more than 50% of tool, workpiece materials, time and power
- The comparative experiments were performed with highest sliding parameters of pin-on-disc tribometer for different sliding conditions like wet and nano-cutting fluids.
- The comparative experiments were performed with highest machining parameters of lathe machine for different machining conditions like wet and nano-cutting fluids.

RESULTS AND DISCUSSION

This chapter has the content about significant results of the presented research work. An approach was made to reach the optimum results. A comprehensive discussion is made which enlighten the trend and cause of behaviour though characterization by SEM, FSEM, EDS, TEM and Raman analysis in accordance to the property and requirement.

6.1 Experiments on pin-disc tribometer (dry and cryogenic)

The experiments were performed on pin-on-disc tribometer under dry and cryogenic cooling with LN₂ at the interface of pin and disc. Probability plot was made to ensure the pattern of distribution of data points within acceptable limits of normal distribution.

Figure 6.1 depicts the probability plot. It is observed that experimental result values obtained are mostly shifted towards the central line and are in the range of normal distribution. P-value is greater than 0.01. This is illustrated that further calculations and interpretation of results could be performed.

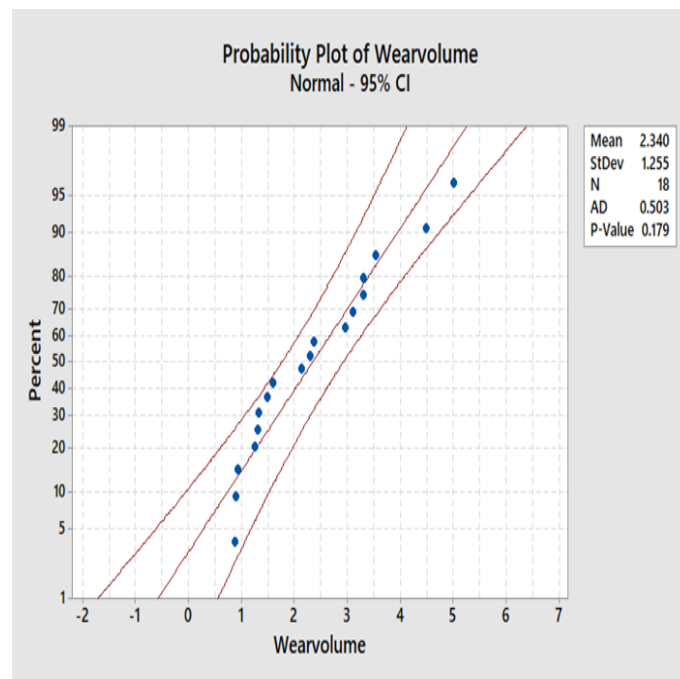


Figure 6 1 Probability plot for Wear volume

Table 6.1 L₁₈ Taguchi orthogonal array [OA]

Run	E'	SS' (m/min.)	SL'(N)	SD'(m)	Wear volume	S/N value of wear volume
1	Dry	30	35	600	1.5891	-4.0230
2	Dry	30	55	1200	2.3723	-7.5034
3	Dry	30	75	1800	2.9493	-9.3944
4	Dry	60	35	600	3.1055	-9.8426
5	Dry	60	55	1200	3.2998	-10.3698
6	Dry	60	75	1800	3.3011	-10.3732
7	Dry	90	35	1200	3.5381	-10.9754
8	Dry	90	55	1800	4.9983	-13.9764
9	Dry	90	75	600	4.4795	-13.0246
10	Cr LN ₂	30	35	1800	0.8786	1.1242
11	Cr LN ₂	30	55	600	0.8932	0.9810
12	Cr LN ₂	30	75	1200	0.9257	0.6706
13	Cr LN ₂	60	35	1200	1.2425	-1.8859
14	Cr LN ₂	60	55	1800	1.3198	-2.4102
15	Cr LN ₂	60	75	600	1.3044	-2.3082
16	Cr LN ₂	90	35	1800	1.4901	-3.4643
17	Cr LN ₂	90	55	600	2.1397	-6.6071
18	Cr LN ₂	90	75	1200	2.2893	-7.1941

Table 6.1 depicts the sequence of parameters used during the performance of experiments according to L₁₈ [OA]. Output values of wear volume is shown with respective S/N values which was calculated by using the lower the better the approach as shown in Eq. (1)

Smaller is the better characteristic $\frac{S}{N} = -10 \log \frac{1}{n} (\sum x^2)$ Eq. (1)

6.1.1 Wear volume loss

Pins were measured on a dedicated measuring scale of least count $\pm 0.0001g$. The difference in weight before and after conducting each experiment was measured and noted. Wear volume loss was measured by using Eq. (1) for each experimental run.

$$\text{Wear volume loss} = \frac{\text{Weight loss}}{\text{Density}} \quad \text{Eq. (2)}$$

The wear volume loss of experimental runs from 10-18 during cryogenic cooling with direct supply of LN₂ at the interface of pin and disc in an enclosed chamber was lower than the wear volume loss for experimental runs from 1-9 during dry sliding condition as shown in Figure 6.2.

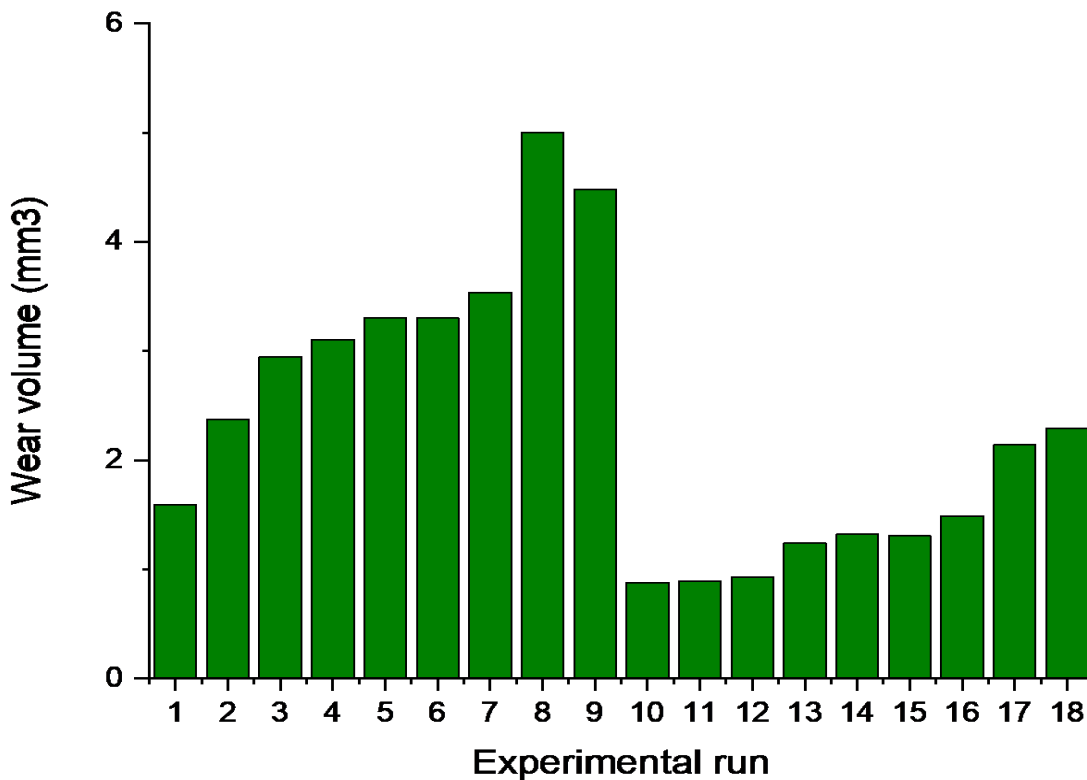


Figure 6.2 Wear volume obtained during experimental run L₁₈ DoE

6.1.2 Optimization on the basis of Taguchi (S/N ratio)

Optimization was based on Taguchi S/N ratio. The smaller the better was used in deriving the value of response at the optimum level.

This is illustrated in Eq. (2). Table 6.2 shows S/N values of response (wear volume).

Delta is the difference between the highest and lowest value in each control factor. The optimized value is calculated by recognizing the highest value of S/N value of each control factor.

Rank is provided showing the influence of factor.

Table 6.2 Response table for S/N ratio Wear volume (mm³)

Response	Level	Sliding Condition	SS'(m/min.)	SL'(N)	SD'(m)
Wv'	1	-9.943	-3.024	-4.845	-5.804
	2	-2.344	-6.198	-6.648	-6.210
	3	-	-9.207	-6.937	-6.416
	Delta	7.599	6.183	2.093	0.612
	Rank	1	2	3	4

Table 6.3 depicts the response values for means of wear volume (mm³). Delta is the difference between the highest and lowest value in each control factor.

Rank is provided showing the influence of factor.

Table 6.3 Response table for means Wear volume (mm³)

Response	Level	Sliding Condition	SS'(m/min.)	SL'(N)	SD'(m)
Wv'	1	3.293	1.601	1.974	2.252
	2	1.387	2.262	2.504	2.278

	3	-	3.156	2.542	2.490
	Delta	1.906	1.554	0.568	0.238
	Rank	1	2	3	4

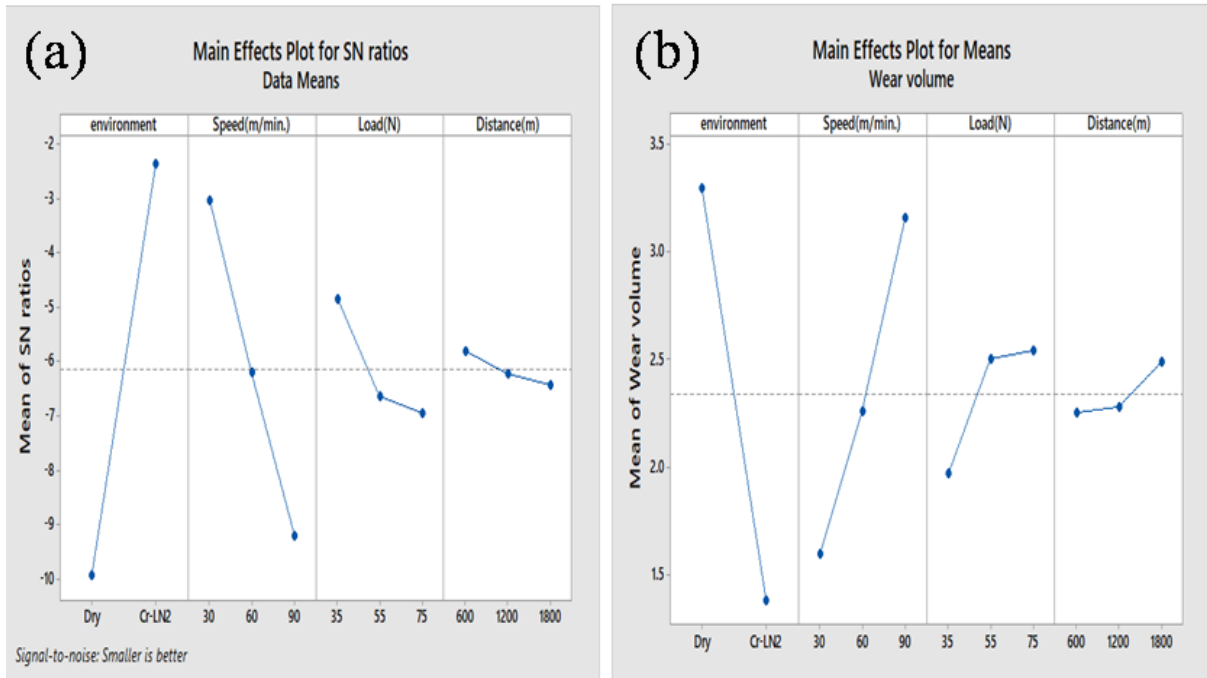


Figure 6.3 Diversification of (a) mean S/N ratio wear volume (b) means of mean wear volume with various factor levels

Diversification of mean S/N ratio Wv' (graphical trend) according to input control factors has been shown in Figure 6.3(a) and numerical values in Table 6.2 respectively. Diversification of mean Wv' (graphical trend) according to input control factors have been shown in Figure. 6.3 (b) and numerical values in Table 6.3 respectively.

On incrementing speed, load and distance wear volume increased. From Table 6.2 the highest S/N ratio was selected for an optimum value of each level.

The optimized sliding parameters at $E' = LN_2$, $SS' = 30m/min.$, $SL' = 35N$ and $SD' = 600m$. Eqs (3) and (4) were used for calculating the predicted value of each response.

Where, $\bar{\delta}_p$ was the average S/N ratios of all variables δ_p was the actual calculated S/N response at optimum level, \bar{S}_{co} was the average S/N ratio when variable E' (sliding condition) was at optimum level, \bar{S}_0 was the average S/N ratio when variable (sliding speed) was at

optimum level, $\overline{L_o}$ was the average S/N ratio when variable (load) was at optimum level and $\overline{Di_o}$ was the average S/N ratio when variable (sliding distance) was at optimum level. Z_p was the predicted responses for wear volume.

$$\delta_p = \overline{\delta_p} + (\overline{S_{co}} - \overline{\delta_p}) + (\overline{S_o} - \overline{\delta_p}) + (\overline{L_o} - \overline{\delta_p}) + (\overline{D_{io}} - \overline{\delta_p}) \quad \text{Eq. (3)}$$

$$Z_p = 10^{-\delta_p/20} \quad \text{Eq. (4)}$$

Using, Eqs (3) and (4) predicted the optimum value of wear volume was 0.7574mm³.

This was enhanced by the statistical analysis of variance (ANOVA). Table of ANOVA consists of a degree of freedom (df), adjoint sum of squares (Adj SS), adjoint mean of square (Adj MS),

F-Value, P-Value and percentage of contribution.

ANOVA Table 6.4 shows that for response friction force sliding condition has the highest effect on the percentage of contribution (64.37%), next followed by sliding speed (28.42%), load (3.82%) and lastly distance (0.24%).

F-value depicted the relative importance of firstly sliding condition, secondly sliding speed, thirdly sliding load and lastly sliding distance.

P-value was significant for sliding condition, sliding speed and load. Since P - value was significant at the value of level equal to or less than 0.05.

Table 6.4 Analysis of variance for means of Wear volume (mm³)

Response	Source	DF	Adj SS	Adj MS	F-Value	P-Value	% Cont.
Wv'	E'	1	259.835	259.835	207.12	0.000	64.37
	SS'(m/min.)	2	114.709	57.354	45.72	0.000	28.42
	SL'(N)	2	15.430	7.715	6.15	0.018	3.82
	SD'(m)	2	1.162	0.581	0.46	0.642	0.29

	Error	10	12.545	1.255	-	-	-
	Total	17	403.681	-	-	-	-

6.1.3 Confirmation Tests

Confirmatory validity experiment was performed in accordance with the predicted parameter for checking the difference between predicted value and confirmation experimental value at optimized level of response at $E'= LN_2$, $SS'= 30m/min.$, $SL'= 35N$ and $SD'= 600m$.

Predicted value of response was $0.7574mm^3$ and actual experimental value was $0.7570mm^3$.

It has been shown that actual value of response at experimental run of optimized level is very close to predicted value.

6.1.4 Wear of pin

Worn out pins of TiN coated carbide material after the performance of experiment on pin-on-disc tribometer used during dry and cryogenic sliding conditions were analyzed for better understanding of wear mechanism.

Figure 6 4(a) Field scanning electron microscope (FSEM) image depicts coating peeling, adhesives, edge fracture and small depressions during dry sliding. Figure 6.4(b) Field scanning electron microscope

(FSEM) image shows a clean & smooth surface of the pin with a minor edge fracture during cryogenic cooling. The surface structural phenomena may be due to the low temperature generated at the interface of pin and disc.

LN_2 provided a fluid film between pin and disc which generated a lubrication effect at the interface.

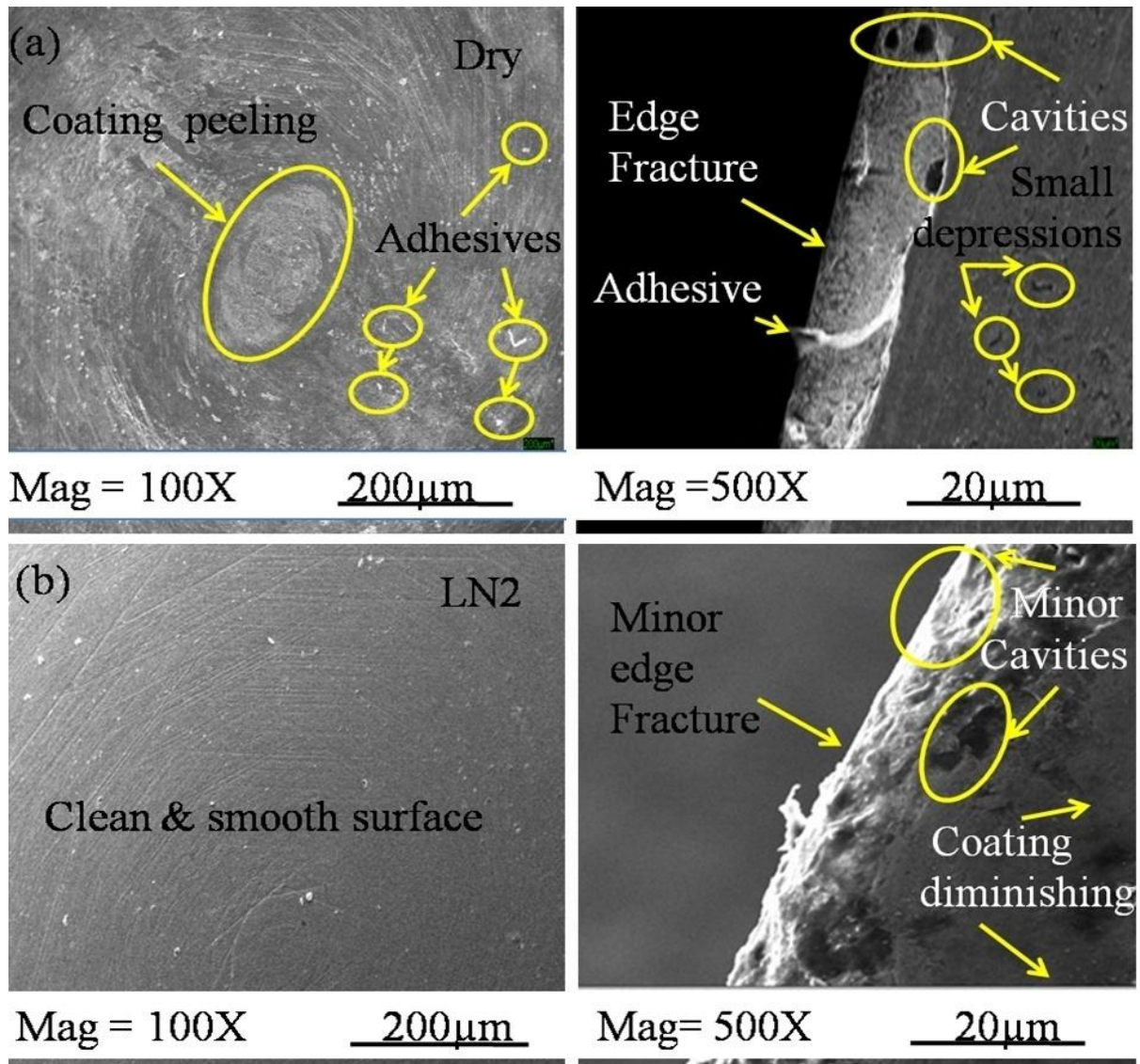


Figure.6.4 (a) Field scanning electron microscope (FSEM) image of used pin during dry sliding at sliding speed = 90m/min, sliding load = 75N, sliding distance = 1200m (b) with LN₂ sliding

6.1.5 Wear of disc

Wear tracks formed on the disc were analysed during dry and cryogenic cooling. Figure 6.5(a) Field scanning electron microscope (FSEM) image depicts cavities, wear debris, plough and delamination during dry sliding. Figure 6.5(b) Field scanning electron microscope (FSEM) image shows minor cavities, plough, clean and smooth surface. The surface structural phenomenon may be due to the pressurised flow of LN₂ that washed away out the debris between pin and disc. The low temperature created and maintained by LN₂ prevented the surface from contamination and deterioration.

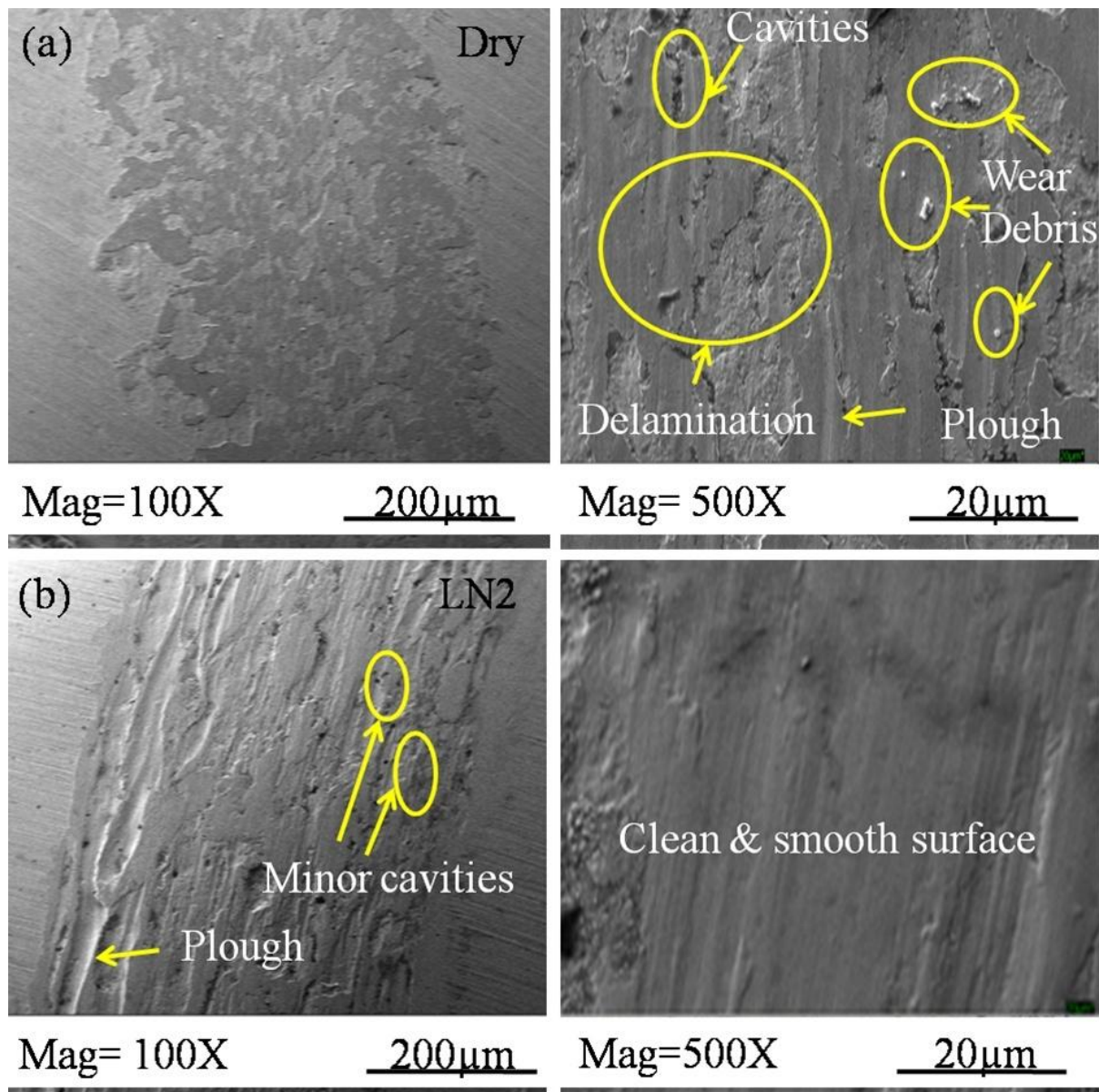


Figure 6.5 (a) Field scanning electron microscope (FSEM) image of wear tracks on disc formed during dry sliding at sliding distance = 90m/min, sliding load = 75N, sliding distance = 600m (b) with LN₂ sliding distance = 1200m

6.2 Experiments on Pin-on- Disc tribometer (Wet and Nano-cutting fluids)

The experiments were carried on pin-on-disc tribometer on sliding parameters at SS'= 90m/min., SL'= 75N and SD'= 1800m during (i) wet using cutting oil and water as a conventional cutting fluid

(ii) nano-cutting fluids at the interface of TiN coated carbide pin and AISI D3 steel disc

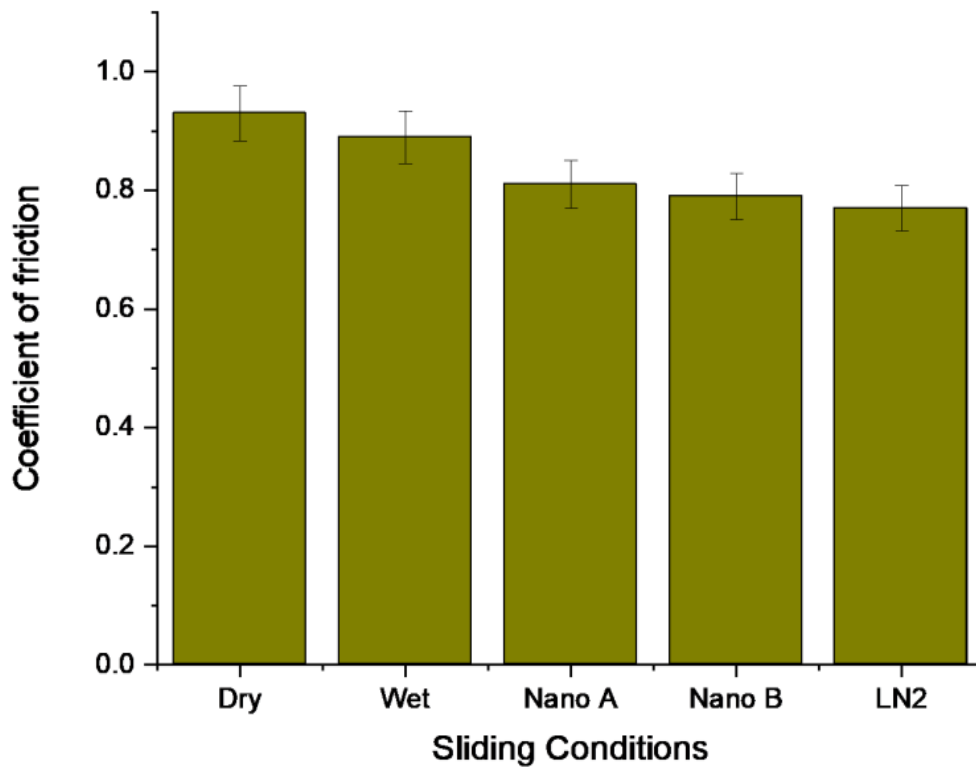


Figure.6.6 Coefficient of friction during different sliding conditions

The measurement of friction force was from the start to the end of the experimental run. Coefficient of friction was calculated for each experiment using Eq.(5)

$$\mu = \frac{\text{Friction force}}{\text{Load}} \quad \text{Eq. (5)}$$

Coefficient of friction calculated during different sliding conditions are shown in Figure. 6.6. It has been found that coefficient of friction was more in a dry condition as compared to wet, Nano A, Nano B and LN₂. The fluid formed a thin layer reduced the metal to metal direct contact.

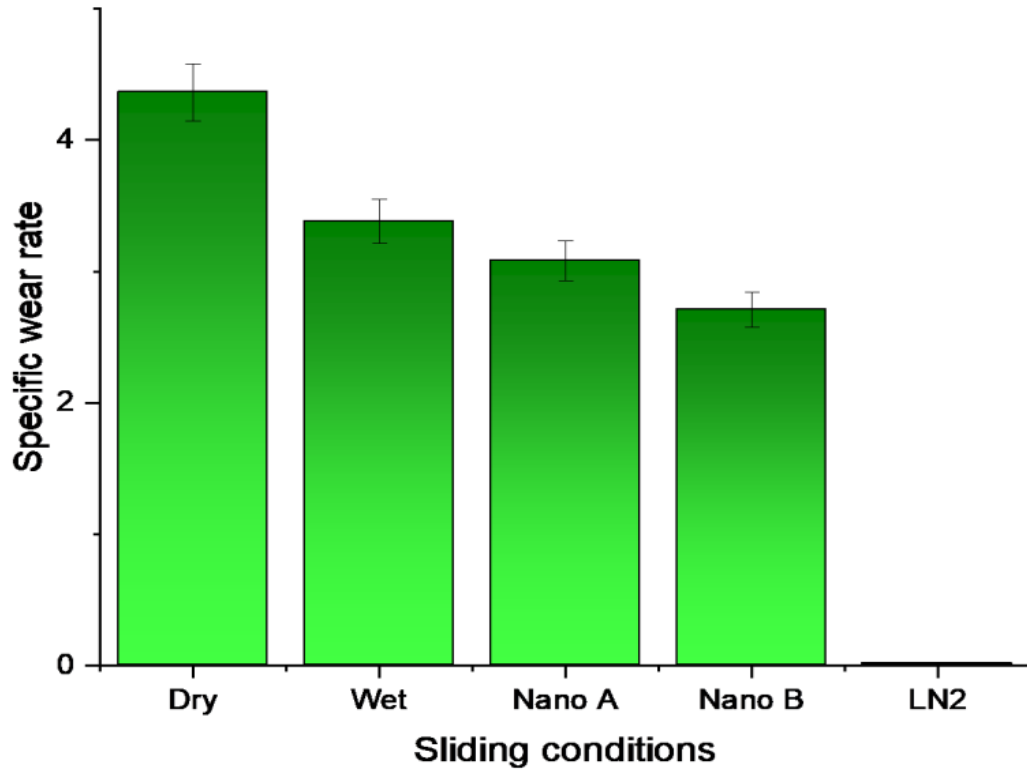


Figure.6.7 Specific wear rate during different sliding conditions

Figure.6.7 shows the variation of specific wear rate with the different environment of sliding condition has been calculated from Eq. (1) and Eq. (6)

$$Swr = \frac{\Delta V}{F' \times S'} \quad \text{Eq.(6)}$$

Where,

ΔV = Wear volume loss

F' = Frictional force (N)

S' = Sliding distance

It has been found that specific wear rate of the pin is negligible during LN₂t direct supply at the interface of pin and disc. This may be due to high rate of heat removing capacity of LN₂ which makes the surface harder and finally lesser wear of the tribo-material. Nano A made with nanoparticles Al₂O₃ was performed better than Nano B with nanoparticles TiO₂, wet and dry due to high specific heat which may transfer heat from the vicinity of pin and disc faster.

6.3 Experiments on lathe machine (dry and cryogenic)

The experiments were performed according to L₁₈ Taguchi based design of the experiment. The sequences of performances of experiments are shown in Table 6.4. The responses have been justified by the probability plot from Figure 6.8. The data values are roughly aligned with the middle line and normally distributed. This can be further used for optimization and investigation.

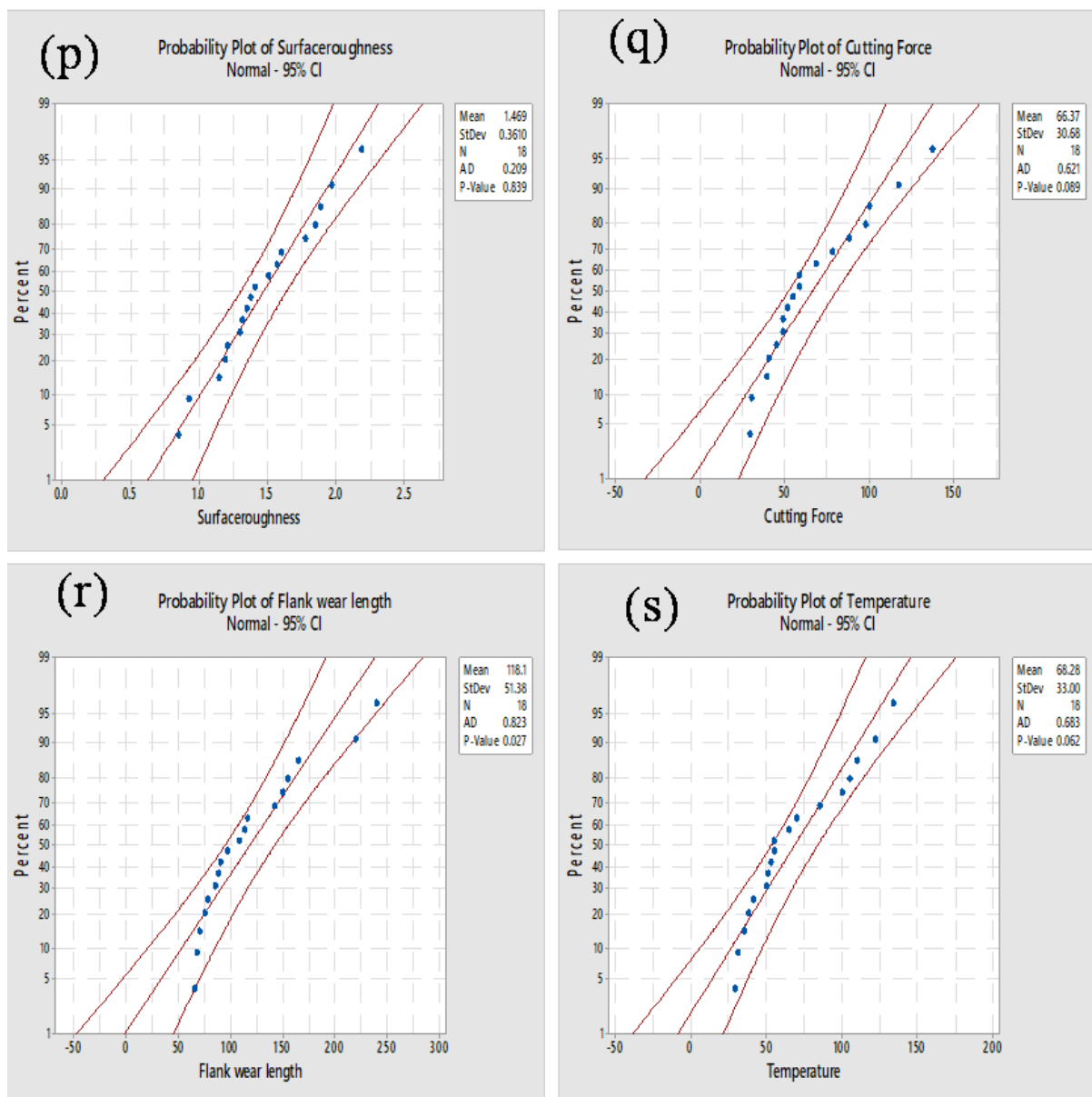


Figure 6.8 Probability plots for (p) surface roughness, (q) cutting force, (r) flank wear length and (s) temperature

Table 6.5 L₁₈ Taguchi orthogonal array basis of performance of experiments

Run	M'	Vc' (m/min.)	Fo' (mm/rev.)	Dc' (mm)
1	Dry	30	0.05	0.25
2	Dry	30	0.08	0.35
3	Dry	30	0.14	0.45
4	Dry	45	0.05	0.25
5	Dry	45	0.08	0.35
6	Dry	45	0.14	0.45
7	Dry	60	0.05	0.35
8	Dry	60	0.08	0.45
9	Dry	60	0.14	0.25
10	LN ₂	30	0.05	0.45
11	LN ₂	30	0.08	0.25
12	LN ₂	30	0.14	0.35
13	LN ₂	45	0.05	0.35
14	LN ₂	45	0.08	0.45
15	LN ₂	45	0.14	0.25
16	LN ₂	60	0.05	0.45
17	LN ₂	60	0.08	0.25
18	LN ₂	60	0.14	0.35

The first column of Table 6.5 shows the machining conditions like (1-9) dry and (10-18) direct supply of LN₂ at the interface of cutting insert and workpiece. Second, third and fourth columns show Vc' (m/min.), Fo' (mm/rev.) and Dc' (mm)

Table 6.6 Experimental results of responses with respective S/N value as per Taguchi L₁₈ orthogonal array

Run	Responses				S/N value of responses			
	Ra'	Fc'	Vb'	T'	Ra'	Fc'	Vb'	T'
1	2.19	59.0	108	38	-6.808	-35.417	-40.668	-31.596
2	1.89	49.0	113	55	-5.529	-33.803	-41.062	-34.810
3	1.97	68.6	116	70	-5.889	-36.726	-41.289	-36.902
4	1.51	78.4	155	85	-3.579	-37.886	-43.806	-38.588
5	1.60	88.2	165	105	-4.082	-38.909	-43.349	-40.423
6	1.85	98.0	150	122	-5.343	-39.825	-43.522	-41.727
7	1.57	117.6	142	134	-3.918	-41.408	-43.046	-42.542
8	1.38	137.2	220	100	-2.796	-42.747	-46.848	-40.000
9	1.78	100.0	240	110	-5.008	-40.000	-47.604	-40.828
10	1.35	29.4	70	29	-2.606	-29.367	-36.902	-29.247
11	1.41	30.2	85	35	-2.984	-29.600	-38.588	-30.881
12	1.30	39.2	90	41	-2.278	-31.866	-39.085	-32.255
13	0.93	40.5	68	31	0.630	-32.149	-36.65	-29.827
14	1.21	49.0	78	50	-1.655	-33.803	-37.842	-33.979
15	1.32	58.8	65	55	-2.411	-35.388	-36.258	-34.807
16	1.19	51.5	75	65	-1.511	-34.236	-37.501	-36.258
17	0.85	55.0	88	51	1.412	-34.807	-38.889	-34.151
18	1.15	45.0	97	53	-1.214	-33.064	-39.735	-34.485

Table 6.6 shows the values of each response for every performed experiment like Ra', Fc', Vb' and T' with respective S/N value which was calculated by Eq. (1)

6.4 Taguchi Based Optimization (Signal to Noise ratio)

The optimization based on Taguchi S/N (ratio) involves a reduction of variability and alignment of mean value to target value. In any process, variability may arise due to factors having no control are termed as uncontrollable factor or noise.

Eq. (1) shows smaller the better characteristic of continuous response function depending on the optimization principle Where x represents the measuring responses (Ra' , Fc' , Vb' and T') & n is the number of experimental data.

Taguchi based S/N values of each response are shown in Table 6.7 The difference between the maximum and minimum S/N value of each control factor is shown as delta. The optimised value of each control factor has been selected by recognizing the highest S/N value of each control factor for a particular response of surface roughness (Ra'), cutting force (Fc'), flank wear length (Vb') and temperature (T'). According to the importance of the control factor, Rank value is present.

Table 6.8 shows the means of mean of surface roughness (Ra'), cutting force (Fc'), flank wear length (Vb') and temperature (T'). Rank value is present on the basis of importance of control factor

This is supported by the statistical analysis of variance (ANOVA).Table 6.9 has a degree of freedom (df), adjoint sum of squares (Adj SS), adjoint mean of square (Adj MS), F-Value, P-Value and percentage of contribution.

The P-value is defined for the significance level of 5% (confidence level of 95%) for all responses. Last column shows the effect of contribution in the terms of percentage.

Table 6.7 Response table for S/N ratio of surface roughness (Ra'), cutting force (Fc'), flank wear length (Vb') and temperature (T')

Response	Level	M'	Vc'(m/min.)	Fo'(mm/rev.)	Dc'(mm)
Ra'	1	-4.773	-4.350	-2.966	-3.23
	2	-1.402	-2.740	-2.606	-2.732
	3	-	-2.173	-3.691	-3.301

	Delta	3.371	2.177	1.085	0.569
	Rank	1	2	3	4
Fc'	1	-38.52	-32.80	-35.08	-35.52
	2	-32.70	-36.33	-35.61	-35.20
	3	-	-37.71	-36.14	-36.12
	Delta	5.83	4.91	1.07	0.92
	Rank	1	2	3	4
Vb'	1	-43.58	-39.60	-39.76	-40.97
	2	-37.94	-40.40	-41.26	-40.65
	3	-	-42.27	-41.25	-40.65
	Delta	5.64	2.67	1.50	0.32
	Rank	1	2	3	4
T'	1	-38.60	-32.61	-34.68	-35.14
	2	-32.88	-36.56	-35.71	-35.72
	3	-	-38.04	-36.83	-36.35
	Delta	5.72	5.43	2.16	1.21
	Rank	1	2	3	4

Table 6.8 Response table for means of surface roughness (Ra'), cutting force (Fc'), flank wear length (Vb') and temperature (T')

Response	Level	M'	Vc'(m/min.)	Fo'(mm/rev.)	Dc'(mm)
Ra'	1	1.749	1.685	1.457	1.510
	2	1.190	1.403	1.390	1.407
	3	-	1.320	1.562	1.492

	Delta	0.559	0.365	0.172	0.103
	Rank	1	2	3	4
Fc'	1	88.44	45.90	62.73	63.57
	2	44.29	68.82	68.10	63.25
	3	-	84.38	68.27	72.28
	Delta	44.16	38.48	5.53	9.03
	Rank	1	2	4	3
Vb'	1	156.56	97.00	103.00	123.50
	2	79.56	113.50	124.83	112.50
	3	-	143.67	126.33	118.17
	Delta	77.00	46.67	23.33	11.00
	Rank	1	2	3	4
T'	1	91.00	44.67	63.67	62.33
	2	45.56	74.67	66.00	69.83
	3	-	85.50	75.17	72.67
	Delta	45.44	40.83	11.50	10.33
	Rank	1	2	3	4

Table 6.9 Analysis of variance for means of surface roughness (Ra'), cutting force (Fc'), flank wear length (Vb') and temperature (T')

Response	Source	DF	Adj SS	Adj MS	F-Value	P-Value	% Cont.
Ra'	M'	1	51.123	51.1229	47.93	0.000	62.42

	Vc'(m/min.)	2	15.296	7.6481	7.17	0.012	18.67
	Fo'(mm/rev.)	2	3.664	1.8321	1.72	0.228	4.47
	Dc'(mm)	2	1.151	0.5756	0.54	0.599	1.40
	Error	10	10.666	1.0666	-	-	-
	Total	17	81.901	-	-	-	-
Fc'	M'	1	152.781	152.781	77.27	0.000	59.77
	Vc'(m/min.)	2	77.045	38.522	19.48	0.000	30.14
	Fo'(mm/rev.)	2	3.420	1.710	0.86	0.450	1.34
	Dc'(mm)	2	2.606	1.303	0.66	0.538	1.02
	Error	10	19.772	1.977	-	-	-
	Total	17	255.624	-	-	-	-
Vb'	M'	1	137.470	137.470	51.40	0.000	70.03
	Vc'(m/min.)	2	23.354	11.677	4.37	0.043	11.89
	Fo'(mm/rev.)	2	8.027	4.013	1.50	0.269	4.09
	Dc'(mm)	2	0.718	0.359	0.13	0.876	0.37
	Error	10	26.745	2.675	-	-	-
	Total	17	196.314	-	-	-	-
T'	M'	1	147.496	147.496	40.45	0.000	49.69
	Vc'(m/min.)	2	94.458	47.229	12.95	0.002	31.83
	Fo'(mm/rev.)	2	13.976	6.988	1.92	0.197	4.71
	Dc'(mm)	2	4.397	2.198	0.60	0.566	1.48
	Error	10	36.467	3.647	-	-	-
	Total	17	296.794	-	-	-	-

6.3.1 Surface roughness

Surface roughness is the measure of service period provided by a machined component. Low surface roughness reduces the stress points and makes an increment in the good service life period. This declined the wastage of energy and cost during machining by a high integrity surface of the machined component. Surface roughness during cryogenic turning with a direct supply of LN₂ at the interface of cutting tool and workpiece is low due to less adhesion between cutting tool insert and machined surface.

Figure 6.9 shows the experimental values of surface roughness in different machining conditions (dry and cryogenic with LN₂). It has been observed that values of surface roughness in dry machining condition L₁₈ DoE (1-9) is more than cryogenic (10-18). The surface phenomenon may be due to high friction and heat generated at the interface of tool and workpiece. The direct supply of LN₂ may wash away debris from the surface of workpiece which might reduce the possibility of debris to be entangled with workpiece and cutting insert and left a smoother surface

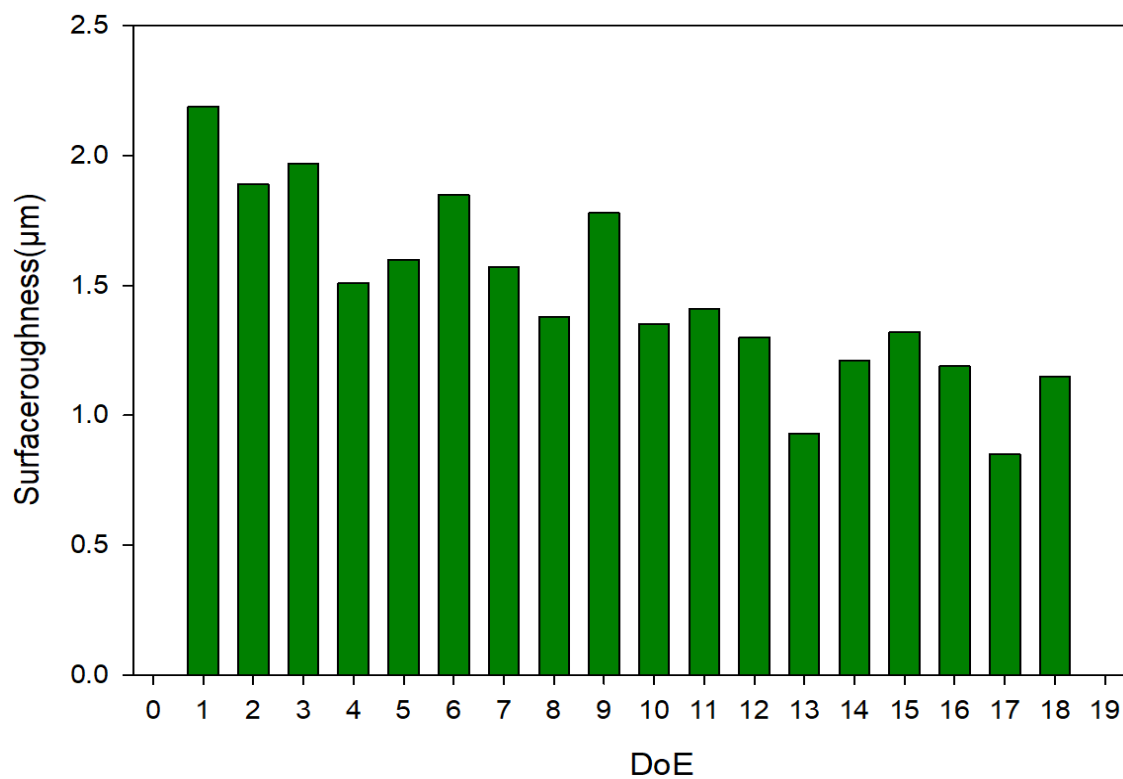


Figure 6.9 Experimental Ra' in accordance with DoE

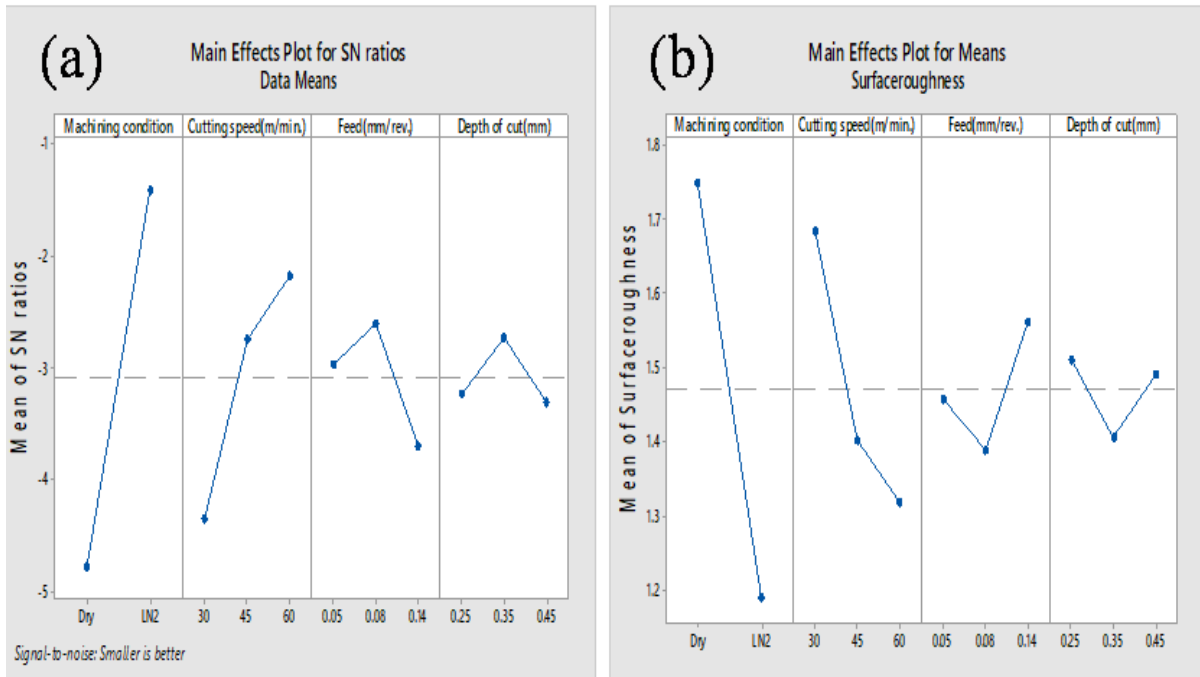


Figure 6.10 (a) Modification of mean S/N ratio Ra' (b) Modification of mean Ra' with various factor levels

Figure 6.10 (a) and Table 6.7 show the modification of mean S/N ratio of Ra'. Figure 6.10 (b) and Table 6.8 show modification of means Ra'. Turning with a direct supply of LN₂ at the interface of tool and workpiece declined surface roughness as compared to dry turning. Figure 6.10(b) shows on incrementing cutting speed surface roughness declined. On incrementing feed and depth of cut surface roughness declined and then increased. The graph shows the representation of both machining condition. Cryogenic cooling with direct supply of LN₂ has significant effect on values obtained of surface roughness. Table 6.7, shows optimum level value of surface roughness at machining condition (level 2 = LN₂), Vc' (level 3 = 60m/min.), Fo' (level 2 = 0.08mm/rev.) and Dc' (level 2 = 0.35mm).

The predicted value of the response is calculated from Eqs. (2) and (3). \overline{dp} is the S/N ratio calculated at optimum level, \overline{dp} is the average S/N ratios of all variables at optimum level, \overline{Mo} is the average s/n ratio when variable M (machining condition) is at optimum level, \overline{No} is the average s/n ratio when variable N (speed) is at optimum level, \overline{Fo} is the average s/n ratio when variable F (feed) is at optimum level and \overline{Do} is the average s/n ratio when variable D (depth of cut) is at optimum level, Rp is predicted responses for surface roughness, cutting force, cutting time, flank wear length and temperature. The predicted value of surface roughness has been calculated from Eqs. (7) and (8) is 0.75 μ m. ANOVA Table 6.9 for

response of surface roughness shows machining condition has the highest effect in percentage of contribution (62.42%), speed has a second higher effect on the percentage of contribution (18.67%), feed has a third higher effect on the percentage of contribution (4.47%) and the depth of cut has fourth higher effect on the percentage of contribution (1.40%). F- value shows the relative importance firstly machining condition, secondly speed, thirdly feed and lastly, is depth of cut. P- value is significant for speed. Since P- value is significant at the value of level equal or less than 0.05.

$$dp = \overline{dp} + (\overline{Mo} - \overline{dp}) + (\overline{No} - \overline{dp}) + (\overline{Fo} - \overline{dp}) + (\overline{Do} - \overline{dp}) \quad \text{Eq. (7)}$$

$$Rp = 10^{-dp/20} \quad \text{Eq. (8)}$$

6.3.2 Cutting force

Cutting force is created during the machining process is related to machining condition. In dry machining (without any coolant) the magnitude of cutting force is large. In wet machining, the magnitude of cutting force is comparatively low

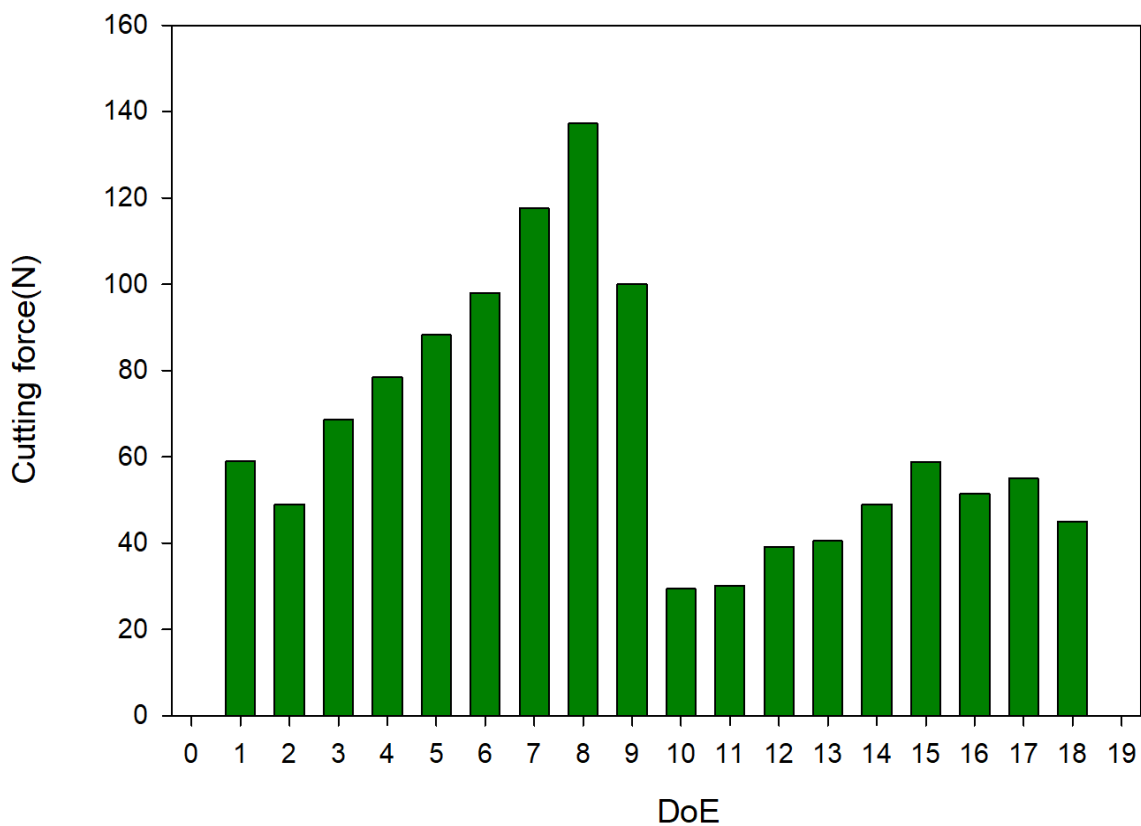


Figure 6.11 Experimental Fc' in accordance with DoE

This may be due to low friction and better cooling and lubrication. But, with the emergence of hard engineering materials, the conventional cutting fluid is not sufficient. The effective alternative may be presently liquid nitrogen. Figure 6.11 shows the experimental values of cutting force in different machining conditions (dry and cryogenic with LN₂). It has been observed that values of cutting force in dry machining condition L₁₈ DoE (1-9) is more than cryogenic (10-18). This may be due to high friction and heat generated at the interface of tool and workpiece. Cryogenic cooling with direct supply of LN₂ has significant effect on values obtained during experimentation. Cutting force is low during cryogenic turning with a direct supply of LN₂ as compared to dry turning due to better lubrication effect created by liquid nitrogen at tool (rake face) chip interface and newly machined surface with the flank face of the cutting tool due to the formation of the fluid. This has reduced adhesion between interacting surfaces

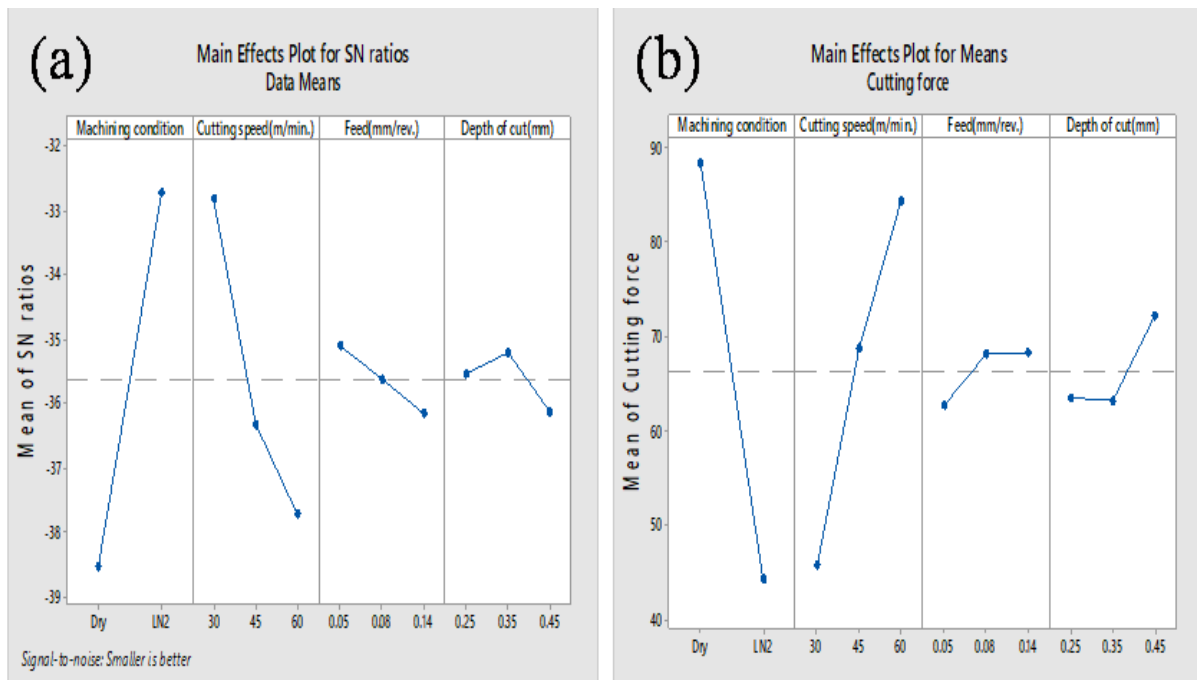


Figure 6.12(a) Modification of S/N Fc' (b) Modification of means Fc' with various factor levels

Figure 6.12(a) and Table 6.7 show modification of S/N ratio of Fc' Figure 6.12(b) and Table 6.8 show modification of means of Fc'. On incrementing Vc', Fo' and Dc' mean of cutting force has been incremented (a) Modification of S/N Fc' (b) Modification of means Fc' with various factor levels eased. Table 6.7 shows optimum level of cutting force at machining (level 2 = LN₂), Vc' (level 1 = 30m/min.), Fo' (level 1 = 0.05mm/rev.) and Do' (level 2 = 0.35mm). The predicted value of cutting force has been calculated from Eqs. (7) and (8) is

28.01N. ANOVA Table 6.9 for response of cutting force shows machining condition has the highest effect on percentage of contribution (59.77%), speed has a second higher effect on the percentage of contribution (30.14%), feed has third higher effect on the percentage of contribution (1.34%) and depth of cut has fourth higher effect on the percentage of contribution (1.02%). F- value shows the relative importance firstly machining condition, secondly speed, thirdly feed and lastly is depth of cut. P- value is significant for machining condition and speed.

6.3.3 Tool wear (Flank wear length)

Tool wear is related to machining condition, tool material and workpiece material. Abrasion and adhesion phenomena are present in flank wear mechanism. Flank surface rubbed with the workpiece which acts as a resultant for dimensional change of cutting edge. The mechanism liable for the occurrence of crater wear is abrasion, adhesion and diffusion. The sliding motion of chip over the rake surface generates high temperature favouring diffusion phenomenon

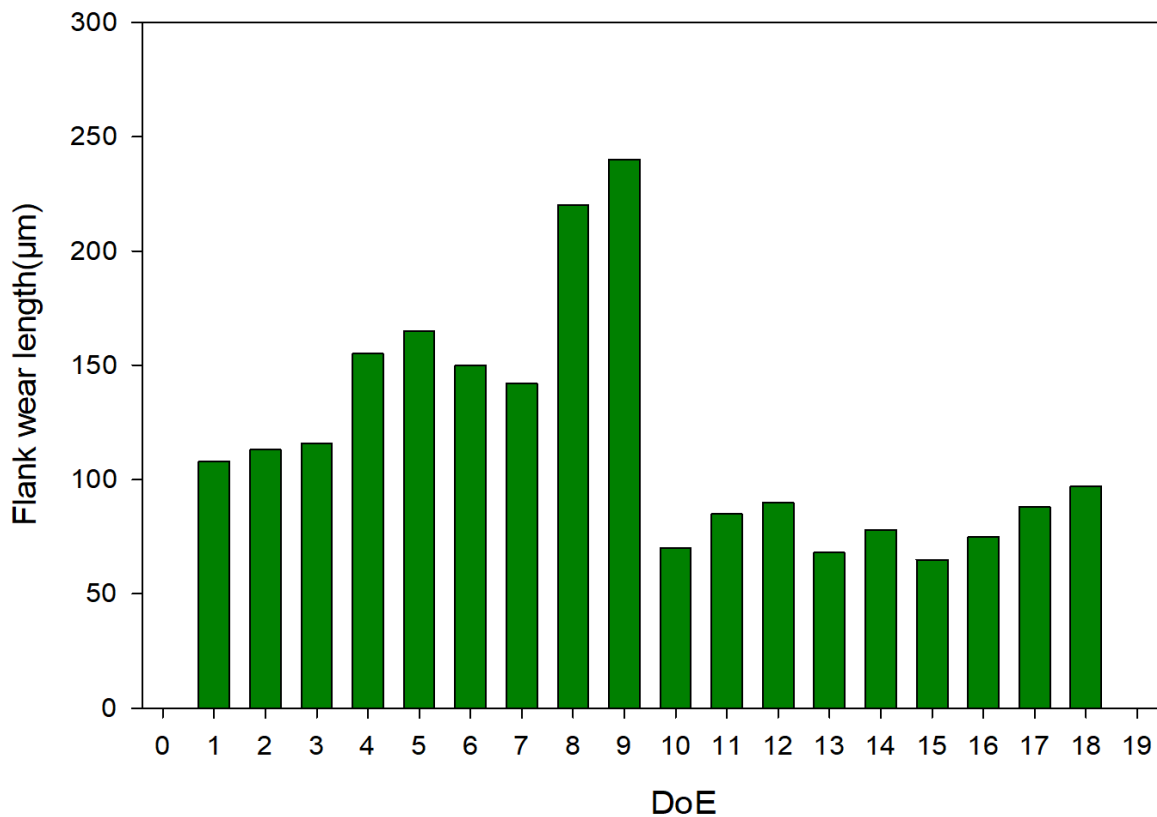


Figure 6.13 Experimental Vb' in accordance with DoE

Figure 6.13 shows the experimental values of flank wear length in different machining conditions (dry and cryogenic with LN₂). It has been observed that values of flank wear length in dry machining condition L₁₈ DoE (1-9) is more than cryogenic (10-18). Flank wear length was more due to high the temperature created at the interface of tool and workpiece LN₂ supply at the interface of cutting tool and workpiece built a film which minimized the direct contact of freshly cut material with atmosphere resulted into lower tool wear.

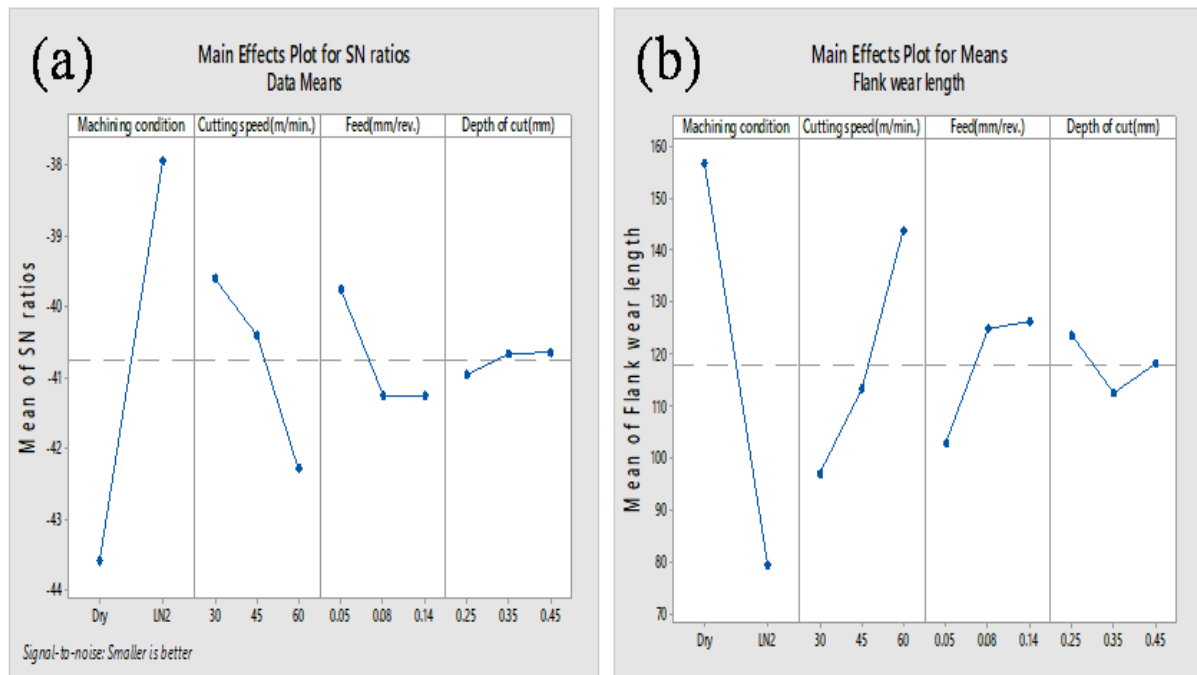


Figure 6.14 (a) Modification of S/N of Vb' (b) Modification of mean Vb' at various factor levels

Figure 6.14(a) and Table 6.7 show modification of S/N ratio of Vb'. Figure 6.14(b) and Table 6.8 show modification of mean of Vb' and on incrementing speed and feed tool wear has increased. On incrementing depth of cut flank wear length marginally decreased than increased. This may be due to a higher cooling efficiency of LN₂. At low cutting speed and depth of cut, flank wear is a marginal difference in dry and cryogenic machining. Table 6.7 shows optimum level of flank wear length at machining (level 2 = LN₂), Vc' (level 1 = 30m/min.), Fo' (level 1 = 0.05mm/rev.) and Dc' (level 2 = 0.35mm). The predicted value of flank wear length has been calculated from Eqs. (7) and (8) is 61.97µm. ANOVA Table 6.9 for response of flank wear length shows machining condition has the highest effect on the percentage of contribution (70.03%), speed has a second higher effect on the percentage of contribution (11.89%), feed has a third higher effect on the percentage of contribution

(4.09%) and depth of cut has fourth higher effect in the percentage of contribution (0.37%) F-value shows the relative importance firstly machining condition, secondly speed, thirdly feed and lastly is depth of cut. P-value is significant for machining condition and speed.

6.3.4 Temperature

Temperature at the interface of tool and workpiece is important in relating tool wear and surface integrity of the machined component. High temperature leads to more tool wear and not good surface properties. Figure 6.15 shows the experimental values of temperature in different machining conditions (dry and cryogenic with LN₂). It has been observed that values of temperature in dry machining condition L₁₈ DoE (1-9) is more than cryogenic (10-18). To reduce the temperature LN₂ is directly supplied at the interface of tool and workpiece. Due to high heat removing rate LN₂ is highly efficient in reducing the temperature in short time duration as compared to conventional cooling fluids.

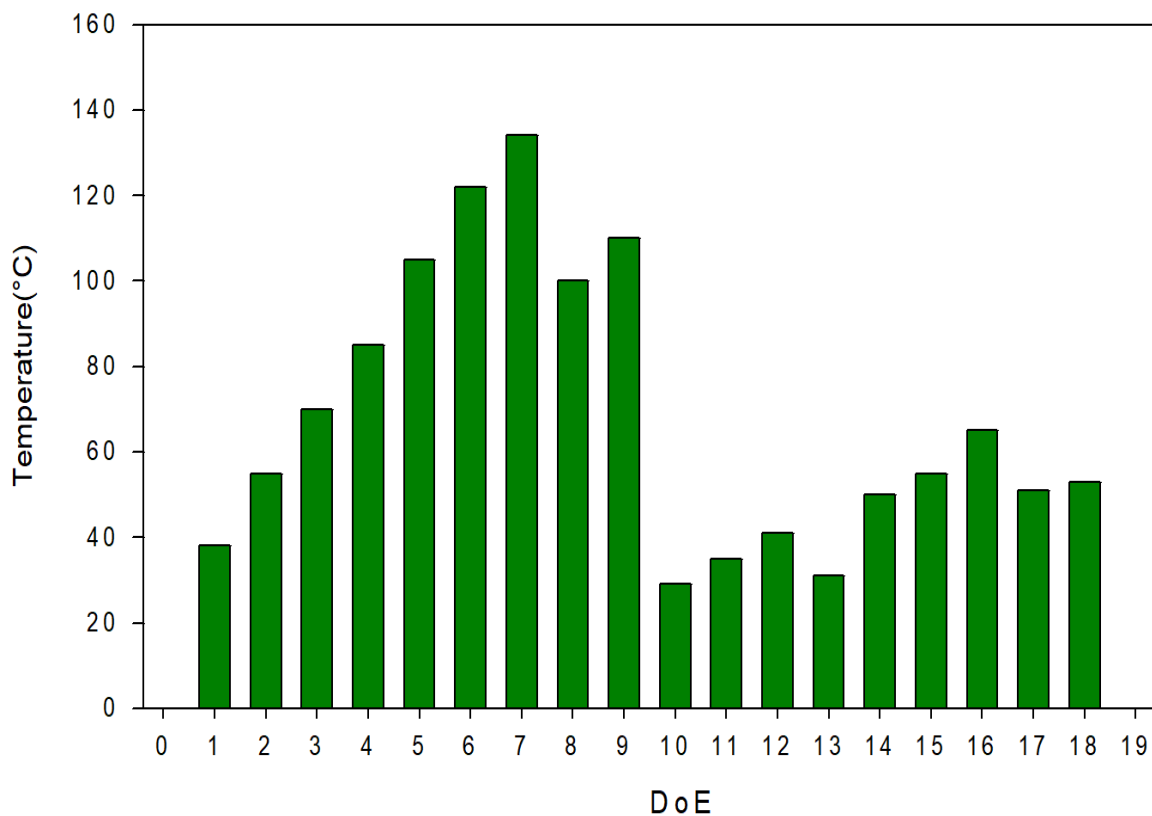


Figure 6.15 Experimental T' in accordance with DoE

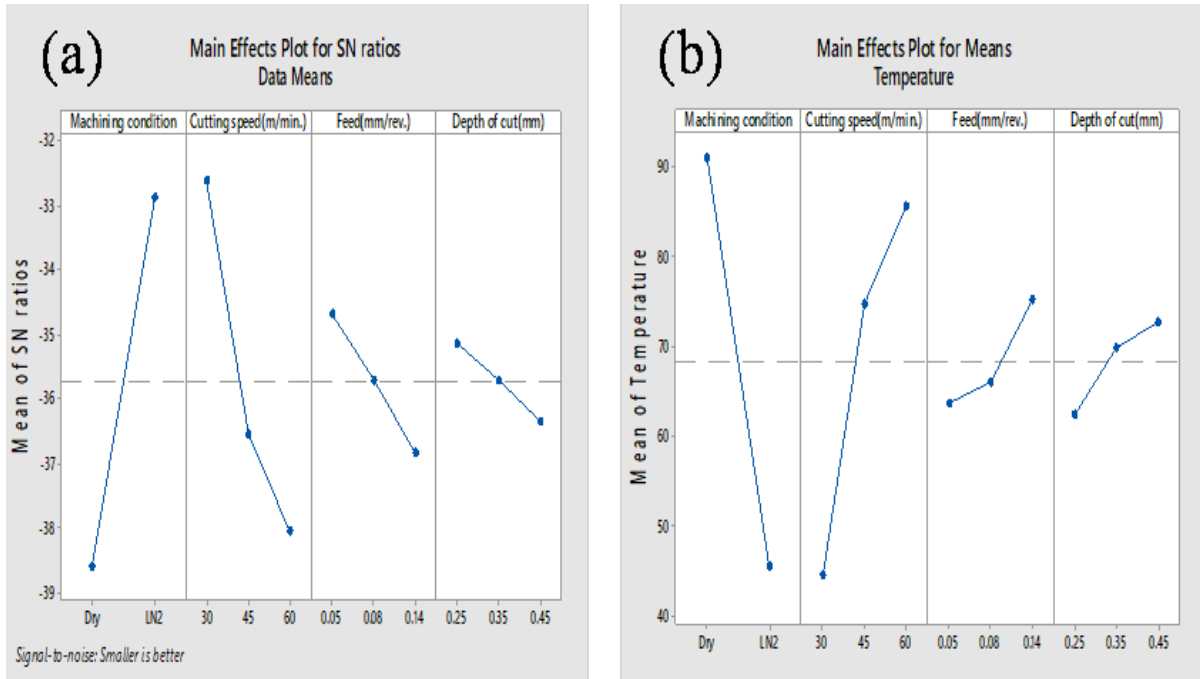


Figure 6.16(a) Modification of mean S/N of T'(b) Modification of mean temperature T' at various factors

Figure 6.16(a) and Table 6.7 show modification of mean of S/N of T'. Figure 6.16(b) and Table 6.8 show the modification of mean of T'. On incrementing V_c' , F_o' and D_c' temperature at the interface of cutting insert and workpiece increased. Table 6.7 shows optimum level of temperature at machining (level 2 = LN2), V_c' (level 1 = 30m/min.), F_o' (level 1 = 0.05mm/rev.) and D_c' (level 1 = 0.25mm). The predicted value of temperature has been calculated from Eqs. (7) and (8) is 25.40°C.

ANOVA Table 6.9 for response of temperature shows machining condition has the highest effect in percentage of contribution (49.69%), speed has a second higher effect on the percentage of contribution (31.83%), feed has a third higher effect on the percentage of contribution (4.71%) and depth of cut has fourth higher effect in the percentage of contribution (1.48%).

P- value was significant for machining condition and speed.

6.3.5 Confirmation Experiments

In Taguchi method Confirmation experiments were performed to calculate the difference between actual values and predicted values of response at optimum levels. If the reliability of the condition is assumed to be 95%, then confidence level (CI) is calculated from Eqs. (9) and (10) [210].

$$CI = \sqrt{\left[F(\alpha, 1, fe) Ve \left\{ \left(\frac{1}{Ne} \right) + \left(\frac{1}{R} \right) \right\} \right]} \quad \text{Eq. (9)}$$

$$Ne = \frac{N}{(1+Td)} \quad \text{Eq. (10)}$$

Where, $F(\alpha, 1, fe)$ is the F-ratio required for $100(1 - \alpha)$ percent confidence level, fe is DOF for error =10, $Ve = \text{AdjMs for error}$, $N = \text{total number of experiment (18)}$, $R = \text{number of replications for confirmation of experiments (0)}$ and $Td = \text{total degree of freedom associated with mean optimum is (7)}$. From standard statistical table, the value of F ratio for $\alpha = 0.05$ is $F(0.05, 1, 10) = 4.96$. Substituting values from ANOVA Table 6.9 with the respective responses. CI value of surface roughness (Ra') is $\pm 1.53\mu\text{m}$, cutting force (Fc') is $\pm 2.09\text{N}$, flank wear length (Vb') is $\pm 2.42\mu\text{m}$ and temperature (T') is $\pm 2.84^\circ\text{C}$.

Experiments have been performed with respective optimum cutting parameters for responses. Surface roughness is $0.80\mu\text{m}$, cutting force is 28N , flank wear length is $63\mu\text{m}$ and temperature is 26°C during machining condition of LN_2 .

The values of responses obtained are within the range of confidence level (CI). The regression models have been generated for studying the relationship between machining parameters and the correlation between independent and dependent parameters

From Table 6.10, this has been observed that R-Sq value is greater than 75% and approaches more than 90% with and a good correlation was obtained between cutting parameters and experimental outputs.

Table 6.10 Regression models

Response	Regression Models	R-Sq
Ra'	$2.586 - 0.5589 M' - 0.1825 Vc'(m/min.) + 0.0525 Fo'(mm/rev.) - 0.0092 Dc' (mm)$	83.02%

Fc'	79.9- 44.16 M'+ 19.24 Vc'(m/min.)+ 2.77 Fo'(mm/rev.) + 4.36 Dc'(mm)	84.58%
Vb'	168.9- 77.0 M'+ 23.33Vc'(m/min.)+ 11.67 Fo'(mm/rev.)- 2.67 Dc'(mm)	77.85%
T'	73.8- 45.44 M'+ 20.42 Vc'(m/min.)+ 5.75 Fo'(mm/rev.) + 5.17 Dc'(mm)	81.09%

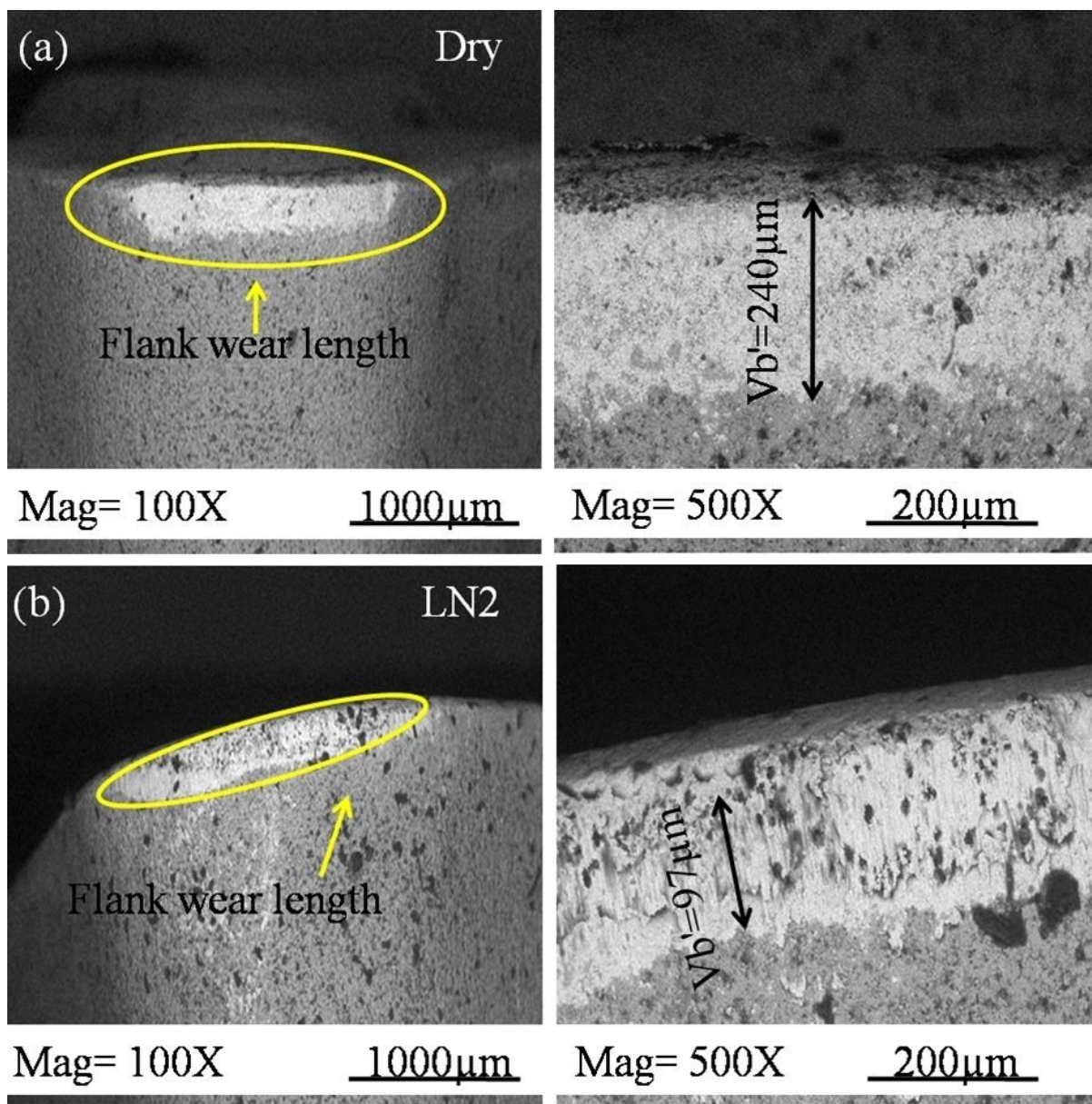


Figure 6.17 (a) SEM image of the used cutting insert during dry turning at Vc' 60m/min., Fo' 0.14mm/rev. & Dc' 0.35mm (b) cryogenic turning with LN₂.

It has been shown in Figure 6.17(a) that at machining parameters of V_c' 60m/min., F_o' 0.14mm/rev. & D_c' 0.35mm during dry turning that flank wear length was 240 μ m and 97 μ m during cryogenic turning with direct supply of LN₂ at the interface of cutting tool insert and workpiece. The property of LN₂ in removing heat generated quickly and released to the surrounding atmosphere was responsible factor. The fluid film developed between the tool and workpiece reduced friction and provided the strength to tool material.

6.3.6 Surface morphology

The surface generated during dry turning has high surface roughness with some adhesives as shown in SEM image Figure 6.18(a). The feed marks are wider in EDS image Figure 6.18(b) shows high peaks of iron followed by chromium, carbon and sulphur. The surface generated during cryogenic turning has low surface roughness and narrow feed marks with a clean and smooth surface as shown in Figure 6.19(a) EDS image Figure 6.19(b) show high peaks of iron and other elements. This may be due to low temperature and high pressurised jet takes away adhesive particles from the machined surface.

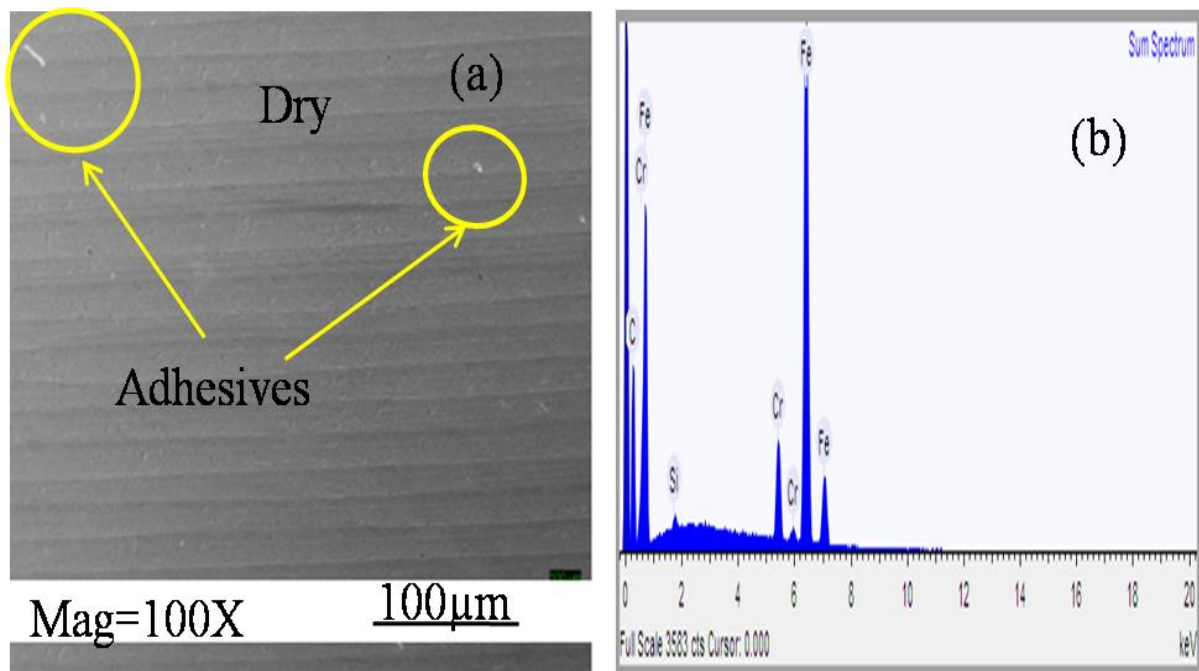


Figure 6.18 (a) SEM image (b) EDS of the machined surface during dry turning at V_c' 60m/min., F_o' 0.14mm/rev. and D_c' 0.35mm

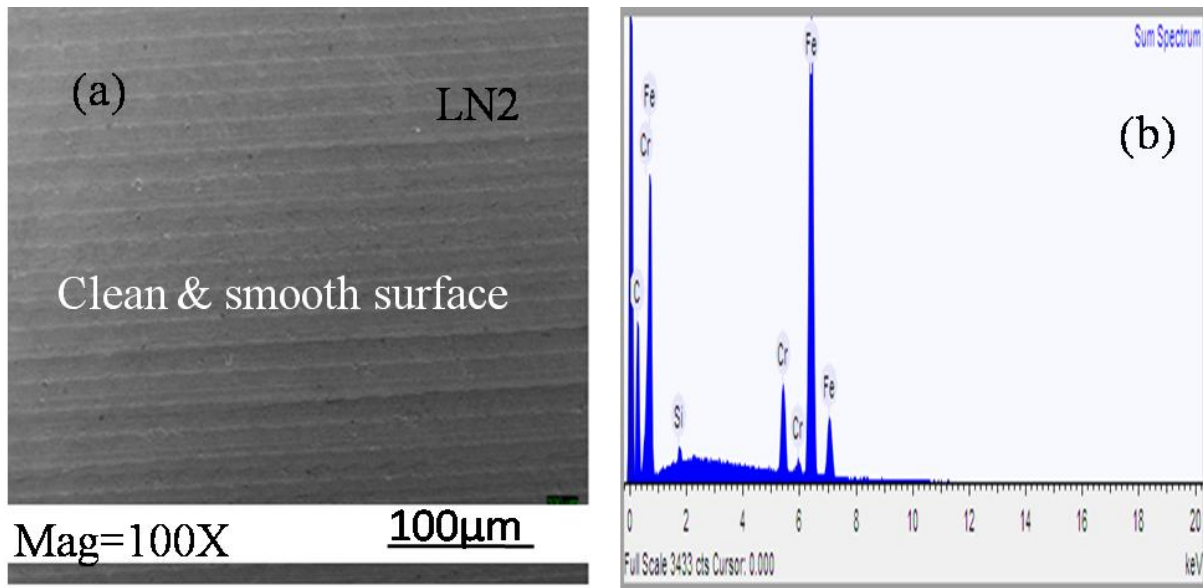


Figure 6.19 (a) SEM image (b) EDS of the machined surface during cryogenic turning with LN_2 at V_c' 60m/min., F_o' 0.14mm/rev. and d_c' 0.35 mm

6.4 Experiments on lathe machine with wet and nano-cutting fluids

The experiments were performed on lathe machine with conventional cutting with an emulsion with water in (1:20) ratio (w/w) is termed as wet. Nano-cutting fluid made with nano particles TiO_2 is termed as Nano A and Nano cutting fluid with nanoparticles Al_2O_3 is termed as Nano B during turning at V_c' 60m/min., F_o' 0.14mm/rev. and d_c' 0.35 mm. The conventional cutting fluid, Nano A and Nano B were supplied at the interface of single point cutting tool and workpiece through specially self made delivery system which supplied fluids dropwise in a controlled manner with negligible wastage.

6.4.1 Surface roughness

The requirement of lower surface roughness and eliminating wastage of cutting fluids etc. is a path towards sustainable machining process. The effective cooling and lubricating through cutting fluids provide a better surface morphology of workpiece.

It has been depicted in Figure 6.20 that surface roughness was more during dry turning then declined towards with wet, Nano A, Nano B and direct supply of LN_2 .

The cryogenic turning with LN_2 had lower surface roughness.

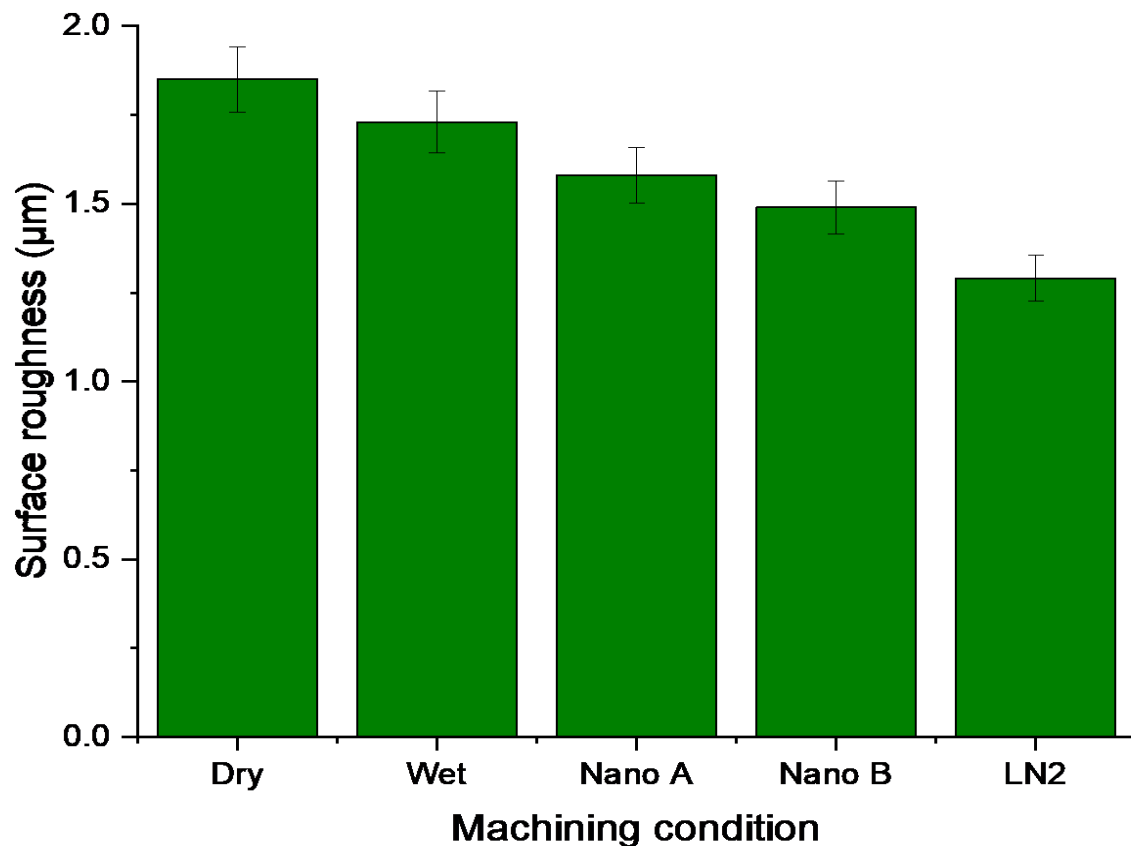


Figure 6.20 Surface roughness (μm) during different machining conditions

6.4.2 Tool Wear (Flank Wear length)

Tool wear is associated with the temperature generated during machining process. The high temperature may affect material by plastic deformation. Therefore, to keep the temperature lower cutting fluids are used. According to tool, workpiece material and machining parameters cutting fluids are selected and discovered.

The change in composition of cutting fluids give better results.

It has been depicted that flank wear length was more during dry turning then became progressively lower with wet, NanoA, Nano B and LN₂

The cryogenic cooling with LN₂ gave lower flank wear length as compared with other machining conditions.

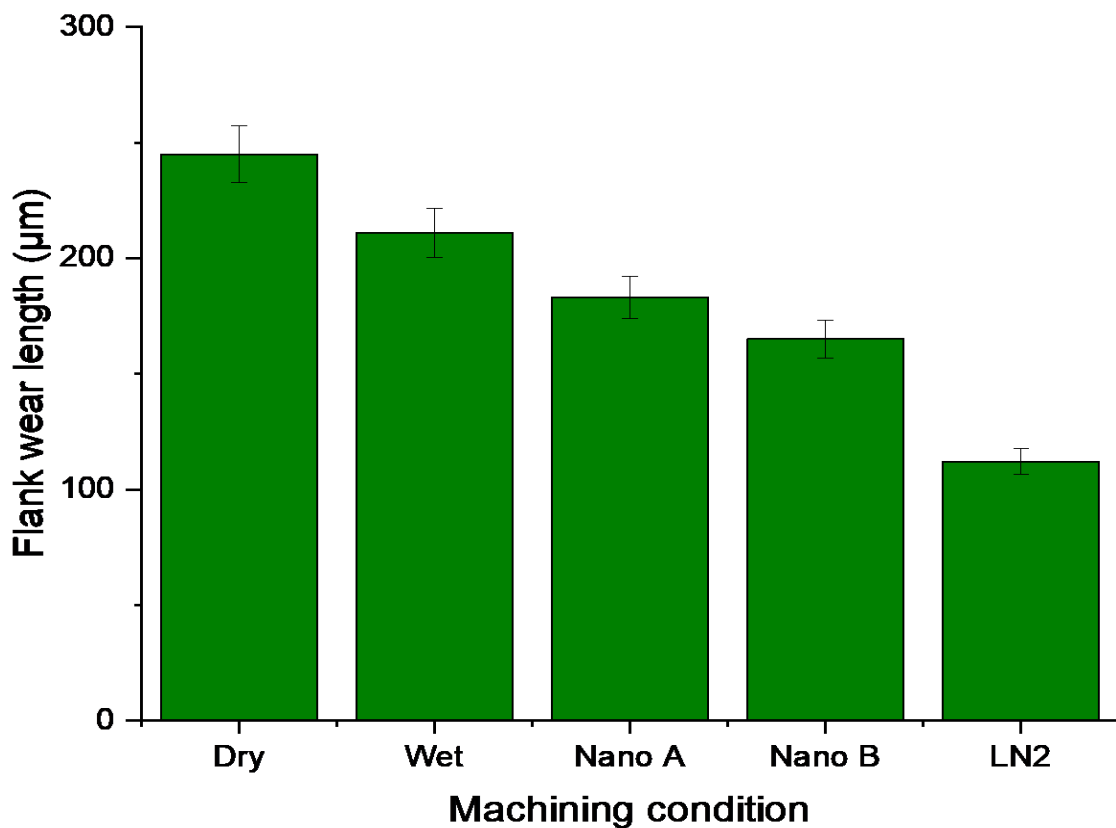


Figure 6.21 Flank wear length (μm) during different machining condition

6.4.3 Cutting Force

The cutting force may be related to the machining condition. In dry turning, the workpiece and cutting tool insert was in direct contact to each other which may increase the friction and enhance rise in cutting force.

It has been shown in Figure 6.22 that cutting force was more dry machining condition as compared to other

In accordance to type of cooling process, it was found that cutting force was lower in LN₂ direct supply at the interface of cutting insert and workpiece.

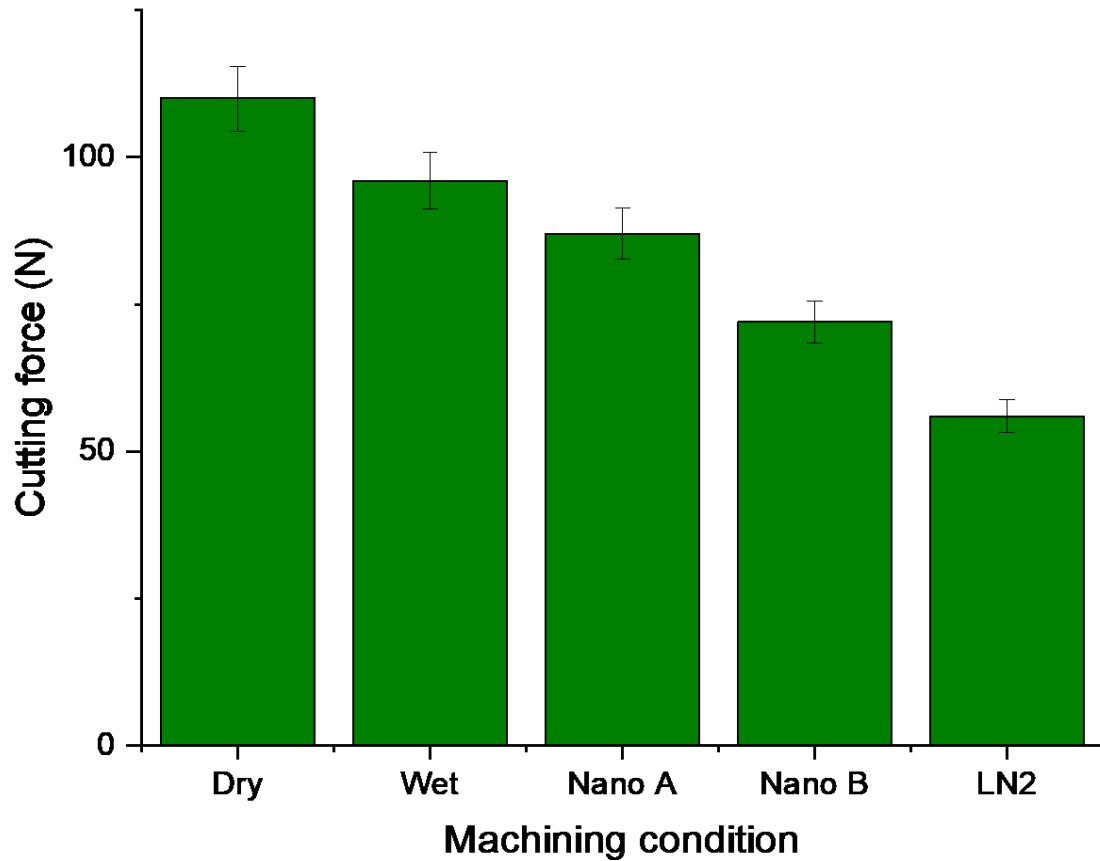


Figure 6.22 Cutting force (N) during different machining condition

6.4.4 Temperature

The temperature was measured at the end of the machining operation. In dry machining due to high friction the temperature was higher than other cooling methods. The coefficient of heat transfer is important.

The high value of coefficient of heat transfer quickly absorbs the heat and releases into atmosphere at faster rate.

It has been shown in Figure 6.23 that temperature was higher during dry machining. With supply of coolants it became progressively lower.

The value of temperature was lower with direct supply of LN2 at the cutting tool and workpiece.

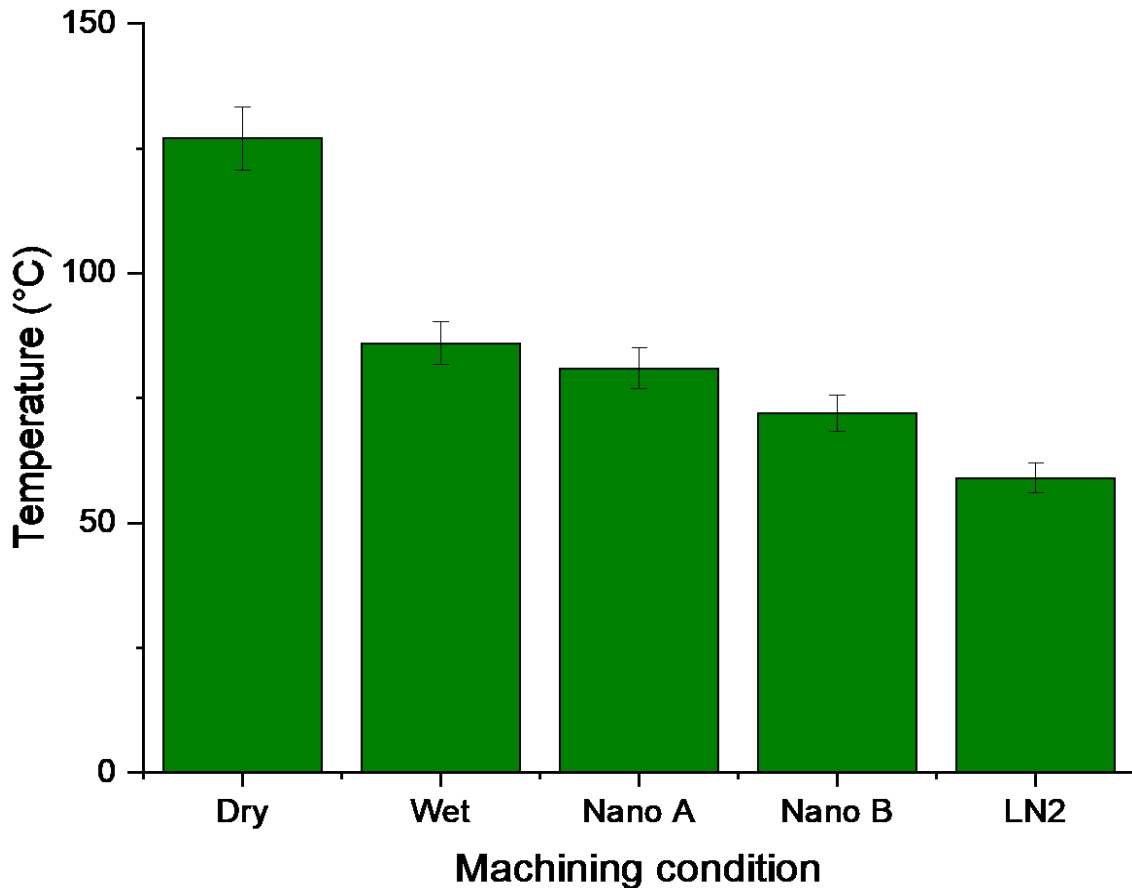


Figure 6.23 Temperature (°C) during different machining condition

6.4.5 Machining time

The machining time was calculated with a dedicated digital stop watch. The time period was observed between start and end of cut. The theoretical time was calculated with Eq. (11)

$$\text{Machining time(seconds)} = \frac{\pi \times D \times L}{f \times V \times 1000} \quad \text{Eq. (11)}$$

Where, π is 3.14, D is diameter of workpiece (mm), L is length of machining, f is feed (mm/rev.) and V is Cutting velocity (m/sec.)

The theoretical machining time calculated = 42.39 seconds.

The machining time during dry turning was 49.31seconds.

The higher machining time during dry machining may be due to high friction, hardness of tool and workpiece material which were not taken into consideration during calculation of theoretical machining time.

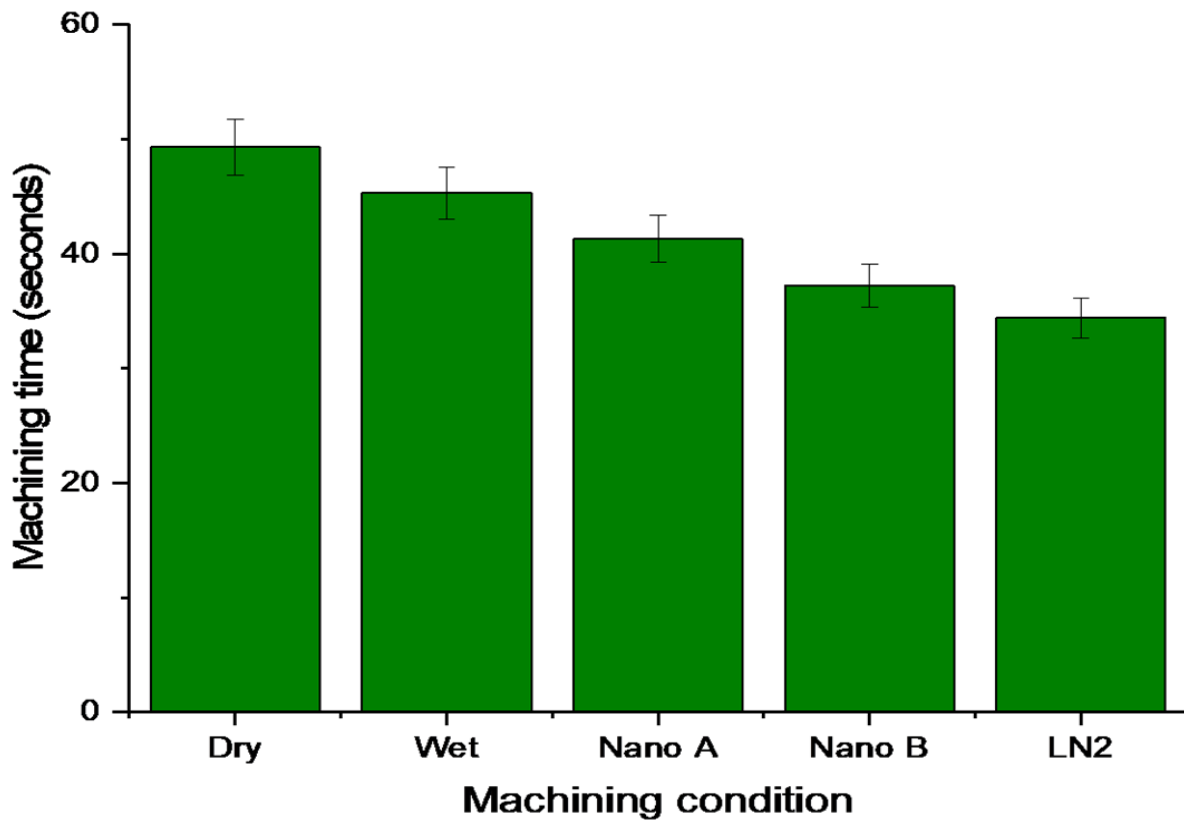


Figure 6.24 Machining time (seconds) during different machining conditions

It has been shown in Figure 6.24 that machining time declined with the cooling capacity of coolants used during different machining conditions. LN₂ supply shows lower machining time as compared to others due to high effectiveness in providing cooling and fluid film generated between cutting tool and workpiece reduced friction and supported faster tool movement.

6.4.6 Chip compression ratio

The chips were collected during different machining conditions. The ratio of deformed chip thickness to undeformed chip thickness is defined as the chip compression ratio by utilizing Eq. (12).

$$\psi = \frac{t_d}{t_u} \quad \text{Eq. (12)}$$

Chip compression ratio showed the frictional condition on the tool surface. From Figure 6.25 it was found that chip compression ratio was more than 2 for dry machining. Further with the use of coolants it become progressively lower. The cooling efficiency decreased chip compression ratio.

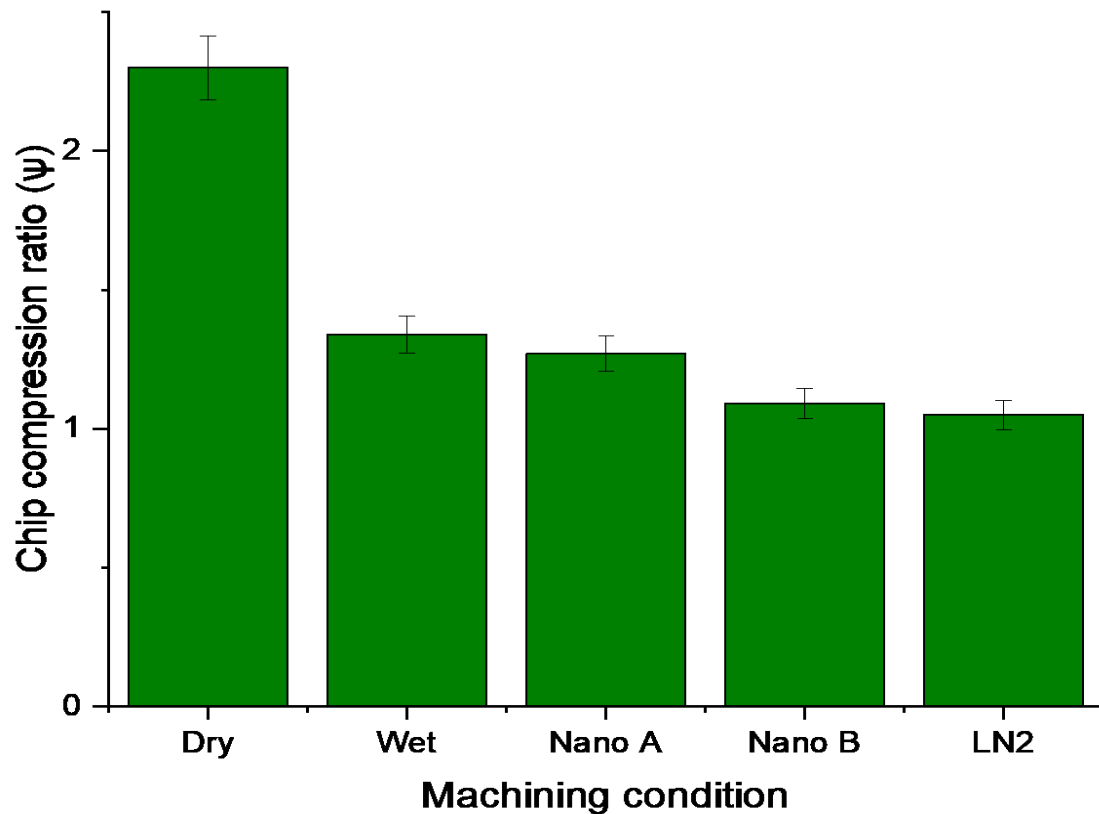


Figure 6.25 Chip compression ratio (ψ) during different machining condition

Summary

- Taguchi based design of experiments L_{18} [OA] have been used for understanding wear volume loss of pin during dry and cryogenic cooling with LN_2 supply at the interface of pin and disc tribometer has been discussed.
- Wear behaviour mechanism of pin and wear tracks of is shown.

- Optimization of sliding parameters which was supported by ANOVA and confirmation test was performed
- A comparative effect of different sliding conditions like dry, wet, Nano A, Nano B and LN₂ on coefficient of friction and specific wear rate is discussed
- Taguchi based design of experiments L₁₈ [OA] have been used for understanding surface roughness, tool wear, cutting force and temperature during dry and cryogenic cooling with LN₂ supply at the interface of pin and disc tribometer have been discussed.
- Optimization of machining parameters and machining condition is discussed and supported by ANOVA
- Confirmation tests were performed and results are shown
- A comparative effect of different machining condition on surface roughness, tool wear, cutting force, temperature, machining time, chip compression ratio has been discussed.S

CONCLUSIONS AND FUTURE SCOPE

This chapter has the content of salient conclusions drawn after the performance of experiments and analysis of results gathered. An introduction regarding some ways of extension of presented research work into new the dimensions of future scope have been enlightened.

Turning of workpiece require appropriate cutting fluid for the definite shape and size of the product. The exhaustive literature review has been carried out for finding the research gap and objective of the work. The experiments were carried on Tribometer and Lathe at room condition and other created cryogenic condition. Following conclusions have been made from this study:

The experimentation on pin-on-disc tribometer as per ASTM G-99 has been carried out

- Dry condition: The coefficient of fiction was 0.93 and specific wear rate was $4.365 \times 10^{-5} \text{mm}^3/\text{Nm}$. FSEM images of pin showed adhesion and abrasion wear mechanism. On higher magnification edge fracture was observed.
- Wet with conventional cutting fluid: On comparing with dry condition, coefficient of fiction was lowered by 4.3% and specific wear rate was lowered by 22.5%.
- Nano-cutting fluid TiO_2 : On comparing with dry condition, coefficient of fiction was lowered by 12.9% and specific wear rate was lowered by 29.5%.
- Nano-cutting fluid Al_2O_3 : As compared with dry condition, coefficient of fiction was lowered by 15% and specific wear rate was lowered by 37.92%.
- Cryogenic cooling with LN_2 : As compared with, coefficient of fiction was lowered by 17.2% and specific wear rate was lowered by 98.5%. FSEM images of pin showed clean smooth surface.
- The experimentation on lathe machine has been carried out
- Dry condition: Surface roughness, flank wear length, cutting force, temperature , machining time and chip compression ratio were found at $1.85 \mu\text{m}$, $245 \mu\text{m}$, 110N, 127°C , 49.31seconds and 2.3 respectively. SEM images showed that flank surface

rubbed with the workpiece which acted as a resultant for dimensional change of cutting edge. The mechanism liable for the occurrence of crater wear was abrasion, adhesion and diffusion. The sliding motion of chip over the rake surface generates high temperature was favouring diffusion phenomenon.

- Wet with conventional cutting fluid: Surface roughness, flank wear length, cutting force, temperature, machining time and chip compression ratio were lowered by 6.48%, 13.87%, 12.72%, 32.28%, 8.09% and 41.73% on comparing with respective values during dry machining condition.
- Nano-cutting fluid TiO_2 Surface roughness, flank wear length, cutting force, temperature, machining time and chip compression ratio decreased by 14.59%, 25.31%, 20.91%, 36.28%, 16.26% and 44.78% on comparing with respective values during dry machining condition.
- Nano-cutting fluid Al_2O_3 Surface roughness, flank wear length, cutting force, temperature, machining time and chip compression ratio were declined by 19.45%, 32.65%, 34.54%, 43.31%, 24.54% and 52.61% on comparing with respective values during dry machining condition.
- Cryogenic cooling with LN_2 Surface roughness, flank wear length, cutting force, temperature, machining time and chip compression ratio were declined by 30.27%, 54.28%, 49.09%, 53.54%, 30.26% and 54.35% on comparing with respective values during dry machining condition. The surface generated during cryogenic turning had low surface roughness and narrow feed marks with a clean and smooth surface.
- Biocompatible surfactant did not produce any harmful effects to hands and human skin during contact during performing experiments on pin-on-disc tribometer and lathe machine.
- The dropwise supply of nano-cutting fluids saved the quantity and did not produce any sedimentation of particles during the entire process of experimentation.
- The mechanism which may be responsible for the nano-cutting fluids was rolling effect. The nanoparticles along with fluid made a film between the cutting tool and workpiece which acted like ball bearing and reduced the friction.
- The chip compression ratio was higher for dry turning and decreased with the coolants supply at the interface of cutting tool and workpiece.
- The chips generated during dry turning were thick, close coiled and bluish in colour.

- The chips generated with nano-cutting fluids were comparatively thin, open coiled and white in colour.
- The chips generated during cryogenic cooling with LN₂ were open coiled with most of the material flow on either of the side.
- The machining time progressively lower for cryogenic cooling which may be due to high rate heat transfer capacity.
- The results showed progressive decrease of surface roughness, flank wear length, cutting force, temperature, machining time and chip compression ratio in respective machining conditions of dry, wet, nano cutting fluid TiO₂, nano-cutting fluid Al₂O₃ and cryogenic with LN₂.
- It has been found through rigorous experiments that nano-cutting fluid with Al₂O₃ was better than dry, wet, nano-cutting fluid with TiO₂ and cryogenic LN₂. The wastage of nano-cutting fluid has been found very low or negligible as compared with cryogenic cooling with LN₂.

Future Scope

1. The selection of cutting tool and workpiece material can be changed like cubic boron carbide as cutting tool material and aerospace material
2. Hybrid combinations of nano-cutting fluids can be made with the change in different compositions.
3. Refrigerated closed-loop cycle can be used with nanofluid in tribometer
4. Models with Grey analysis and Fuzzy cycles can be made for analyzing the results.
5. EDX analysis may be done on the chips for understanding the adhering of nanoparticles to them surfaces and then discussion.
6. SEM micrographs may be taken from worn or machined surfaces for dry, wet, nanoA and nanoB, and LN₂ may be discussed and given as an evidence for lower or higher wear.
7. The effects of LN₂ may also depends on altered material properties of the tip and the workpiece by the cryogenic heat treatment applied during the tests and machining durations. The effects of change of properties can be done in future research work.

Summary

- The major conclusions are discussed with comparative percentage with dry sliding condition for pin-on-disc tribometer and dry machining condition for lathe machine
- The lower numerical value was obtained during cryogenic cooling with LN₂ supply
- The results with nano cutting fluid with nanoparticles Al₂O₃ were better considering the self made delivery system with controlled supply drop wise without any wastage at the interface of pin and disc on (pin-on-disc tribometer) and cutting tool insert with workpiece on lathe machine.
- The wear mechanism involved during dry and cryogenic sliding conditions has been discussed for pin-on disc tribometer.
- The wear mechanism involved during dry and LN₂ machining condition have been discussed for lathe machine
- The wear mechanism involved during nano-cutting fluid during turning and pin-on-disc have been discussed
- The compression ratio of chips and nature of generated are discussed
- Some future scope and extension of present research work are discussed.

References

1. Sahoo P., "Engineering Tribology", (2015) PHI Learning, ISBN-978-81-203-2724-5.
2. Hirani H., "Tribology", <http://www.nptelvideos.in/2012/12/tribology.html>.
3. Juneja B. L., Sekhon G. S., Seth N., "Fundamentals of metal cutting and machine tools", (2015) New age international (p) limited, ISBN-978-81-224-1467-7.
4. Bhattacharyya A., "Metal cutting, theory and practice", (2006) New central book agency, ISBN-81-7381-228-4.
5. Boothroyd G., Knight W. A. "Fundamentals of machining and machine tools", (1988) CRC Press, ISBN-08247-7852-9.
6. Sen G. C., Bhattacharyya A., "Principles of machine tools", (2013) New central book agency, ISBN-978-81-7381-155-5.
7. Goindi G. S., Sarkar P., "Dry Machining: A Step towards Sustainable Machining - Challenges and Future Directions", *Journal of Cleaner Production*, vol. (2017) doi: 10.1016/j.jclepro.2017.07.235.
8. Deshpande S. Deshpande Y., "A review on cooling systems used in machining processes", *Materials Today: Proceedings*, vol. 18 (2019) 5019-5031.
9. Chetan, Behera B.C., S Ghosh S., Rao P.V., "Application of nanofluids during minimum quantity lubrication: A case study in turning process", *Tribology International*, vol.101, (2016) 234–246.
10. Rech J., "Influence of cutting tool coatings on the tribological phenomenon at tool chip interface in orthogonal dry turning", *Surface & Coatings Technology*, vol. 200 (2006) 5132-5139.
11. Samad M. A., Satyanarayana N., Sinha S.K., "Tribology of UHMWPE film on air-plasma treated tool steel and effect of PFPE overcoat", *Surface & Coatings Technology*, vol. 204 (2010) 1330-1338.
12. Jin J., Chen Y., Gao K., Huang X., "The effect of ion implant at on tribology and hot rolling contact fatigue of Cr4Mo4Ni4N bearing steel", *Applied Surface Science*, vol. 305 (2014) 93-100.
13. Barnes C. J., Childs T. H. C., Henson B., Southee C. H, "Surface finish and touch a case study in a new human factors tribology", *Wear*, vol. 257 (2004) 740-750.
14. Tichy J. A., Meyer D. M., "Review a solid mechanics in Tribology", *International Journal of Solids and Structures*, vol. 37 (2000) 391-400.

15. Olah N., Forgarassy Z., Sulyok A., Szivos J., Csanadi T., “Ceramic TiC/a: C protective nano- composite coatings: Structure and composition versus mechanical properties and tribology”, *Ceramics International*, vol. 42 (2016) 1215-1220.
16. Kovalchenko A. M., Milman Y. N., “On the cracks self healing mechanism at ductile mode cutting of silicon”, *Tribology International*, vol. 80 (2014) 166-171.
17. Kopac J., Sokovic M., Dolinsek S., “Tribology of coated tool in conventional HSC machining”, *Journal of Materials Processing Technology*, vol. 118 (2001) 377-384.
18. Errico G. E. D., Bugliosi S., Guglielmi E., “A tribological evolution of coated cermets system for cutting tools”, *Surface coatings & Technology*, vol. 94-95 (1997) 627-631.
19. Rechberger M., Paschke H., Fischer A. Bertling J., “New tribological strategies for cutting tools following nature”, *Tribology International*, vol. 63 (2013) 243-249.
20. Chardon G., Klinkova O., Rech J., Drapier S., Bergheau J.M., “Characterization of friction properties at work material/cutting tool interface during machining of randomly structured carbon fibers reinforced polymer with polycrystalline diamond tool under dry conditions”, *Tribology International*, vol. 81 (2015) 300-308.
21. Bonnet C., Valigorgve F., Rech J., Claudin C., Hamdi H, Bergheau J.M., Gilles P. “Identification of friction model—application to the context of dry cutting of an AISI 316L austenite stainless steel with Tin Coated carbide tool”, *International Journal of Machine Tools & Manufacture*, vol. 48 (2008) 1211-1223.
22. Grzesik W., “The influence of tin hard coatings on frictional behaviour in orthogonal cutting process”, *Tribology International*, vol. 33 (2000) 131-140.
23. Grzesik W., “Experimental investigation of influence of adhesive on the frictional conditions in cutting process”, *Tribology International*, vol. 32 (1999) 15-23.
24. Pottirayil, Kailash S. V., Biswas S. K., “Experimental estimation of friction force in lubricated cutting of steel”, *Wear*, vol. 269 (2010) 552-564.
25. Saoubi R. M., Axinte D., Soo S. L., Nobel C., Attia H., Kappmeyer G., Engin S., Sim W. M., “High performance cutting of advanced aerospace alloys and composite materials”, *CIRP Annals-Manufacturing Technology*, vol. 64 (2015) 557-580.
26. Chamani H. R., Ayatollahi M. R., “The effect of Berkovich tip orientations on friction coefficient in nano scratch testing of metals”, *Tribology International*, vol. 103 (2016) 25-36
27. Gresik W., Rech J., Zak K., “Determination of friction in metal cutting with tool wear and flank face effects”, *Wear*, vol. 317 (2014) 8-16.

28. Grzesik W., Kowalczyk D., Zak K., "A new mechanistic friction model for oblique cutting with tool wear effect", *Tribology International*, vol. 66 (2013) 49-53.
29. Schuh J. K., Ewoldt R. H., "Asymmetric surface textures decreases friction with Newtonian fluids in full film lubricated sliding contact", *Tribology International*, vol. 97 (2016) 490-498.
30. Abdelali H. B., Claudin C., Rech J., Salem W. B., Kapsa P., Dogui A., "Experimental characterization of friction coefficient at the tool-chip-workpiece interface during dry cutting AISI 1045", *Wear*, vol. 286-287 (2012) 108-115.
31. Brinksmeier E., Meyer D., A. G. Cordes A. G. H., Herrmann C., "Metalworking fluids- Mechanisms and performance", *CIRP- Annals-Manufacturing Technology*, vol. 64 (2015) 605-628.
32. Kawasegi N., Sugimori H., Morimoto H., Morita N., Hori I., "Development of cutting tools with microscale and nanoscale texture to improve frictional behavior", *Precision Engineering*, vol. 33 (2009) 248-254.
33. Smolenicki D., Boos J., Kuster F., Roelofs H., Wyen C. F., "In process measurement of friction coefficient in orthogonal cutting", *CIRP Annals-Manufacturing Technology*, vol. 63 (2014) 97-100.
34. Rech J., Claudin C., Eramo E. D., "Identification of a friction model application to the context of dry cutting AISI 1045 annealed steel with TiN-coated carbide tool", *Tribology International* 42 (2009) 738-744.
35. Tlili B., Barkaoui A., Walcok M., "Tribology and wear resistance of stainless steel. The sol-gel coating impact on the friction and damage", *Tribology International*, vol. 102 (2016) 348-354.
36. Wang H., Chang L., Williams J. G., Ye L., Mai Y.W., "On machinability and surface finish of cutting nanoparticle and elastomer modified epoxy", *Materials and Design*, vol. 109 (2016) 580-589.
37. Yahiaoui M., Paris J. Y., Delbe K., Denape J., Gerbaud L., Dourfaye A., "Independent analyses of cutting and frictional force applied on a single polycrystalline diamond compact cutter", *International Journal of Rock Mechanics & Mining*, vol. 85 (2016) 20-26.
38. Kurniawa R., Kiswanto G., Ko T. J., "Micro dimple pattern places and orthogonal cutting force analysis of elliptical vibration texture" *International Journal of Machine Tool & Manufacture*, vol. 106 (2016) 127-140.

39. Granados G. H., Morita N., Hidai H., Matsusaka S., Chiba A., Ashida K., Ogura I., Okazaki Y., "Development of a non-rigid micro-scale cutting mechanism applying a normal cutting force control system", *Precision Engineering*, vol. 43 (2016) 544-553.
40. Sugihara T., Enomoto T., "Improving anti adhesive in aluminum alloy cutting by micro stripe texture", *Precision Engineering*, vol. 36 (2012) 229-237.
41. Ahmed A., Bahadur S., Russell A. M., Cook B. A., "Belt abrasion resistance and cutting tool studies on new ultra hard boride materials", *Tribology International*, vol. 42 (2009) 706-713.
42. Shalaby M. A., Hakim M. A. E., Abdelhameed M. M , Krzanowski J. E., Velhuis S. C., Dosbaeva G. K., "Wear Mechanisms of several cutting tool material in hard turning of high carbon-chromium tool steel", *Tribology International*, vol. 70 (2014) 148-154.
43. Pilkington A., Dowey S. J., Toton J. T., Doyle E. D., "Machining with AlCr-oxinitride PVD coated cutting tools", *Tribology International*, vol. 65 (2013) 303-313.
44. Ramanujacha K., Subramanian S. V., "Micromechanisms of tool wear in machining free cutting steels", *Wear*, vol. 197 (1996) 45-55.
45. Komanduri R., Chandrasekaran N., Raff L. M., "MD Simulation of nanometric cutting of a single crystal aluminium-effect of orientation and direction of cutting", *Wear*, vol. 242 (2000) 60-88.
46. Nouari M., Iordanoff I., "Effect of third-body particle on tool-chip contact and tool wear behaviour during dry cutting of aeronautical titanium alloy" *Tribology International*, vol. 40 (2007) 1351-1359.
47. Zhu D., Luo S., Yang L., Chen W., Yan S., Ding H., "On energetic assessment of cutting mechanism in robot-assisted bolt grinding of titanium alloys", *Tribology International*, vol. 90 (2015) 55-59.
48. Bhat D. G., Johnson D. G., Malshe A. P., Naseem H., Brown W. D., Schaper L. W., Shen C. H., "A preliminary investigation of effect of post deposition polishing of diamond films on machining behaviour of diamond coated tools", *Diamond and Related Materials*, vol. 4 (1995) 921-929.
49. Komanduri R., Chandrasekaran N., Raff L. M., "Orientation effects in Nano metric cutting of single crystal material, An MD simulation approach", *Annals of CIRP*, vol. 48 (1) (1999) 67-72.
50. Komandori R., Chandrasekaran N., Raff L. M., "Effect of tool geometry in nano metal cutting a molecular dynamics simulation approach", *Wear*, vol. 219 (1998) 84-97.

51. Kosaraju S., Chandraker S., “Taguchi analysis on cutting force and surface roughness in turning MD N 350 Steel”, *Materials Today Proceedings*, vol. 2 (2015) 3388-3393.
52. Yuefeng Y., Wuyi C., Liansheng G., “Tools materials Rapid selection based on initial wear”, *Chinese Journal of Aeronautics*, vol. 23 (2010) 386-392.
53. Bahi S., List G., Sutter G., “Analysis of adhered contact and boundary conditions of secondary shear zone”, *Wear*, vol. 330-331 (2015) 608-617.
54. Caliskan H., Kucukkose M., “The effect of CN/Tin Al Coating tool wear, cutting forces, surface finish and chip morphology in face milling of Ti6Al4V superalloy”, *Int. Journal of Refractory Metals and Hard materials*, vol. 50 (2015) 304-312.
55. Buse H., Feinle P., “Model system studies of wear mechanism of hard metal tools when cutting CFRP”, *Procedia Engineering* vol. 149 (2016) 24-32.
56. Sugihara T., Enomoto T., “Crater and Flank wear resistance of cutting tools having micro textured surface”, *Precision Engineering*, vol.37 (2013) 888-896.
57. Thakur A., Gangopadhyay S., “State of the art in surface integrity in machining of nickel based super alloys”, *International Journal of Machine Tools & manufacture*, vol. 100 (2016) 25-54.
58. Hakim M. A. E., Abad M. D., Abdelhamed M. M, Shalaby M. A., Veldhuis S. C., “Wear behavior of some cutting tool materials in hard turning of HSS”, *Tribology International*, vol. 44 (2011) 1174-1181.
59. Monaghan J., Macginley T., “Modeling in the orthogonal machining process using coated carbide cutting tools”, *Computational Materials Science*, vol. 16 (1999) 275-284.
60. Zhou M., Ngoi B. K. A., Yusoff M. N., Wang X. J., “Tool wear and surface finish in diamond cutting of optical glass”, *Journal of Materials Processing Technology*, vol. 174 (2006) 29-33.
61. Ozbek N. A., Cicek A., Gulesin M., Ozbek O., “Effect of cutting condition on wear performance of cryogenically treated tungsten carbide insert of dry turning of stainless steel”, *Tribology International*, vol. 94 (2016) 223-233.
62. Remadna M., Rigal J. F., “Evolution during time tool wear and cutting forces in case of hard turning with CBN inserts”, *Journal of Materials Processing Technology*, vol. 178 (2006) 67-75.
63. Kumar A. S., Durai A. R., Sornakuma T., “Wear behaviour of alumina based ceramic cutting tools on machining steels”, *Tribology International*, vol. 39 (2006) 191-197.

64. Woydt M., Mohrbacher H., “The use of niobium carbide (NbC) as cutting tools and for wear resistant tribosystems”, *Int. Journal of Refractory Metals and Hard Materials*, vol. 49 (2015) 212-218.
65. Settineri L., Faga M. G., “Laboratory tests for performances evaluation of nano composite coating for cutting tools”, *Wear*, vol. 260 (2006) 326-332.
66. Talib N., Rahim E. A., “The effect of tribology on machining performances when using bio-based lubricants as a sustainable metal working fluid”, *Procedia CIRP*, vol. 40 (2016) 504-508.
67. Simonovic K., Kalin M., “Methodology of a statistical and DOE approach to the predication of performance in tribology- A DLC boundary case study”, *Tribology International*, vol. 101 (2016) 10-24.
68. Sugihara T., Enomoto T., “Development of cutting tool with a nano/micro- textured surface improvement of anti-adhesive effect by considering texture patterns”, *Precision Engineering*, vol. 33 (2009) 425-429.
69. Claudin C., Mondelin A., Rech J., Fromentin G., “Effects of a straight oil on friction at the tool-work material interface in machining”, *International Journal of Machine Tools & Manufacture*, vol. 50 (2016) 681-688.
70. Pottirayil A., Kailash S. V., Biswas S. K., “Lubricity of an oil in water emulsion in metal cutting: The effect of Hydrophilic/ lyophilic balance of emulsifiers”, *Colloids and Surface A: Physicochemical and Engineering Aspects*, vol. 384 (2011) 323-330.
71. Zhao C., Chen Y. K., Jiao Y., Loya A., Ren G. G., “The preparation and tribological properties of zinc borate ultra fine powder as a lubricant additive in liquid paraffin”, *Tribological International*, vol. 70 (2014) 155-164.
72. Enomoto T., Sugihara T., “Improvement of anti adhesive properties of cutting tool by nano/micro texture and its mechanism”, *Procedia Engineering.*, vol. 19 (2011) 100-105.
73. Battez A. H, Blanco D., Gonzalez A. F., Mallada M. T., Gonzalez R., Viesca J. L., “Friction, wear and tribofilm formation with(NTf₂) anion-based ionic liquid as neat lubricant”, *Tribology International*, vol. 103 (2016) 73-86.
74. Shyha I., Gariani S., Bhatti M., “Investigation of cutting tools and working conditions effects when cutting Ti-6 Al-4V using vegetable oil-based cutting fluids”, *Procedia Engineering*, vol. 132 (2015) 577-584.

75. Deshayes L., "Analysis of an equivalent tool face for cutting speed range prediction of complex grooved tools", *Journal of Materials Processing Technology*, vol. 190 (2007) 251-262.
76. Zhu P. Z., Hu Y. Z., Ma T. B., Wang H., "Study AFM Based nano metals cutting process using molecular dynamics", *Applied surface*, vol. 256 (2010) 7160-7165.
77. Klocke F., Krieg T., "Coated tools for metal-cutting features and applications", *Annals of CIRP*, vol. 48 (2) (1999) 57-88.
78. Romero O. M., Romeu M. L. G., Trejo D. O., Bagudanch I., Zuniga A. E., "Tool dynamics during single point incremental forming process", *Procedia Engineering*, vol. 81 (2014) 2286-2291.
79. Mansori M. E., Mkaddem A., "Surface plastic deformation in dry cutting at magnetically assisted machining", *Surface & Coatings Technology*, vol. 202 (2007) 1118-1122.
80. Gao Y., Sun R., Leopold J., "Analysis of cutting stability in vibration assisted machinery using an analytical predictive force model", *Procedia CIRP*, vol. 31 (2015) 515-520.
81. Cascon I., Sarasua J. A., "Mechanistic model for prediction of cutting forces in turning of non-axisymmetric parts", *Procedia CIRP*, vol. 31 (2015) 435-440.
82. Sagapuram D., Yeung H., Guo Y., Mahato A., Saubi R. M., Compton W. D., Trumble K. P., Chandrashekar S., "On control flow instabilities in cutting of metals", *CIRP Annals-Manufacturing Technology*, vol. 64 (2015) 49-52.
83. Wang X., Da Z. J., Balaji A. K., Jawahir I. S., "Performance Based Predictive Models and optimization methods for turning operations and applications. Part-3 options cutting conditions and selection of cutting tools", *Journal of Manufacturing Processes*, vol. (9) 2007 61-74.
84. Rao C. J., Sreeramulu D., Mathew A. T., "Analysis of Tool life during Turning operations by determining optimal Process Parameters", *Procedia Engineering*, vol. 97 (2014) 241-250.
85. Aagapiou J., Breher C., Clewett M., Ericson R., Huston F., Kadowaki Y., Lenz E., Moriwaki T., Pitsker A., Shimizu S., Schulte T., Schumiuz M. H., Smith K. S., Tsutsumi M., Yokama K., "Tooling structure: Interface between cutting edge and machine tools", *Annals of CIRP*, vol.49 (2) (2000) 591-634.

86. Elmadagli M., Alpas T. A., "Metallographic analysis of deformation micro-structure of copper subjected to orthogonal cutting", *Materials Science and Engineering A*. vol. 355 (2003) 249-259.
87. Beauchamp Y., Thomas M., Youssef Y. A., Masounave J., "Investigation of cutting parameter effects on surface roughness in lathe boring of operations by use of a full factorial design", *Computers Industrial Engineering*, vol. 31 (1996), 645-651.
88. Venuvinod P. K, Jin W. L., "Three Dimensional cutting force analysis based on lower boundary of the shear zone Part I: Single edge oblique cutting", *International J. Mach. Tools Manufacture*", vol. (36) (1996) 307-323.
89. Grzesik W., Rech J., Zak K., Claudin C., "Machining performance of pearlitic-ferritic nodular cast iron with coated carbide and silicon nitride ceramic tools", *International Journal of Machine Tools & Manufacture*, vol. 49 (2009) 125-133.
90. Shoba C., Ramanaiah N., Rao D. N., "Effect of reinforcement on cutting forces while machining metal matrix composites - an experimental approach", *Engineering Science and Technology, An International Journal*, vol. 18 (2015) 658-663.
91. Kilic Z. M., Altintas Y., "Generalized Mechanics and dynamics of metal cutting operation for united simulations", *International Journal of Machine Tools & Manufacture*, vol. 104 (2016) 1-13.
92. Wegener K., Kuster F., Weikert S., Weisis L., Stirnimann J., "Success Story Cutting", *Procedia, CIRP* vol. 46 (2016) 512-524.
93. Tanaka H., Sugihara T., Enomoto T., "High speed machining of Inconel 718 focusing of wear behaviour of PCBN cutting tool", *Procedia CIRP*, vol. 46 (2016) 545-548.
94. Sparham M., Sarhan A. A. D., Marti N. A, Dahari M., Hamdi M., "Cutting force analysis to estimate the friction force in linear guideways of CNC machines", *Measurement*, vol. 85 (2016) 65-79.
95. Alagan N. T., Beno T., Wretland A., "Investigation of modified cutting insert with forced coolant application in machining alloy 718", *Procedia CIRP*, vol. 42 (2016) 481-486.
96. Huang K., Yang W., "Analytical modeling of residual stress formation in work piece material due to cutting", *International Journal Mechanical Science*, vol. 114 (2016) 21-34.
97. Su G. S., Guo Y. K., Song X. L., Tab H., "Effects of high pressure cutting fluid with different jetting paths on tool wear in cutting compact graphite iron", *Tribology International*, vol. 103 (2016) 289-297.

98. Katuku K., Koursaris A., Sigalas I., “Structured features of the austempered ductile iron - PCBN Cutting tool interaction interface as captured through static diffusion couple experiment”, *Solid State Ionics*, vol. 224 (2012) 41-50.
99. Goel S., Kolvalchenko A., Stukouski A., Goss G., “Influence of micro structure on cutting behaviour of silicon”, *Acta Materialia*, vol. 105 (2016) 464-478.
100. Schneider F., Bischof R., Kirsch B., Kuhn C., Muller R., Aurich J. C., “Investigation for chip formation and surface integrity when micro cutting cp- titanium with ultra fine grain cemented carbide”, *Procedia CIRP*, vol. 45 (2016) 115-118.
101. Mauclair C., Pietroy D., Maio Y. D., Baubeau E., Colombier J. P., Stoian R., Pigeon F., “Ultrafast laser micro- cutting of stainless steel and PZT using a line of multiple foci formed by spatial beam shaping”, *Optics and lasers in Engineering*, vol. 67 (2015) 212-217.
102. Sonam A., Anbarasan N., Haresh P., Kukkan P., “Experimental study on effect of electric current applied at the interface of cutting tool and workpiece for turning operation”, *Procedia Engineering* , vol.97 (2014) 220-229.
103. Abouridouane M., Klocpe F., Lung D., Veseloc D., “The mechanism of cutting in-situ measurement and modelling”, *Procedia CIRP*, vol. 31 (2015) 246-251.
104. Piska M., Sliwkova P., “Surface parameters, tribological tests cutting performance of coated HSS tap”, *Procedia Engineering*, vol. 100 (2015) 125-134.
105. Chengzhang Y., Outeiro J. C., Mabrouks T., “On the selective of Johnson - Cook constitute model parameters for Ti-6Al-4V using three types of numerical models of orthogonal cutting”, *Procedia CIRP*, vol. 31 (2015) 112-117.
106. Baksa T., Kroupa T., Hanzl P., Zetek M., “Durability of cutting tools during machining very hard and solid metal”, *Procedia Engineering*, vol. 100 (2015) 1414-1423.
107. Pilkington A., Dowey S. J., Toton J. J., Doyle E. D., “Machinery with AlCr-oxinitride PVD cutting tools”, *Tribology International*, vol. 65 (2013) 303-313.
108. Venkateson K., Ramanujan R., Kuppan P., “Analysis of cutting forces and temperature in laser assisted machining of Inocel 718 using Taguchi method”, *Procedia Engineering*, vol. 97 (2014) 1637-1646.
109. Shihab S. K., Khan Z. A., Mohammad A., Siddiqueed A. N., “RSM based study of cutting and during hard turning with multi layer coated carbide insert”, *Procedia Materials Science*, vol. 6(2014) 1233-1242.

110. Kannan S., Deiab I. M., Surappa M. K., "On the role of reinforcements on tool performance during cutting of metal matrix components", *Journal of Manufacturing Process*, vol. 8 (2006).67-75.
111. Dhananchezian M., Kumar M. P., "Cryogenic turning of Ti- 6Al- 4V alloy with modified cutting tool insert", *Cryogenics*, vol. 51 (2011) 34-40.
112. Jiang W., "Bio-inspired self-sharpening cutting tool surface for finish hard turning of steel", *CIRP Annals Manufacturing Technology*, vol. 63 (2014) 517-520.
113. Soussia A. B., Makadden A., Mansori M. E., "Effect of coating type on dry cutting of glass/epoxy composite", *Surface & Coatings Technology*, vol. 215 (2013) 413-420.
114. Lakic G. G., Sredanovic B., Kramer D., Nedic B., Kopac J., "Experimental research using MQL in metal cutting", *Tribology in Industry*, vol. 35 (2013) 276-285.
115. Kramar B.M., "Tribology aspects in metal cutting", *Journal of Engineering for Industry, ASME*, vol. 115 (1993), 372-376.
116. Gupta, M. K., Kumar P., "Optimizing Multi Characteristics in machining of AISI 4340 Steel using Taguchi's approach and utility concept", *Journal of Engineering India Ser. C*, vol. (97) (1), (2016) 63-69.
117. Mandal, N., Mondal B., "Surface roughness predication model using Zirconia toughened alumina (ZTA) turning inserts: Taguchi method and regression Analysis", *Journal of Engineering India Ser. C*, vol. (97) (1) (2016) 77- 84.
118. Nagapal S., Jain N. K., Sanyal S., "Three dimensional parametric analyses of stress concentration factor and its mitigation in isotropic and orthotropic plate with central circular hole under axial in plane loading", *Journal of Institution of Engineers (India) Ser. C*, vol. (97) (1) (2016) 85-92.
119. Sundeepan J., Kumar K., Barman T.K., "Mechanical And Tribological behavior of ABS/TiO₂ polymer composites and optimization of tribological properties using grey relation analysis", *Journal of Institution of Engineers (India)*, vol. (97) (1) (2016) 41-53.
120. Bleicher F., Pollak C. , Brier J., Siller A., "Reduction of built up edge formation in machining Al and cast iron hybrid components by internal cooling of cutting inserts", *CIRP Annals-Manufacturing Technology*, vol.65 (2016) 97-100.
121. Shokoohi Y., Shekarian, E. "Application of nano fluids in machining process- A Review", *Journal of Nano-Science and Techonology*, vol.(2) (1) (2016) 59-63.
122. Rech J., Kusiak A., Battaglia J. L., "Tribological and thermal function of cutting tool coatings", *Surface & coatings technology*, vol. 186 (2004) 364-371.

123. Komanduri R., Hou Z. B., “Thermal modeling of metal cutting process — Part II: temperature rise distribution due to frictional heat sources at tool-chip interface”, *International Journal of Mechanical Sciences*, vol. 42 (2001) 57-88.
124. Moufki A., Devillez A., Dudzinshi D., Molinari A., “Thermo mechanical modeling of oblique cutting and experimental validation”, *International Journal of Machine Tools & Manufacture*, vol. 44 (2004) 971-989.
125. Rajifar B., “Enhancement of the performance of double layered micro channel heat sink using PCM slurry and nano fluid coolant”, *International Journal of Heat and Mass Transfer*, vol. 88 (2015) 627-635.
126. Cotterell M., Ares E., Yanes J., Lopez F., Hernandez P., Pelaez G., “Temperature and strain measured during chip formation in orthogonal cutting conditions applied to Ti-6 AL-4V”, *Procedia Engineering*, vol. 63 (2013) 922-930.
127. Chiffre L. D., Belluco W., “Comparison of methods for cutting fluid, performance testing”, *Annals of CIRP*, vol. (49) (1) (2000) 57-60.
128. Gosai M., Bhavsar S. N., “Experimental study on temp. measured in turning operation of hardened steel (EN36)”, *Proceedings Technology*, vol. 23 (2016) 311-318.
129. Savan A., Simmonds M. C., Huang Y., Constable C. P., Creasey S., Gerbig Y., Haefke H., Lewis D. B., “Effects of temperature on the chemistry and tribology of co-sputtered MoS_x - Ti composite thin films”, *Thin Solid Films*, vol. 489 (2015), 137-144.
130. Augspurger T., Brockmann M., Frekers Y., Kocke F., Kneer R., “Experimental Investigation of thermal boundary conditions during metal cutting”, *Procedia CIRP*, vol. 46 (2016) 119-122.
131. Courbon C., Mabrouki T., Rech J., Mazuyer D., Eramo E. D., “On the existence of a thermal contact resistance at the tool chip interface in dry cutting of AISI 1045: Formation mechanism and Influence on cutting process”, *Applied Thermal Engineering*, vol. 50 (2013) 1311-1325.
132. Mkadden A., Zeramdin B., Mansori M. E., Mezlini S., “Evaluation of tribothermal effectiveness of Ti AlN - based bilayer coatings in cutting fiber-reinforced polymers”, *Tribology International*, vol. 103 (2016) 176-186.
133. Nandy A. K., Gowrishankar M. C., Paul S., “Some studies on high pressure cooling in turning of Ti-6Al-4V”, *International Journal of Machine Tools & Manufacture*, vol. 49 (2009) 182-198.

134. Jawhir I. S., Attia H., Biermann D., Duflou J., Klocke F., Meyer D., Newman S. T., Pusavec F., Putz M., Rech J., Schulze V., Umbrello D., "Cryogenic Manufacturing Processes", *CIRP Annals-Manufacturing Technology*, vol.65 (2016) 713-736.
135. Madanchi N., Kurle D., Winter M., Thiede S., Herrmann C., "Energy Efficient process chain: The impact of cutting fluids strategies", *Procedia CIRP*, vol. 29 (2015) 316-365.
136. Naves V. T. G, Silva M. B. D., Silva F. J. D., "Evaluation of the effect of application of cutting fluid at high pressure on tool wear during turning operation of AISI 316 austenitic stainless steel", *Wear*, vol. 302 (2013) 1201-1208.
137. Mosleh, M., Ghaderi M., Shirvani K. A., Belk J., Grzina D. J., "Performance of cutting nanofluids in tribological testing and conventional drilling", *Journal of Manufacturing Processes*, vol. 25 (2017) 70-76.
138. Paul P. S., Varadarajan A. S., Cnandurai R. R., "Study on the influence of fluid application parameters on tool vibration and cutting performance during turning of hardened steel", *Engineering Science and Technology an International Journal*, vol. 19 (2016) 241-253.
139. Shokrani A., Dhokia V., Newman S. T., "Environmentally, conscious machining of difficult to machine materials with regard to cutting fluids", *International Journal of Machine Tools & Manufacture*, vol. 57 (2012) 83-101.
140. Jayal A. D., Balaji A. K., "Effects of cutting fluid application on tool wear in machining: Interaction with tool surface features", *Wear*, vol. 267 (2009) 1723-1730.
141. Verschaka A. A., Grigoriev S. N., Vereschaka A. S., Popov A. Y., Batako A. D., "Nano-scale multilayered composite coatings for cutting tools operating under heavy cutting conditions", *Procedia CIRP*, vol. 14(2014) 239-244.
142. Bork C. A. S., Goncalves J. F. D. S., Gomes J. D. O., Gheller J., "Performance of the jatropha vegetable base soluble cutting oil as a renewable source in the aluminum alloy 7050-T7451 milling", *CIRP Journal of Manufacturing Science and Technology*, vol. 7 (2014) 210-221.
143. Sokovic M., Mijanovic K., "Ecological aspects of the cutting fluids and its influence on quantifiable parameters of the cutting processes", *Journal of Material Processing Technology*, 190 (2011) 181-189.
144. Hermoso J., Boza F. M., Gallegos C., "Influence of viscosity modifier and concentration on the viscous flow behaviour of oil based drilling fluids at high pressure", *Applied Clay Science*, vol. 87 (2014) 14-21.

145. Khan M. M. A., Mithu M. A. H., Dhar N. R., “Effects of minimum quantity lubrication on turning AISI 9310 Alloy steel using vegetable oil-based cutting fluid” *Journal of Materials Processing Technology*, vol. 209 (2009) 5573-5583.
146. Xu D. L. J., Ding W., Fu Y., Yang C., “Tool wear in milling Ti40 burn resistant titanium alloy using pneumatic mist jet impinging cooling”, *Journal of Materials Processing Technology*, vol. 229 (2016) 641-650.
147. Baradie M. A. E., “Cutting Fluids: Part II, Recycling and clean machining”, *Journal of Materials Processing Technology*, vol. 56 (1996) 798-806.
148. Lotierzo A., Piffier V., Artizzone S., Pasqualin P., Cappelletti G., “Insight into the role of amines in metal working fluids”, *Corrosion Science*, vol. 110 (2016) 192-199.
149. Rakic R., Rakic Z., “Tribological aspects of choice of metal working fluid in cutting processes”. *Journal of Materials Processing Technology*, vol. 124 (2002).25-31.
150. Courbon C., Sajn V., Kramar D., Rech J., Kosel F., Kopac J., “Investigation of machining performance in high pressure jet assisted turning of Inconel 718: A numerical model”, *Journal of material processing Technology*, vol. 211 (2011) 1834-1851.
151. Xavior M. A., Adithan M., “Determining the influence of cutting fluids on tool wear and surface roughness during turning of AISI 304 austentic stainless steel” *Journal of Material Processing Technology*, vol. 209 (2009) 900-909.
152. Chan C. Y., Lee W. B., Wang H., “Enhancement of surface finish using water – miscible nano cutting fluid in ultra precision turning”, *International Journal of machine tools & manufacture*, 73 (2013) 62-70.
153. Zong W. J., Sun T., Cheng D. L. K., Liang Y. C., “XPS analysis of the groove wearing marks on flank face of diamond tool in nano metric cutting of silicon wafer”, *International Journal of Machine Tools & manufacture*, vol. 48 (2008) 1678-1687.
154. Yin Z., Huang C., Zou B., Liv H., Zhu H., Wang J., “High temperature mechanical properties of AlO₂O₃/Tic micro nano – composite ceramic tool materials” *Ceramic International* 39 (2013) 8877- 8883.
155. Kumar K. M, Ghosh A., “Assessment of cooling lubrication and wettability characteristics of nano engineered sunflower oil as cutting fluid and its impact on SQCL grinding performance”, *Journal of Material Processing Technology*, vol. 237 (2016) 55-64.

156. Zhang K., Deng J., Meng R., Go P., Yue H., “Effect of nano scale textures on cutting performance of WC/Co-based Ti₅₅Al₄₅N coated tools in dry cutting”, *Int. Journal of Refractory Metals and Hard Material*, vol. 51 (2015) 35-49.
157. Amrita M., Shariq S. A., Manoj, Gopal C., “Experimental investigation on application of emulsifier oil based nano cutting fluid in metal cutting process”, *Procedia Engineering*, vol. 97 (2014) 1115-124.
158. Sharma A. K, Singh R. K., Dixit A. R, Tiwari A. K., “Characterization and experimental investigation of Al₂O₃ nanoparticle based cutting fluid in turning AISI 1040 steel under minimum quantity lubrication (MQL)”, *Materials Today, Proceedings* 3 (2016), 1899-1906.
159. Sharma A. K., Tiwari A. K., Singh R. K., Dixit A. R., “Tribological Investigation of TiO₂ Nano particle based cutting fluid in machining under minimum quantity lubrication (MQL)”, *Materials Today: Proceedings*, vol. 3 (2016) 2155-2162.
160. Padmini R., Krishna P. V., Rao G. K. M., “Effectiveness of vegetable oil based nano fluids as potential cutting fluid in turning steel AISI 1040 Steel”, *Tribology International*, vol. 94 (2016) 490-501.
161. Uysal A., Demiren F., Atlan E., “Applying minimum quantity lubrication (MQL) method on milling of martensitic stainless steel by using Nano MoS₂ reinforced vegetable cutting fluid”, *Procedia social and Behavioral Sciences*, vol. 195 (2015) 2742-2747.
162. Wu W., Chen W., Yang S., Lin Y., Zhang S., Cho T. Y., Lee G. H., Kwon S. C., “Design of AlCrSiN multilayers and nanocomposites coating for HSS cutting tools”, *Applied Surface Science*, vol. 351 (2015) 803-810.
163. Dobrzanski L. A., Golomek K., “Structure properties of cutting tools made from cemented carbides and cermets with TiN + mono - , gradient - or multi (Ti, Al, Si)N + TiN nano crystalline coatings”, *Journal of Material Processing Technology*, vol 164-165 (2005) 805-815.
164. Esfe M. H., Afrand M., Rostamian S. H., Toghraie D., “Examination of rheological behavior of MWCNTS/ZnO-SAE40 hybrid nano-lubricants under various temperatures and solid volume fractions”, *Experimental Thermal and Fluid science*, vol. 80 (2017) 384-390.
165. Ali M. K. A., Xianjun H., Mai L., Qingping C., Turkson R. F., Bicheng C., “Improving the tribological characteristics of piston ring assembly in automotive

- engines using Al₂O₃ and TiO₂ nanomaterials as nano-lubricant additives”, *Tribology International*, vol.103 (2016) 540-554.
166. Asadi A., Asadi M., Rezari M., Siahmargoi, Asadi F., “The effect of temperature and solid concentration on dynamic viscosity of MWCNT /MgO (20-80)-SAE50 hybrid nano-lubricant and proposing a new correlation: An experimental study”, *International Communications in Heat and Mass Transfer*, vol. 78 (2016) 48-53.
167. Ali M. K. A., Xianjuh H., Mai L., Bicheng C., R. Turkson R. F., Ping, C. Q. “Reducing frictional power losses and improving the scuffing resistance in automotive engines using hybrid nanomaterials as nano-lubricant additives”, *Wear*, vol. 364-365 (2016) 270-281.
168. Esfe M. H., Afrand M., Yan W. M., Yarmand H., Toghraie D., Dahari M., “Effects of temperature and concentration on rheological behavior of MWCNTs, SiO₂(20-80)-SAE 40 hybrid nano-lubricant”, *International Communications in Heat and Mass Transfer*, vol. 76 (2016) 133-138.
169. Maheswaran R., Sunil J., “Effect of nano sized garnet particles dispersion on the viscous behaviour go extreme pressure lubricant”, *Journal of Molecular Liquids*, vol. 223 (2016) 643-651.
170. Callisti M., Polcar T., “The role of Ni-Ti (Cu) interlay on the mechanical properties and nano scratch behaviour of solid lubricant W-S-C coatings”, *Surface & Coatings Technology*, vol. 254 (2014) 260-269.
171. Afrand M., Najafabadi K. N., Sina N., Safaei M. R., Kherbeet A. S., Wongwises S., Dahari M., “Prediction of dynamic viscosity of a hybrid of a hybrid nano-lubricant by an optimal artificial neural network”, *International Communications in Heat and Mass Transfer*, vol. 76(2016) 209-214.
172. Kumar N. S., Sammaiah P., Rao K. V., M. Sneha M., Ashok C., “Influence of Nano solid Lubricant emulsions on surface roughness of mild steel when machining of lathe machine”, *Materials Today: Proceedings*, vol. 2 (2015) 4413- 4420.
173. D. H. Cho, J. S. Kim, S. H. Kwon, C. Lee, Y. Z. Lee, “Evaluation of hexagonal boron nitride nano sheets as a lubricant additive in water”, *Wear*, vol. 302 (2013) 981-986.
174. Shahnazar S., Begheri S., Hamid S. B. A., “Enhancing lubricant properties by nano particle additives”, *International Journal of Hydrogen Energy*, vol.41 (2016) 3153-3170.

175. Hu C., Bai M., Lv J., Li X., “Molecular dynamics simulation of mechanism of nano particle in improving load carrying capacity of lubricant film”, *Computational Materials Science*, vol. 109 (2015) 97-103.
176. Liu Y., Hu K., Hu E., Guo J., Han C., Hu X., “Double hollow MoS₂ nano-spheres: Synthesis, tribological properties, and functional conversion from lubrication to photocatalysis”, *Applied surface science*, vol. 392 (2017) 1144-1152.
177. Tao Y., Tao Y., Wang B., Tai Y., “Preparation and investigation of nano - AlN lubricant with high performance”, *Materials Chemistry and Physics*, vol. 147 (2014) 28-34.
178. Zheng J., Ren X., Hao J., Li A., Liu W., “Carbon nanohoops as attractive toughening and lubricant agents in TiN porous films”, *Applied Surface Science* vol. 393 (2017) 60-66.
179. Yang C., Hou X., Li Z., Li X., Yu L., Zhang Z., “Preparation of surface modified lanthanum fluoride - graphene oxide nanohybrids and evaluation of their tribological properties as lubricant additives in liquid paraffin”, *Applied Surface Science*, vol. 388 (2016) 497-502.
180. Xiang L., Gao C., Wang Y., Pan Z., Hu D., “Tribological and tribo chemical properties of magnetite nanoflakes as additives in oil lubricants”, *Particuology*, vol. 17(2014) 136-144.
181. Zovari M., Kharrat M., Dammak M., Barletta M., “A comparative investigation of the tribological behavior and scratch response of polyester powder coatings filled with different solid lubricants”, *Progress in Organic Coatings*, vol. 77 (2014) 1408-1417.
182. Tang Z., Li S., “A review of recent developments of friction modifiers for liquid lubricants (2007- present)”, *Current Opinion in Solid State and Materials Science*, vol. 18 (2014) 119-139.
183. Putz M., Dix M., Neubert M., Schmidt G., Wertheim R., “Investigation of turning elastomers assisted with cryogenic cooling”, *Procedia CIRP*, vol. 401 (2016) 631-636.
184. Bermingham M. J., Kirsch J., Sun S., Palanisamy S., Dargusch M. S., “New Observations on tool life cutting forces and chip morphology in cryogenic machining Ti-6Al-4V”, *International Journal of Machine Tools & Manufacture*, vol. 51 (2011) 500-511.
185. Huang X., Zhang X., Mou H., Zhang X., Ding H., “The influence of cryogenic cooling on milling stability”, *Journal of Material Processing Technology*. 214 (2014) 3169-3178.

186. Yuvaraj N., Kumar M. P., "Cutting of aluminum alloy with abrasive water jet and cryogenic abrasive water jet: A comparative study of the surface integrity approach", *Wear* 362-363 (2016) 18-32.
187. Schoop J., Effgen M., Balk T. J., Jawahir I. J., "The effects of depth in of cut and pre cooling on surface porosity in cryogenic machining of porous tungsten", *Procedia CIRP*, vol. 8 (2013) 357-362
188. Aggarwal A., Singh H., Kumar P., Singh M., "Optimization of multiple quality characteristics for CNC turning under cryogenic cutting environment using desirability function", *Journal of Materials Processing Technology*, vol. 205 (2008) 42-50.
189. Hong S. Y., Ding Y., "Cooling approaches and cutting temperatures in cryogenic machining of Ti-6Al-4V", *International Journal of Machine Tools and Manufacture*, vol. 41 (2001) 1417-1437.
190. Aslantas K., Cicek A., Ucun I., Percin M., Hopa H. E., "Performance evaluation of a hybrid cooling lubrication system in micro milling of Ti-6Al-4V alloy", *Procedia CIRP*, vol. 46 (2016) 492-495.
191. Fredj N. B., Sidhem H., Braham C., "Ground surface improvement of the austenitic stainless steel AISI 304 using cryogenic cooling", *Surface & Coatings Technology*, vol. 200 (2006) 4846-4860.
192. Chiffre L. D., Andreasen J. L., Lagerberg S., Thesken I. B., "Performance testing of cryogenic CO₂ as cutting fluid in parting /grooving and threading austenitic stainless steel", *Annals of the CIRP*, vol. 56 (1) (2007) 101-104.
193. Wu W., Gui J., Sai W., Xie Z., "The reinforcing effect of graphene nano platelets on the cryogenic mechanical properties of GNPs/Al₂O₃ composites", *Journal of Alloys and compounds*, vol. 691 (2017) 778-785.
194. Kayank Y., Karaca H. E., Noebe R. D., Jawahir I. S., "Tool-wear analysis in cryogenic machining of NiTi shape memory alloys: A comparison of tool-wear performance with dry and MQL machining", *Wear*, vol. 306 (2013) 51-63.
195. Chinchankar S., Choudhury S. K., "Machining of hardened steel-Experimental investigations, performance modeling and cooling techniques: A review", *International Journal of Machine Tools & Manufacture*, vol. (89) (2015) 95-109.
196. Rubio E. M., Agustina B., Marin M., Bericua A., "Cooling Systems based on cold compressed air: a review of the applications in machining processes", *Procedia Engineering*, vol. 132 (2015) 413-418.

197. Sharma V. S., Dogra M., Suri N. M., "Cooling techniques for improved productivity in turning", *International Journal of Machine Tools & Manufacture*, vol. 49 (2009) 435-453.
198. Courbon C., Pusavec F., Dumont F., Rech J., Kopac J., "Tribological behaviour of Ti6Al4V and Inconel 718 under dry and cryogenic conditions-Application to the context of machining with carbide tools", *Tribology International*, vol. 66 (2013) 72-82.
199. Gao Y., Luo B. H., Bai Z. H., Zhu B., Ouyang S., "Effects of deep cryogenic treatment on the microstructure and properties of WC-Fe-Ni cemented carbides", *Int. Journal of Refractory Metals and Hard Materials*, vol. 58 (2016) 42-50
200. Tyshchenko A. I., Theisen W., Oppenkowski A., Siebert S., Razumov O. N., Shoblik A. P., Sirosh V. A., Petrov Y. N., Gavriljuk V. G., "Low temperature martensitic transformation and deep cryogenic treatment of a tool steel", *Materials Science and Engineering*, vol. A 527 (2010) 7027-7039.
201. Shokrani A., Dhokia V., Newman S. T., "Investigation of the effects of cryogenic machining on surface integrity in CNC end milling of Ti-6Al-4V titanium alloy", *Journal of Manufacturing Processes*, vol. 21 (2016) 172-179.
202. Schoop J., Ambrosy F., Zanger F., Schelze V., Balk T. J., Jawahir I. S., "Cryogenic machining of porous tungsten for enhanced surface" *Journal of Material Processing Technology*, vol. 229 (2016) 614-621.
203. Podgornik B., Majdic F., Leskovsek V., Vizinth J., "Improving tribological properties of tool steels through combination of deep cryogenic treatment and plasma nitriding", *Wear*, vol. 288 (2012) 88-93.
204. Li S., Min N., Li J., Wu X., Li C., Tang L., "Experimental verification of segregation of carbon and precipitation of carbide due to deep cryogenic treatment for steel by internal friction method", *Materials Science & Engineering A*, 575 (2013) 51-60.
205. Hong S. Y., Ding Y., "Micro-temperature manipulation in cryogenic machining of low carbon steel", *Journal of Material Processing Technology*, vol. 116 (2001) 22-30.
206. Pusavec F., "Porous tungsten machining under cryogenic conditions", *Int. Journal of Refractory Metals and Hard Materials*, vol. 35 (2012) 84-89.

207. Leskovsek V., Podgornik B., “Vacuum heat treatment deep cryogenic treatment and simultaneous pulse plasma nitriding and tempering of P/M S390MC steel”, *Material Science and Engineering A*, vol. 531 (2012) 119-129.
208. V.G. Dhokia, Newman S. T., Crabtree P., Ansell M. P., “A process control system for cryogenic CNC elastomer machining”, *Robotics and Computer Integrated Manufacturing*, vol. 27 (2011) 779-784.
209. Li S., Deng L., Wu X., Min Y., Wang H., “Influence of deep cryogenic treatment of microstructure and evaluation by internal friction of tool steel”, *Cryogenics*, vol. 50 (2010) 754-758.
210. Ross P. J. Taguchi “Techniques for quality engineering”, (1996) Newyork, McGraw-Hill.

Patent

- Patent on the topic “ Delivery Container” has been submitted to Intellectual Property Rights Cell of Delhi Technical University

Research Papers Published/Accepted in Journals

- [1] **A Sharma**, R C Singh, R M Singari, Effect of direct LN₂ single jet supply during turning of AISI D3 steel alloy using an optimization technique, *Material Research Express* 6 (2019),<https://doi.org/10.1088/2053-1591/ab2ded>
- [2] **A Sharma**, R C Singh, R M Singari, Optimization of cutting parameters during cryogenic turning of AISI D3 steel,*Sadhna*45 (2020) <https://doi.org/10.1007/s12046-020-01368-4>
- [3] **A Sharma**, R C Singh, R M Singari, Effect on wear property during LN₂ sliding, *Indian Journal of Engineering & Materials Sciences* (Accepted)
- [4] **A Sharma**, R C Singh, R M Singari, S L Bhandarkar, Force and temperature analysis during distinct machining environment using an optimization approach, *Indian Journal of Pure & Applied Physics* (Accepted)
- [5] **A Sharma**, R C Singh, R M Singari, Impact of cryogenic cooling during machining: A Literature Review, *International Journal of New Innovations in Engineering and Technology*, 11(2019), 1-5

Research Papers Published/ Accepted in International / National Conference Proceedings

- [1] **A Sharma**, R C Singh, R M Singari, Experimental study of effect of temperature on lubricating oil and grease on Rheometer, International conference on advanced production and industrial engineering(ICAPE 2016) December 2016, 153-170, ISBN: 978-93-85909-51-1
- [2] **A Sharma**, R C Singh, R M Singari, Emergence of Cryogenic Cooling and its Impact in Machining Processes: A Review, 1st International Conference on New Frontiers in Engineering Science & Technology, January, 2018, 726- 730, January, 2018
ISBN: 978-93-86238-41-2
- [3] **A Sharma**, R C Singh, R M Singari, Optimization of cutting parameters of machinability aspects during dry turning, National Conference on Advances in Mechanical Engineering, NCAME 2019, Lecture Notes in Mechanical Engineering,79-94, ISSN: 2195-4356, https://doi.org/10.1007/978-981-15-1071-7_8

Research Papers presented in International/National Conferences

- [1] **A Sharma**, R C Singh, R M Singari, Tribological study of single cutting tool: A Review, International Conference of advanced research and innovation (ICAEI-2017) 29 January, 2017
- [2] **A Sharma**, R C Singh, R M Singari, Emergence of nanoparticles engineering application: A Review, International conference on advanced production and industrial engineering, (ICAPIE 2017), 6-7October, 2017
- [3] **A Sharma**, R C Singh, R M Singari, Investigations of tribological behaviour in machining operations for a single point cutting tool in presence of coolant; A Review, International conference on advanced production and industrial engineering (ICAPIE 2018), 5-6October, 2018.
- [4] **A Sharma**, R C Singh, R M Singari, Experimental study of effect of temperature on lubricating oil and grease on Rheometer, International conference on advanced production and industrial engineering (ICAPIE2016), ISBN: 978-93-85909-51-1, December, 2016, pp 153-170
- [5] **A Sharma**, R C Singh, R M Singari, Emergence of Cryogenic Cooling and its Impact in Machining Processes: A Review, 1st International Conference on New Frontiers in Engineering, Science & Technology, ISBN: 978-93-86238-41-2, January, 2018. pp 726- 730
- [6] **A Sharma**, R C Singh, R M Singari, Optimization of cutting parameters of machinability aspects during dry turning, Lecture Notes in Mechanical Engineering Springer, (2019) https://doi.org/10.1007/978-981-15-1071-7_8